# SYNTHESES OF POLYMERS USING ACTIVATED S-TRIAZINES AND AN INVESTIGATION OF S-TRIAZINE THERMAL REARRANGEMENT

by

Emir Hakan Şamat

B.S., Chemistry, Boğaziçi University, 2023

Submitted to the Institute for Graduate Studies in
Science and Engineering in partial fulfillment of
the requirements for the degree of
Master of Science

Graduate Program in Chemistry

Bogazici University

2025

*Dedicated to my dear sister*

# ACKNOWLEDGEMENTS

First and foremost, I wish to express my deepest gratitude to my advisor, A. Ersin Acar, for welcoming me into his laboratory and agreeing to supervise my research, undoubtedly one of the greatest privileges of my life. He taught me what it means to be a Boğaziçi student and a chemist, and his scientific outlook has fundamentally reshaped how I understand nature. Like all his students, I hope to emulate his wisdom and kindness one day.

I would also like to thank my committee members, Prof. Tarık Eren and Prof. Şaron Çatak, for generously devoting their time and insight to evaluating this thesis.

My sincere thanks go to my "big sisters" Halenur, Göknil, and Ayşenur. You were there for me even when I did not realize I needed help—listening to my complaints, wiping my tears, and asking the simple but powerful question, "Hakan, are you okay?" Scientifically, your constant support, questioning, and fruitful discussions pushed me forward; I owe much of my growth to you.

I am indebted to Sedef, who entrusted me with significant responsibilities from the very beginning and shared the joys and headaches of triazine chemistry, allowing me to gain invaluable synthetic experience.

Special thanks to Elif for long commutes and heartfelt conversations, Hüseyin for lively banter, Atakan for his colorful spirit, and Nazlıcan for her infectious laughter.

I am also grateful to our kind neighbors, Fatma and Sezin, and to my friends in the chemistry department, Aleyna and Yusuf, for their constant support.

During my time in the lab, I had the pleasure of working with many interns. Ceyda and Gonca deserve particular mention for their substantial contributions to this thesis. I am lucky to call them colleagues and friends.

My close friends Furkan and Yasin have stood behind me throughout my academic journey, illuminating my path with their own experiences and serving as inspiring examples of young scholars.

I owe a heartfelt thank-you to Süyümbike for always being there when I needed her most. Her unwavering effort—especially while I was writing—allowed me to stay focused, and her companionship has been a constant source of trust and comfort.

To my family, who meet every challenge on my behalf and approach every request with love: thank you. You encouraged me to pursue my aspirations even when I chose unconventional paths. I hope to achieve the success you envision for me and make you even prouder.

Finally, I am grateful to God, who grants me the strength to persevere, nourishes my curiosity and diligence, and blesses me with good friends, a caring family, and supportive lab mates. Any success I attain is only by His grace.

# ABSTRACT

**SYNTHESES OF POLYMERS USING ACTIVATED S-TRIAZINES AND AN INVESTIGATION OF S-TRIAZINE THERMAL REARRANGEMENT**

Polycyanurates hold remarkable potential applications and are worth in-depth research. The study focused on synthesizing a novel *s*-triazine monomer for the melt-polycondensation. The monomer, activated *s*-triazine, was synthesized in two steps from commercially available starting materials. Activated s-triazine was polymerized with bisphenol-A under reduced pressure in the presence of a basic catalyst. Initial polymerizations were found to show thermal rearrangement, which was further investigated. The thermal rearrangement reaction of *s*-triazines was studied through thermal exposure experiments, instrumental, and kinetic analyses. To suppress the thermal rearrangement in polycyanurates, solution polymerization at a lower temperature was performed with activated *s*-triazine in the presence of a basic catalyst.

# ÖZET


## AKTİF *S*-TRİAZİNLER KULLANILARAK POLİMER SENTEZİ VE *S*-TRİAZİNLERİN TERMAL YER DEĞİŞTİRMESİNİN İNCELENMESİ

Polisiyanüratlar son derece dikkate değer uygulama potansiyeline sahiptir ve derinlemesine araştırılmalıdır. Bu çalışma, eriyik polikondenzasyon için yeni bir s-triazin monomerinin sentezine odaklanmıştır. Aktif s-triazin olarak adlandırılan bu monomer, ticari olarak temin edilebilen başlangıç maddelerinden iki adımda sentezlenmiştir. Aktif s-triazin, bazik bir katalizör eşliğinde ve düşürülmüş basınç altında bisfenol A ile polimerleştirilmiştir. İlk polimerleşmelerde gözlenen termal yer değiştirme, daha sonra ayrıntılı olarak incelenmiştir. s-Triazinlerin termal yer değiştirme reaksiyonu, termal maruziyet deneyleri, enstrümantal analizler ve kinetik çalışmalar aracılığıyla araştırılmıştır. Polisiyanüratlarda bu yer değiştirmeyi baskılamak amacıyla, bazik katalizör varlığında daha düşük sıcaklıkta çözelti polimerizasyonu uygulanmıştır.

# TABLE OF CONTENTS

ACKNOWLEDGEMENTS ..... IV

ABSTRACT ..... VI

ÖZET ..... VII

LIST OF FIGURES ..... X

LIST OF TABLES ..... XV

LIST OF SYMBOLS ..... XVI

LIST OF ACRONYMS/ABBREVIATIONS ..... XVII

1. INTRODUCTION ..... 1

1.1. s-Triazines ..... 1

1.1.1. Reactions of s-Triazines ..... 3

1.1.1.1. Nucleophilic Aromatic Substitution Reactions ..... 4

1.1.1.2. Transesterification-Type Reactions ..... 4

1.1.1.3. Polymerization Reactions ..... 5

1.1.1.4. Thermal Rearrangement ..... 7

1.2. Activated Carbonates ..... 14

2. AIM OF THE STUDY ..... 15

3. EXPERIMENTAL ..... 16

3.1. Materials ..... 16

3.2. Synthesis of *s*-Triazine Derivatives ..... 16

3.2.1. Synthesis of 4,6-Dichloro-2-methoxy-1,3,5-triazine (ST1) ..... 16

3.2.2. Synthesis of Methoxy-bis(methyl salicyl)-*s*-triazine (MMST) ..... 17

3.2.2.1. Procedure A ..... 17

3.2.2.2. Procedure B ..... 17

3.2.3. Synthesis of Methoxy-diphenoxy-*s*-triazine (MPhT) ..... 18
3.2.4. Synthesis of Triphenoxy-*s*-triazine (TPT) ..... 18
3.2.5. Synthesis of Trimequinol-*s*-triazine (TMT) ..... 19
3.2.6. Synthesis of Methoxy-dimequinol-*s*-triazine (MDMT) ..... 19
3.3. Melt Polymerization Reactions ..... 20
3.4. Solution Polymerization Reactions ..... 21
3.5. Thermal Exposure Experiments ..... 21
3.6. Kinetic and Thermal Analysis ..... 21
3.7. Measurements ..... 22
4. RESULTS AND DISCUSSION ..... 23
4.1. Synthesis of Activated *s*-Triazines ..... 23
4.2. Melt Polymerization of Activated *s*-Triazines ..... 25
4.3. Thermal Rearrangement ..... 31
4.3.1. Alkyl Rearrangement ..... 32
4.3.2. Kinetic and Thermodynamic Study ..... 37
4.3.3. Solution Polymerization ..... 40
4.3.4. Aryl Shift ..... 43
5. CONCLUSION ..... 48
6. FUTURE WORK ..... 49
REFERENCES ..... 50
APPENDIX A: SUPPLEMENTARY DATA ..... 56
APPENDIX B: COPYRIGHT LICENCES ..... 74

# LIST OF FIGURES

Figure 1.1. Well-known derivatives of *s*-triazines [2]. ..... 1

Figure 1.2. Trimerization reactions of cyanates to cyanurates (top) and isocyanates to isocyanurates (bottom) [10], [11]. ..... 2

Figure 1.3. Structure of cyanurate (left) and isocyanurate (right), highlighting their key structural differences. ..... 3

Figure 1.4. Stepwise substitution of CC [5]. ..... 4

Figure 1.5. The transesterification reaction mechanism for cyanurate, replacing its alcohol substituent with another [17]. ..... 5

Figure 1.6. Interfacial polymerization of dichloro-*s*-triazines. Redrawn and adapted from Ref [22]. ..... 6

Figure 1.7 Synthesis of polycyanurates from amino-*s*-triazine compounds by dephenoxylation [28]. ..... 7

Figure 1.8. Thermal rearrangement of cyanurates [10]. ..... 7

Figure 1.9. Rearrangement of dimethoxy-aniline-*s*-triazine *via* pTSOH catalyst [31]. ..... 8

Figure 1.10. Disproven homolytic mechanism of thermal rearrangement. ..... 9

Figure 1.11. Proposed mechanism of the first rearrangement in trimethoxy-*s*-triazine [33]. ..... 9

Figure 1.12. Exchange of Methyl Cations with $H^+$ in the Presence of Molten Acid. Redrawn and adapted from Ref [33]. ..... 10

Figure 1.13. DSC Thermograms of several dialkoxy-amino-*s*-triazines. Redrawn and adapted from Ref [36]. ..... 11

Figure 1.14. Alkaline hydrolysis of cyanurates (top) and isocyanurates (bottom) [11]. ..... 11

Figure 1.15. Alcohol to alkylamine synthesis from the work of Harrington and co-workers. Redrawn and adapted from Ref [37]. ..... 12

Figure 1.16. Model compound from the work of Saito and colleagues. Redrawn and adapted from Ref [39]..... 13

Figure 1.17. DSC thermograms of two polycyanurate examples from Saito and co-workers. Used as it is from Ref [39]..... 13

Figure 1.18. Solution polymerization of BMSC with BPA [45]. ..... 14

Figure 2.1. Targeted polycondensation reaction of activated *s*-triazine monomer and BPA..... 15

Figure 4.1. Synthetic pathway for the synthesis of polycyanurates..... 23

Figure 4.2. Synthesis of ST1 from CC..... 24

Figure 4.3. Procedure A-B for the synthesis of MMST monomer. ..... 24

Figure 4.4. Targeted polycondensation reaction of MMST and BPA. ..... 25

Figure 4.5. LiOMe Catalyzed targeted polymerization of MMST and BPA. ..... 26

Figure 4.6. Temperature, pressure, and torque values recorded for P1. ..... 26

Figure 4.7. Temperature, pressure, and torque values recorded for P2. ..... 27

Figure 4.8. The $^{1}$H-NMR spectrum shows the shift of the methyl signal from MMST to the possible repeating unit structure of the P1..... 29

Figure 4.9. $^{1}$H-NMR spectrum of P1. ..... 29

Figure 4.10. $^{1}$H-NMR spectra of polymerization P2 at the second and third hours. ..... 30

Figure 4.11. $^{1}$H-NMR spectrum of P2. ..... 31

Figure 4.12. The possible thermal rearrangement of MMST. ..... 32

Figure 4.13. Photos of the heating experiment of MMST and TLC Plate (Mobile Phase Hexane: EtOAc) .....32

Figure 4.14. FTIR spectra of MMST and heated MMST samples. .....33

Figure 4.15. The 1H-NMR spectra of MMST and 10 min/30 min thermal exposure. $^{15}N$-$^{1}H$ HMBC correlations highlighted.....34

Figure 4.16. Comparison of $^{15}N$-$^{1}H$ HMBC invisible (left) and visible (right) structures. .35

Figure 4.17. $^{1}H$-NMR (A) and $^{13}C$-NMR (B) spectra of MPhT before and after rearrangement. .....36

Figure 4.18. DSC thermogram of MPhT at 3 °C $min^{-1}$ heating rate. .....37

Figure 4.19. Close-up of normalized, DSC exotherms of MPhT (a) and MMST (b) in different heating rates. .....38

Figure 4.20. DSC Graph of MMST (a) with different heating rates 3, 5, 7 °C °C/min and Kissinger Kinetic Analysis Plot (b). .....39

Figure 4.21. Solution polymerization scheme of MMST with BPA in o-DCB.....40

Figure 4.22. $^{1}H$-NMR (A) and $^{13}C$-NMR (B) spectra of SP. .....41

Figure 4.23. $^{1}H$-NMR spectra of pristine SP (red) and thermally rearranged SP (blue). ....42

Figure 4.24. Close-up of normalized, DSC exotherms of SP in different heating rates. .....43

Figure 4.25. Synthesis and thermal rearrangement of the model compound from the work of Tsuchiya and co-workers. Used as it is from Ref [39].....44

Figure 4.26. Possible structures of repeating units where no aryl shift (a), semi-aryl shift (b), and complete aryl shift (c) occur. .....44

Figure 4.27. FTIR spectra of TPT, heated TPT samples at 15, 45, and 90 minutes (from top to bottom). .....45

Figure 4.28. FTIR spectra of TMT and heated TMT samples at 30 and 60 minutes (from top to bottom). ..... 46

Figure 4.29. $^{13}$C-NMR spectrum of the rearranged MDMT. ..... 47

Figure A.1. $^{1}$H-NMR spectrum of MMST. ..... 56

Figure A.2. $^{13}$C-NMR spectrum of MMST. ..... 56

Figure A.3. $^{1}$H-NMR spectrum of MPhT. ..... 57

Figure A.4. $^{13}$C-NMR spectrum of MPhT. ..... 57

Figure A.5. $^{1}$H-NMR spectrum of TPT. ..... 58

Figure A.6. $^{13}$C-NMR spectrum of TPT. ..... 58

Figure A.7. $^{1}$H-NMR spectrum of TMT. ..... 59

Figure A.8. $^{13}$C-NMR spectrum of TMT. ..... 59

Figure A.9. $^{1}$H-NMR spectrum of MDMT. ..... 60

Figure A.10. $^{13}$C-NMR spectrum of MDMT. ..... 60

Figure A.11. $^{1}$H-NMR spectrum of P1. ..... 61

Figure A.12. $^{13}$C-NMR spectrum of P1. ..... 61

Figure A.13. $^{15}$N-$^{1}$H HMBC NMR spectrum of P1. ..... 62

Figure A.14. $^{1}$H-NMR spectrum of P2. ..... 62

Figure A.15. $^{13}$C-NMR spectrum of P2. ..... 63

Figure A.16. $^{15}$N-$^{1}$H HMBC NMR spectrum of P2. ..... 63

Figure A.17. $^{1}$H-$^{13}$C HSQC NMR spectrum of P2. ..... 64

Figure A.18. $^{1}$H-NMR spectrum of SP. ..... 64

Figure A.19. $^{13}$C-NMR spectrum of SP. ..... 65

Figure A.20. $^{1}$H-NMR spectrum of thermally rearranged SP ..... 65

Figure A.21. $^{13}$C-NMR spectrum of thermally rearranged SP. ..... 66

Figure A.22. $^{15}$N-$^{1}$H HMBC NMR spectrum of thermally rearranged SP. ..... 66

Figure A.23. FTIR spectrum of ST. ..... 67

Figure A.24. FTIR spectrum of MMST. ..... 67

Figure A.25. FTIR spectrum of P1. ..... 68

Figure A.26. FTIR spectrum of P2. ..... 68

Figure A.27. FTIR spectrum of MMST heated for 10 minutes at 240 °C. ..... 69

Figure A.28. FTIR spectrum of MMST heated for 30 minutes at 240 °C. ..... 69

Figure A.29. FTIR spectrum of MMST heated for 45 minutes at 240 °C. ..... 70

Figure A.30. FTIR spectrum of MPhT. ..... 70

Figure A.31. FTIR spectrum of TPT. ..... 71

Figure A.32. FTIR spectrum of TPT heated for 90 minutes. ..... 71

Figure A.33. FTIR spectrum of TMT. ..... 72

Figure A.34. FTIR spectrum of TMT heated for 60 minutes. ..... 72

Figure A.35. FTIR spectrum of SP. ..... 73

Figure B.1. Copyright of Figure 1.6. ..... 75

Figure B.2. Copyright of Figure 1.12. ..... 76

Figure B.3 Copyright of Figure 1.6 and Figure 4.25. ..... 77

# LIST OF TABLES

Table 1. Synthesis ratios, SEC, and DSC results of polymers P1 and P2. .....28

Table 2. $T_p$'s of exotherms, activation energies, regression of linear fit, and enthalpies of MPhT and MMST. .....39

# LIST OF SYMBOLS

| | |
|---|---|
| $M_n$ | Number-average molar mass (kDa) |
| Mw | Weight-average molar mass (kDa) |
| Tg | Glass-transition temperature (°C) |
| Tp | Peak temperature (°C) |
| | |
| β | Heating Rate (°C $min^{-1}$) |
| ΔH | Enthalpy change of rearrangement (kJ $mol^{-1}$) |

# LIST OF ACRONYMS/ABBREVIATIONS

| | |
|---|---|
| BMSC | Bis-methyl-salicylate carbonate |
| BPA | Bisphenol A |
| CC | Cyanuric chloride |
| DCM | Dichloromethane |
| DMF | Dimethylformamide |
| DSC | Differential scanning calorimetry |
| FTIR | Fourier-transform infrared spectroscopy |
| GPC | Gel-permeation chromatography |
| HMBC | Heteronuclear multiple-bond correlation |
| HSQC | Heteronuclear single-quantum coherence |
| IPA | Isopropyl alcohol |
| MDMT | Methoxy-dimequinol-*s*-triazine |
| MMST | Methoxy-bis(methyl salicyl)-*s*-triazine |
| MPhT | Methoxy-diphenoxy-*s*-triazine |
| NMP | N-Methyl-2-pyrrolidone |
| NMR | Nuclear magnetic resonance |
| o-DCB | Ortho-dichlorobenzene |
| SEC | Size-exclusion chromatography |
| TBAB | Tetrabutyl-ammonium bromide |
| THF | Tetrahydrofuran |
| TLC | Thin-layer chromatography |
| TMT | Trimequinol-*s*-triazine |
| TPT | Triphenoxy-*s*-triazine |
| UV | Ultraviolet |

# 1. INTRODUCTION

## 1.1. s-Triazines

Triazines are notable members of heterocyclic compounds with three nitrogens in a six-membered ring. Among *vic*-triazine (1,2,3-triazine), *as*-triazine (1,2,4-triazine), and *s*-triazine (1,3,5-triazine), the latter is the most widely used one [1]. The symmetric nature of *s*-triazine grants its aromaticity *via* the delocalisation of π-orbitals. The electron-withdrawing effect of nitrogens distributed in the *s*-triazine ring intensifies its susceptibility to nucleophilic attacks. The key attribute of *s*-triazines is the control over their degree of substitution, unlocking possibilities for various applications.

Well-known derivatives of *s*-triazines can be prepared *via* nucleophilic and electrophilic substitutions and hydrolysis. These well-known derivatives are cyanuric acid, cyanurate, melamine, isocyanurate, and cyanuric chloride (CC) (Figure 1.1) [2].

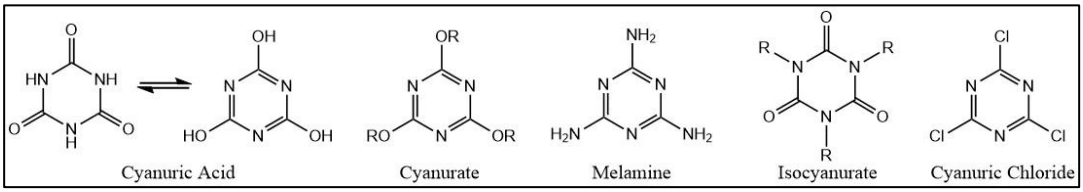



Figure 1.1. Well-known derivatives of *s*-triazines [2].

A vast variety of *s*-triazine derivatives are commercially available. Versatile tailoring in *s*-triazine design enables many derivatives to be used in various applications such as thermal stabilizers, UV stabilizers, pesticides, surface active agents, dyestuffs, and therapeutic agents [1].

The most critical derivative and a building block for a wide range of *s*-triazine derivatives is 2,4,6-trichloro-1,3,5-triazine, commonly named as cyanuric chloride (CC). Cyanuric chloride can undergo controlled nucleophilic aromatic substitution reactions, which makes it valuable for designing *s*-triazines with different substitutions [3], [4]. Along with its functional strengths, cyanuric chloride owes its prevalence to its affordability. Cyanuric chloride is used in many organic syntheses due to the reactivity of its chloride-bearing carbon toward nucleophiles [5]. CC is regarded as an acid chloride analogue [6]. Similarly, cyanurates can be referred to as ester analogues [7].

Cyanurates are *s*-triazine cores with three alkoxy substitutions (Figure 1.2). They are usually synthesized from cyanuric chloride and alcohols through nucleophilic aromatic substitution reactions. Trimerization of cyanates is further exploited in cyanurate synthesis, mainly for the formation of cyanate ester resins. Their chemical and thermal strength is leveraged for high-performance resins and thermosetting systems [8]. Apart from polymer structures, small molecules of cyanurates can be found in many industries. Some cyanurates are shown to rearrange wholly and partially to their isocyanurate counterparts at elevated temperatures.

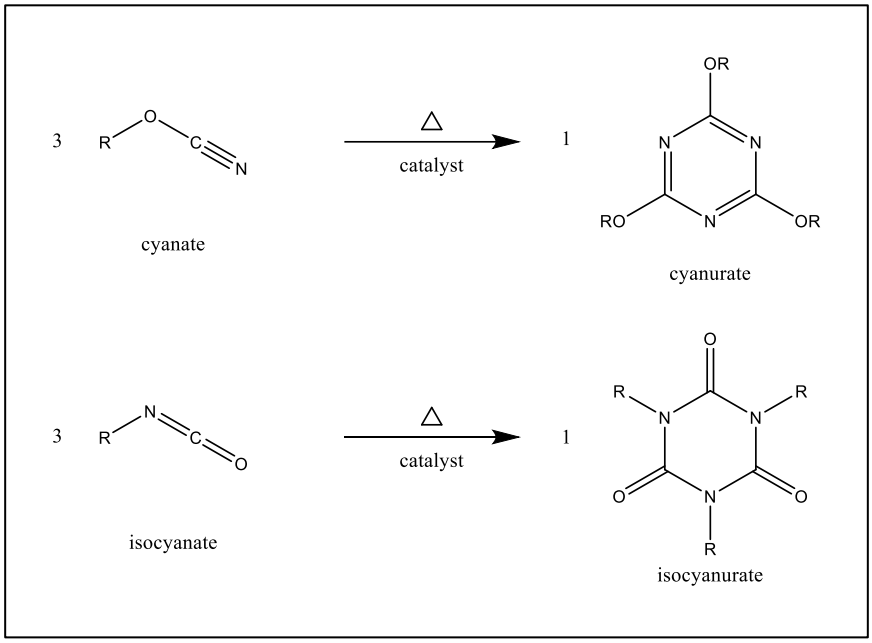



Figure 1.2. Trimerization reactions of cyanates to cyanurates (top) and isocyanates to isocyanurates (bottom) [9].

Even though isocyanurates are regarded as *s*-triazine derivatives, their core structure and atom connectivity differ. Isocyanurates resemble more of a fused N-substituted ureas. In contrast, *s*-triazines have a six-membered benzene-like heterocyclic core (Figure 1.3).

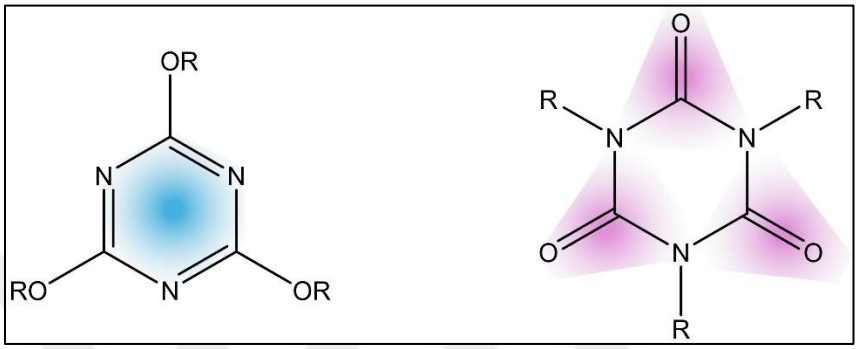



Figure 1.3. Structure of cyanurate (left) and isocyanurate (right), highlighting their key structural differences.

This difference in atom connectivity further lessens the aromatic behaviour [10]. Isocyanurates are used in many industries, including coating, textiles, and plastics. A notable example of an isocyanurate is triglycidyl isocyanurate (TGIC). TGIC is used as a crosslinker in powder coating formulations [11]. Their robust chemical and thermal stabilities make them excellent candidates for insulation materials—for example, polyisocyanurate (PIR) foams are used in rigid insulations. Isocyanurates are used in polyurethane chemistry and poly(urethane-isocyanurate) networks to enhance polyurethane's mechanical and thermal properties [12].

### 1.1.1. Reactions of s-Triazines

The electron-deficient and heterocyclic nature of *s*-triazines gives rise to various reactions. *s*-Triazines are used as reactants and reagents in diverse syntheses such as chlorination, reduction, and cycloaddition reactions [2], [5]. The following chapter will focus on four relevant reaction types.

1.1.1.1. Nucleophilic Aromatic Substitution Reactions. Nucleophilic aromatic substitution reaction is a fundamental reaction of cyanuric chloride, allowing the design of cyanurates with different substituents. The most crucial feature of CC is that its substitution reaction can be controlled *via* temperature. This ability of stepwise substitution yields *mono- di- tri-* substituted *s*-triazines with various substitutions. Effective reactivity is provided by the electron-withdrawing and easy displacement of chloride atoms, which allow nucleophiles such as amines and alcohols to react easily. Several parameters affect the substitution rate, such as the reactant's nucleophilicity, the CC's solubility, and the medium's temperature. Experimental studies have shown a generalized trend between temperature and the number of substitutions. For the first substitution, the temperature is usually kept below 0 °C, the second is at room temperature, while the third requires 60 °C or more (Figure 1.4) [5]. This trend is explained by the loss of reactivity on cyanuric chloride due to increased π-orbital electron density after each reaction. The drop in the *s*-triazine ring's reactivity pushes the reaction temperature to higher degrees.

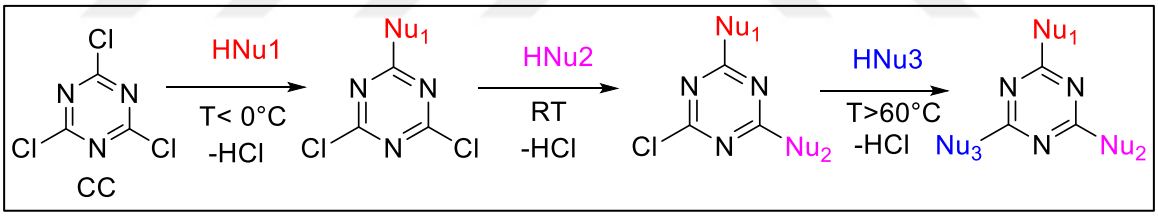



Figure 1.4. Stepwise substitution of CC [5].

Sequentially adding nucleophiles and tuning the degree of substitution paves the way for one-pot synthesis of cyanurate compounds [13].

1.1.1.2. Transesterification-Type Reactions. As stated before, cyanurates are analogous to esters. Just as esters can participate in transesterification reactions, cyanurates can undergo similar processes as well. In suitable conditions, alcohol will react with cyanurate to replace its aryloxy/alkoxy substituent (Figure 1.5). This transesterification-type reaction takes place when the nucleophilicity of the incoming alcohol is high enough to displace the pre-attached

substituent(s) of the cyanurate. Reaction is usually kept above 80 °C, and catalysts are employed [14], [15].

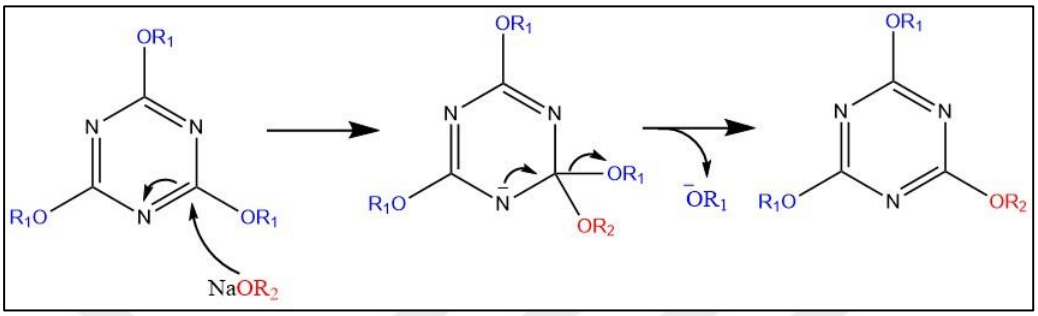



Figure 1.5. The transesterification reaction mechanism for cyanurate, replacing its alcohol substituent with another [14].

1.1.1.3. Polymerization Reactions. The first known examples of polycyanurates were synthesized from amino-*s*-triazines and dialkoxy-*s*-triazines in the 1950s [9]. Later, Bayer AG synthesized polymers containing *s*-triazines in their backbones *via* trimerization [16]. Radical polymerization from 2,4-dimethyl-6-vinyl-*s*-triazine is conducted to obtain linear polymers containing *s*-triazines [17]. Linear polycyanurates are mainly synthesized from dichloro-*s*-triazine monomers with different third substituents, using interfacial polymerization (Figure 1.6) [18]. Through nucleophilic aromatic substitution reactions, dichloro-*s*-triazines react with diols in a polycondensation fashion. The resulting HCl is scavenged with the help of a base. Preferred diols are aromatic diols such as resorcinol, BPA, and Bisphenol S (BPS) [19].

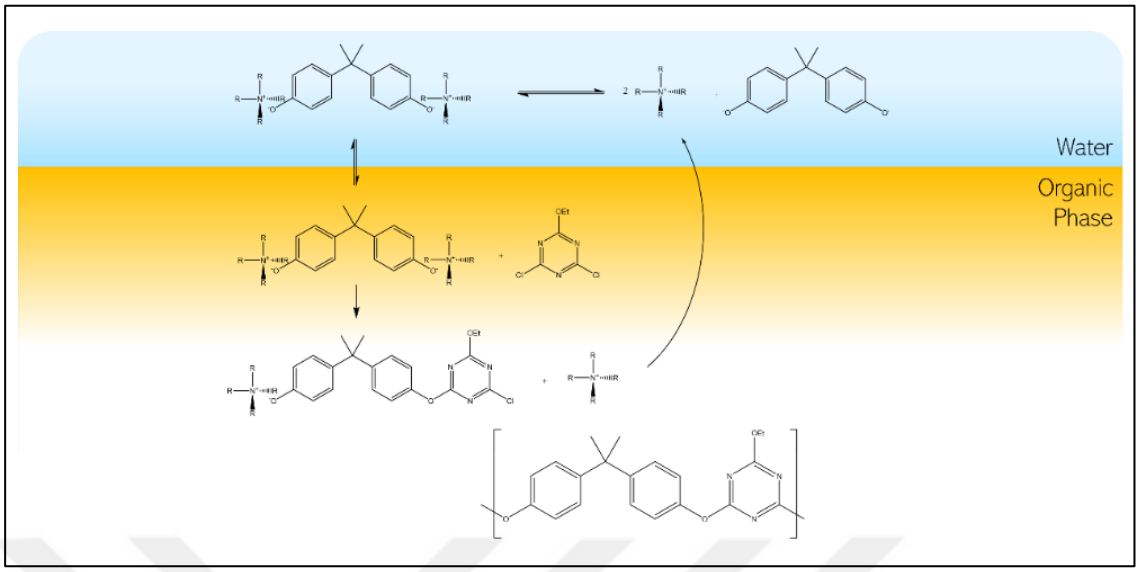



Figure 1.6. Interfacial polymerization of dichloro-*s*-triazines. Redrawn and adapted from Ref [18].

The solution polymerization of dichloro-*s*-triazine monomers is described in several patents [20], [21]. Aldalbahi and co-workers presented a solution polymerization alternative for flame retardant bishydrazino-*s*-triazine based polymers from *s*-triazine bishydrazino monomers [22].

The transesterification-type reaction of cyanurates gives a possibility of a polycondensation reaction [14], [23]. Nakamura and co-workers synthesized polycyanurates from amino-*s*-triazine compounds containing phenol leaving groups through melt polymerization (Figure 1.7). In this reaction, diols such as Bisphenol A (BPA) engage with the *s*-triazine monomer via a transesterification mechanism. The release of phenolic byproducts facilitates the progression of the polymerization process [24].

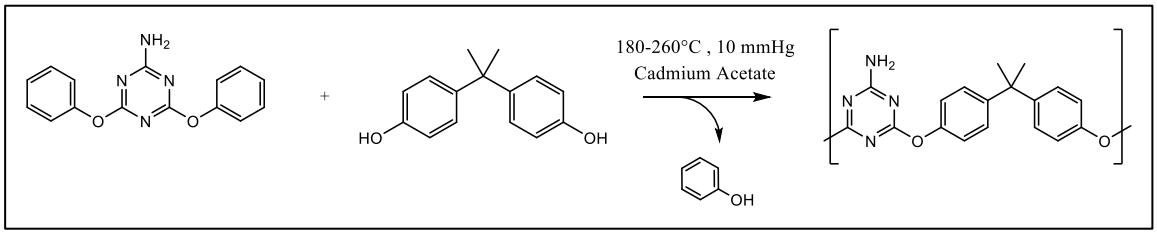



Figure 1.7 Synthesis of polycyanurates from amino-*s*-triazine compounds by dephenoxylation [24].

1.1.1.4. Thermal Rearrangement. The thermal rearrangement of cyanurates into isocyanurates was first identified by Hofman and Olshausen in 1870 [25] (Figure 1.8). Evidence for this isomerisation process has emerged from heating experiments with s-triazine compounds, which showed significant changes in reactivity, especially related to their melting points. Klason's 1885 study focused on the reactivity of cyanurates with silver salts and bases and their hydrolysis, including thiocyanurates [26]. It was suggested that heating causes changes in atomic connections, leading to the formation of constitutional isomers.

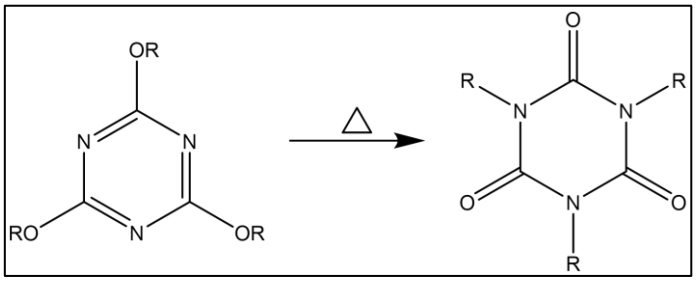



Figure 1.8. Thermal rearrangement of cyanurates [9].

Smolin and colleagues reported that trimethyl cyanurate boils at 265 °C, accompanied by some slight decomposition. However, conversion to trimethyl isocyanurate occurs when heated under reflux, resulting in a boiling point increase to 274 °C [9].

An isomerisation reaction with methyl iodide has been observed, suggesting the presence of a cationic pathway. Amyl and aryl triesters of these isocyanurates have not been observed to form their s-triazine analogues [9]. Substituents on the cyanurates can alter the ring activity, affecting the rearrangement temperature. A study on 2,4-dialkoxy-6-amino-*s*-triazines showed that it is possible to obtain rearranged and semi-rearranged s-triazine moieties by prolonged heating at milder temperatures (Figure 1.9) [27]. Moreover, the same study showed that an acidic catalyst, such as pTSOH, accelerated the rearrangement. Similarly, another research study states that the alkaline treatment produces rearranged intermediates during hydrolysis [9]. To date, literature limits thermal rearrangement to neutral or acidic conditions. However, we have encountered a clean thermal rearrangement during our base-catalyzed polymerization with no sign of hydrolysis. Related findings will be presented in the Results and Discussion. Additionally, the literature has reported that the solvent is among many variables influencing the activation energy for the isomerization [28].

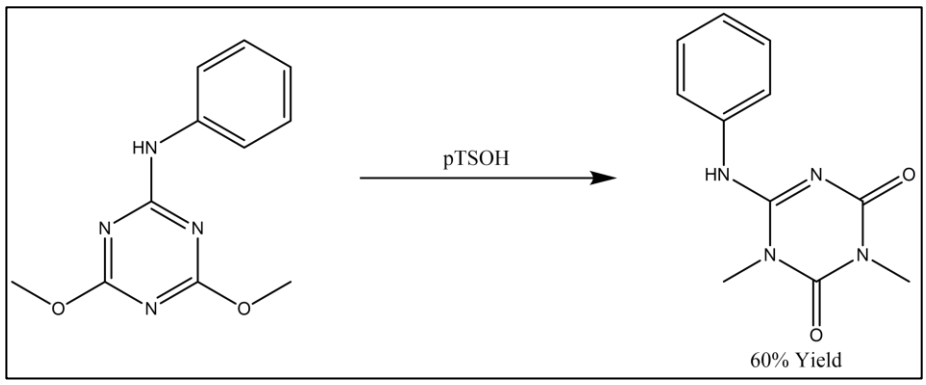



Figure 1.9. Rearrangement of dimethoxy-aniline-*s*-triazine *via* pTSOH catalyst [27].

Paoloni conducted a more comprehensive mechanistic study. Firstly, the radical pathway was ruled out due to the absence of methyl radicals and side products (Figure 1.10).

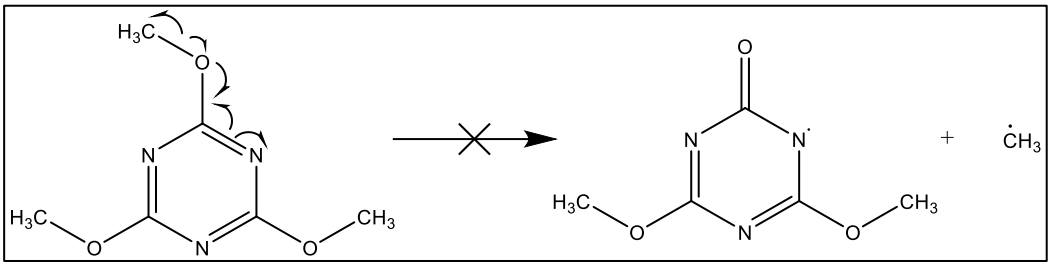


Figure 1.10. Disproven homolytic mechanism of thermal rearrangement.

Paoloni and his friends focused on the methyl ester of cyanuric acid, the isomerisation of trimethoxy-s-triazine to N,N,N-methyl isocyanurate [29]. Isotopic studies used O-18 and D-2 atoms, forming isocyanurate analogues with different masses. Hybrid masses were formed when these *s*-triazines were mixed and heated, which is only possible through intermolecular reactions. A reverse reaction could not be observed, meaning that trimethoxy-*s*-triazines rearrange to form stable isocyanurate analogues. The kinetic study indicated an activation energy of 28.3 ± 0.8 kcal/mol. The proposed mechanism of the stated trimethoxy-*s*-triazine involves the dissociation of the molecule to form $Me^+$ and an anion from the molecule, and a shift onto neighbouring molecules along the mean free path. Neighbouring molecules then likewise dissociate to yield $Me^+$. Overall, methyl groups on cyanurates' oxygens migrate to nitrogens, forming methyl isocyanurate (Figure 1.11).

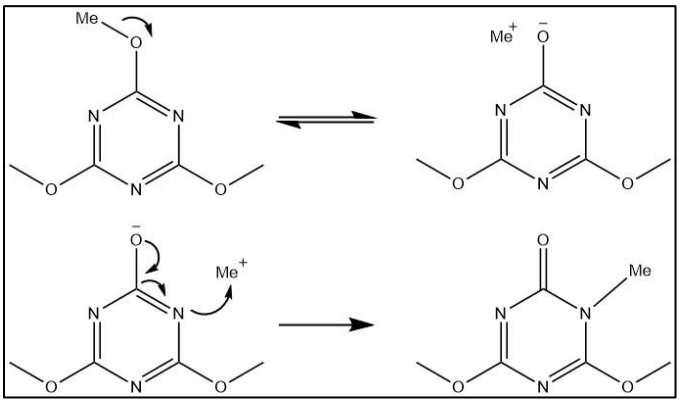


Figure 1.11. Proposed mechanism of the first rearrangement in trimethoxy-*s*-triazine [29].

Mechanical claim of the attack of $Me^+$ is further reinforced by the exchange of $Me^+$ to $H^+$ in molten acid (Figure 1.12). An attack will be easier since $H^+$ has a longer mean free path. It is important to note that these thermal isomerisation experiments were conducted in a neutral environment, allowing the so-called double-ionic pathway [30].

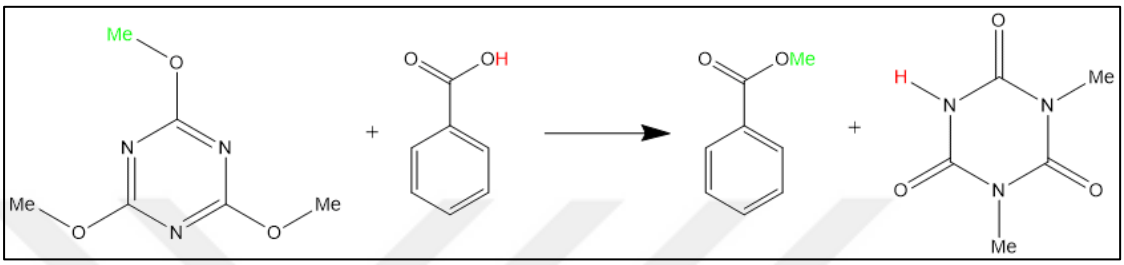



Figure 1.12. Exchange of Methyl Cations with $H^+$ in the Presence of Molten Acid. Redrawn and adapted from Ref [29].

It is important to note that the rearrangement of cyanurates is not limited to methyl cyanurates. 4,6-diethoxy-2-(phenylamino)-1,3,5-triazine is reported to rearrange at 255 °C, 70 °C higher than its methyl counterpart [30]. This increase in reaction temperature is compatible with the mean free path explanation

During thermal isomerisation, the breaking and forming of bonds suggests a change in enthalpy [31]. This change in enthalpy was first measured using differential scanning calorimetry (DSC) (Figure 1.13). The thermal behavior of different cyanurates, as well as that of dialkoxy amino *s*-triazines, were investigated [32]. Exotherms visible in DSC thermograms enabled the calculation of a given molecule's enthalpy change and rearrangement temperature [30]. Similar DSC thermograms were conducted to analyze thermal rearrangements in the present research as well. Resulting exotherms are dissected to gather information on the activation energy. Method and DSC thermograms are discussed in Section 4.

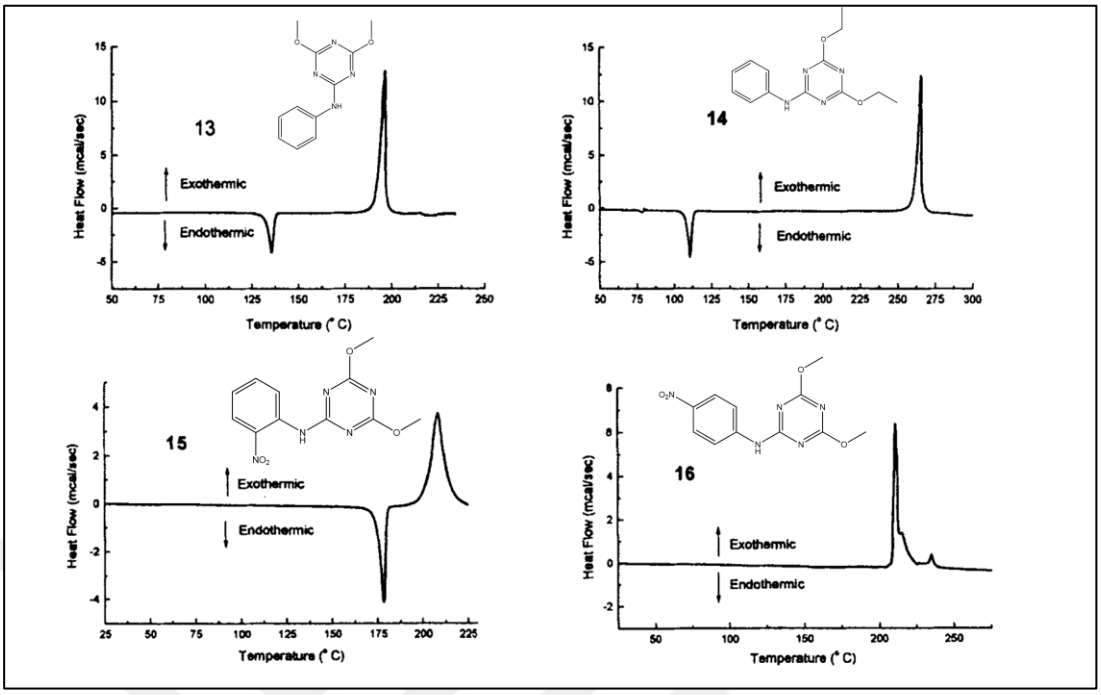



Figure 1.13. DSC Thermograms of several dialkoxy-amino-*s*-triazines. Redrawn and adapted from Ref [32].

The thermal rearrangement of *s*-triazines was also employed as a synthetic approach. Alkyl amine and carbon dioxide are produced during the alkaline hydrolysis of isocyanurates, where cyanuric acid and alcohol are the products resulting from the alkaline hydrolysis of cyanurates [9].

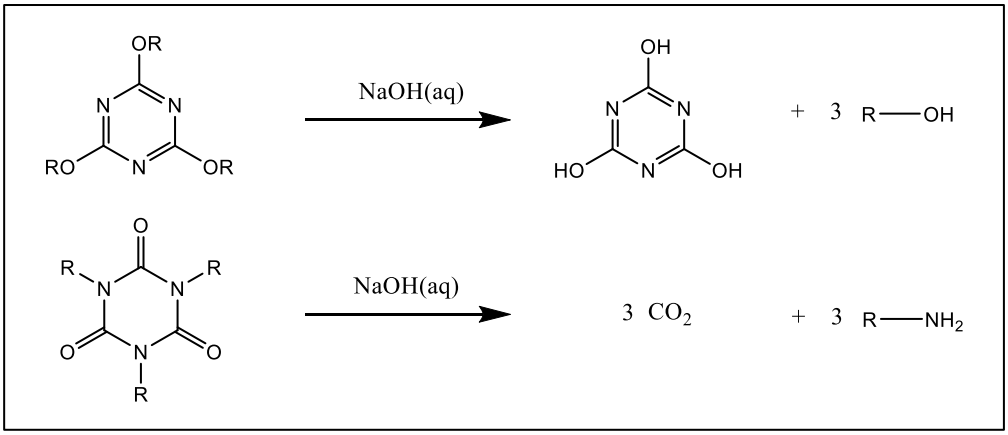



Figure 1.14. Alkaline hydrolysis of cyanurates (top) and isocyanurates (bottom) [9].

The alkaline hydrolysis product of isocyanurates serves as the basis for amine synthesis, enabling the exploitation of this process. Harrington and co-workers were the first to use the rearrangement to obtain an amine (Figure 1.15) [33]. 2-(2-Thienyl)ethylamine was synthesized from its alcohol counterpart. 2-(2-Thienyl)ethanol first reacts with cyanuric chloride to form a cyanurate, then is rearranged to its isocyanurate. The resulting isocyanurate is hydrolyzed to yield 2-(2-thienyl)ethylamine and carbon dioxide, offering a functional approach to alcohol-to-amine synthesis.

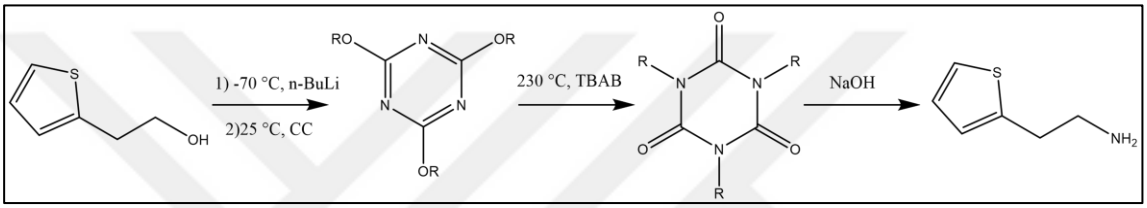



Figure 1.15. Alcohol to alkylamine synthesis from the work of Harrington and co-workers. Redrawn and adapted from Ref [33].

As expected, rearranging relatively long alkyl chains is more challenging and requires higher temperatures. To overcome this challenge, Harrington and others used quaternary ammonium and phosphonium bromides, which are favorable catalysts for rearrangement compared to alkyl iodides. Tetrabutylammonium bromide (TBAB) for example is used to lower the temperature of rearrangement by more than 100 °C. TBAB later became a widely used catalyst for cyanurate rearrangements [40 - 43].

Despite older studies assert that aryl cyanurates cannot undergo such rearrangements, recent literature contains several examples. It is noted that aryl rearrangements in cyanurates follow a Chapman Rearrangement type of intramolecular rearrangement. Chapman Rearrangement is a special case of rearranging aryl N-arylbenzimidates to N-aroyldiphenylamines [38]. Saito and co-workers claimed that rearrangement is a potential tool to alter the characteristics of a polymer and suggested a model study to track the changes during the rearrangement [35] (Figure 1.16).

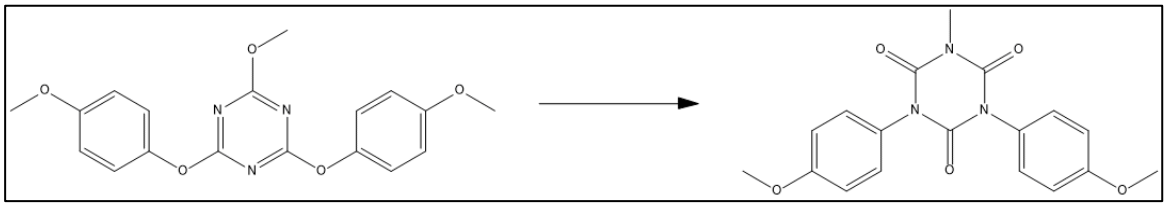


Figure 1.16. Model compound from the work of Saito and colleagues. Redrawn and adapted from Ref [35].

Accordingly 2-methoxy-4,6-bis(4-methoxyphenoxy)-1,3,5-triazine was heated in neutral media with 2% TBAB. The $^{1}$H-NMR spectrum indicated a rearrangement to the isocyanurate form. Later, methoxy-capped polycyanurates of aromatic diols were synthesized, and polymers were rearranged to their corresponding polyisocyanurates with the help of TBAB. When these polymers were subjected to thermal analysis *via* DSC, they exhibited an exotherm (Figure 1.17) [36], [39].

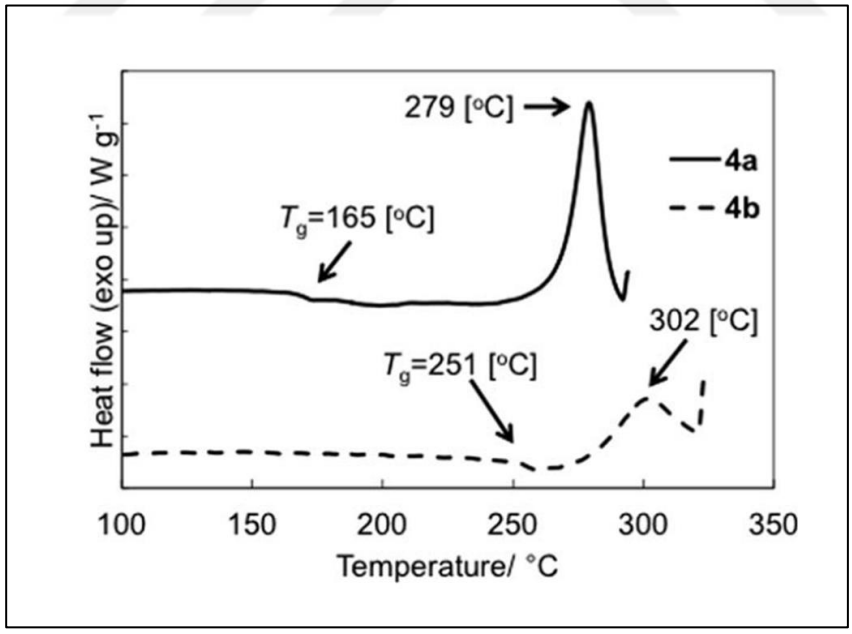



Figure 1.17. DSC thermograms of two polycyanurate examples from Saito and co-workers. Used as it is from Ref [35].

## 1.2. Activated Carbonates

Carbonates that contain methyl salicylate moieties as a leaving group, bis-methyl-salicyl carbonate (BMSC), are named activated carbonates. BMSC is named activated because the carbonyl in BMSC is 100 times more electrophilic than diphenyl carbonate under similar conditions. Apart from the reactivity advantage of BMSC, leaving group methyl salicylate forms an intermolecular H-bonding to create a stable byproduct, which prevents chain scission. This advantage of BMSC makes it a valuable candidate for polycarbonate synthesis. High reactivity lowers the temperature for the melt polymerisation to polycarbonates. The mild byproduct, methyl salicylate, is removed after the melt polycondensation involving Bisphenol A (BPA) [40]. The solution polymerization of BMSC with BPA is shown below.

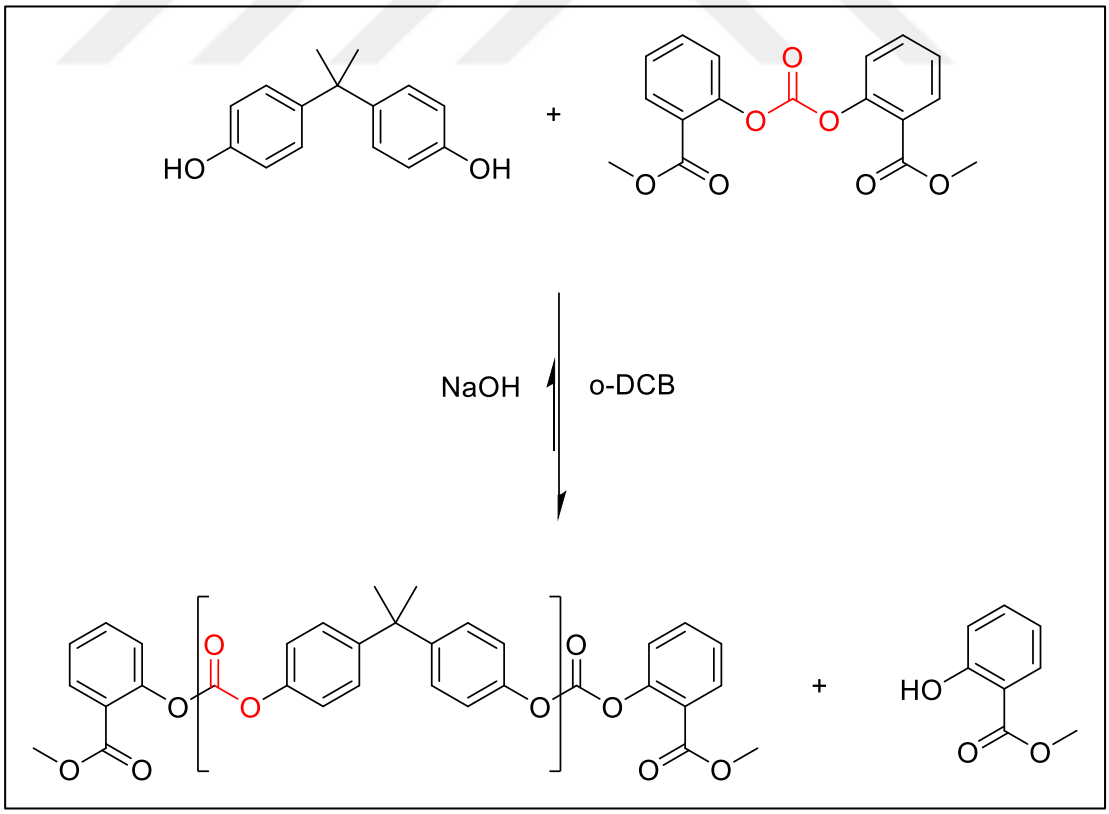



Figure 1.18. Solution polymerization of BMSC with BPA [41].

# 2. AIM OF THE STUDY

The potential applications of polycyanurates are substantial and worth thorough exploration. Inspired by the synthesis of polycarbonates from activated carbonates, a similar activated *s*-triazine monomer was targeted. Melt-polycondensation can be facilitated by an activated s-triazine monomer that contains a methyl salicylate leaving group. Polymerization of activated *s*-triazine monomers and bisphenol A (BPA) was conducted with the help of a basic catalyst, while byproduct methyl salicylate was removed under reduced pressure.

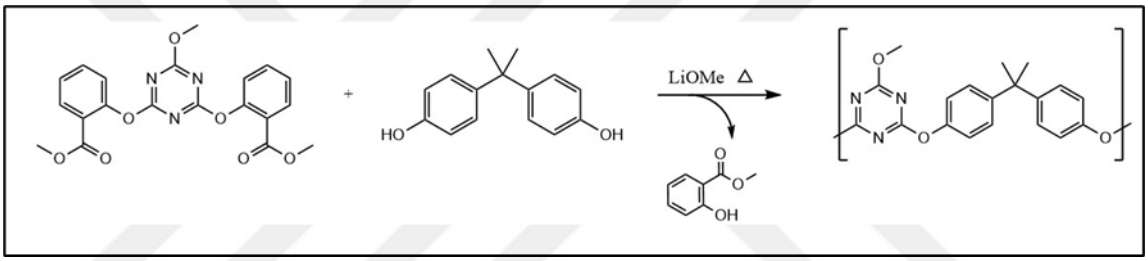



Figure 2.1. Targeted polycondensation reaction of activated *s*-triazine monomer and BPA.

During our initial experiments, we noticed unexpected behavior that was thought to be related to the rearrangement of cyanurate. Consequently, an investigation was carried out into the nature and the extent of the rearrangement through model compounds, instrumental analyses, and kinetic studies.

# 3. EXPERIMENTAL

## 3.1. Materials

Cyanuric Chloride (99%, Sigma-Aldrich), phenol (99%, Merck), BPA (> 99%, TCI), NaOH (Merck), $NaHCO_3$ (Merck), Dichloromethane (99%, analytical grade, Merck), Chloroform-d (99.8%, Sigma Aldrich), THF (99%, analytical grade, Merck & HPLC-isocratic grade, Carlo Erba), MeOH (> 99%, VWR Chemicals), MeOH (90%, Technical Grade), HCl (%37 fuming, Merck) and TLC (Merck), 4-methoxyphenol (99% Sigma-Aldrich), TBAB (99%, Acros Organics), Methyl salicylate (>98%, Sigma-Aldrich), NaH (60 % dispersion in mineral oil, Sigma-Aldrich), $Na_2SO_4$ (anhydrous, Merck), Hexane (Merck), IPA (Merck), o-DCB (99%, Merck), LiOMe (>99%, TCI) were used as received. NMP (Sigma-Aldrich), DMF (Merck) were stored under activated 4 Å molecular sieves (baked at 300 °C, ≥ 3 h) for at least 24 h prior to use.

## 3.2. Synthesis of *s*-Triazine Derivatives

### 3.2.1. Synthesis of 4,6-Dichloro-2-methoxy-1,3,5-triazine (ST1)

An excess amount of methanol (10 mL for every 1 g of cyanuric chloride) was placed in an ice-salt bath at approximately -5 °C. Then, one equivalent of cyanuric chloride (CC) was gradually added to the solution. Next, one equivalent of $NaHCO_3$ was added in portions. The reaction mixture was stirred for about one hour until the consumption of CC was completed. The completion of the reaction was confirmed using TLC. Following this, the mixture was washed with water, and the resulting solution was extracted twice with dichloromethane (DCM). The DCM phase was dried using anhydrous sodium sulfate (Na2SO4) and then filtered. The clear solution was evaporated in a rotary evaporator,

resulting in the formation of white crystals. The yield ranged from 79% to 83%. $^{1}$H NMR (400 MHz, CDCl3) δ 4.07 (s, 1H). $^{13}$C NMR (101 MHz, CDCl3) δ 172.72, 171.65, 57.10.

### 3.2.2. Synthesis of Methoxy-bis(methyl salicyl)-*s*-triazine (MMST)

3.2.2.1. Procedure A. In a 100 mL 3-neck round-bottom flask (RBF), 2.10 equivalents of NaH (60% disp.) were weighed and washed three times with hexane. Next, 2.10 equivalents of methyl salicylate were dissolved in dry NMP and added to the RBF drop by drop under a nitrogen atmosphere. Once the addition was complete, the temperature was set to 80 °C, and 1 equivalent of the ST1 solution in dry NMP was added to the flask. The progress of the reaction was monitored using TLC. After 3 hours, the reaction was considered complete.

The reaction mixture was then poured into 100 mL of ice-cold water containing a few drops of HCl. The resulting precipitate was dissolved in DCM. The DCM solution was washed with NaOH, HCl, water, and brine. The organic phase was dried over $Na_2SO_4$ and then filtered. The clear solution was concentrated using a rotary evaporator, yielding a yellowish viscous liquid. This liquid was subsequently dissolved in THF and precipitated in ice-water. The final yield was found to be 54%. The melting point was found to be 125 °C by DSC analysis. $^{1}$H NMR (400 MHz, CDCl3) δ 7.99 (d, J = 9.0 Hz, 2H), 7.55 (t, J = 7.7 Hz, 2H), 7.31 (t, J = 7.6 Hz, 2H), 7.17 (d, J = 8.1 Hz, 2H), 3.91 (s, 3H), 3.77 (s, 6H). $^{13}$C NMR (101 MHz, CDCl3) δ 173.98, 173.81, 164.93, 151.34, 134.10, 131.99, 126.33, 123.61, 123.38, 55.69, 52.31.

3.2.2.2. Procedure B. Sodium salt of methyl salicylate (NaMS) was freshly prepared for each reaction. Methyl salicylate was dissolved in isopropyl alcohol (IPA) and precipitated in a 5% aqueous sodium hydroxide solution. The resulting precipitate was filtered, washed with hexane, and dried using a rotary evaporator.

2.4 equivalents of NaMS were dissolved in DMF. To this solution, one equivalent of ST1 was added dropwise under a nitrogen atmosphere. The reaction mixture was then heated

to 45 °C, and the progress of the reaction was monitored using TLC. Once the reaction was complete, the work-up procedure was performed as described in Procedure A (Section 3.2.2.1). The final product obtained was white solids with a yield of 37%, and the melting point, determined by DSC analysis, was found to be 125 °C.$^{1}$H NMR (400 MHz, CDCl3) δ 7.99 (d, J = 9.0 Hz, 2H), 7.55 (t, J = 7.7 Hz, 2H), 7.31 (t, J = 7.6 Hz, 2H), 7.17 (d, J = 8.1 Hz, 2H), 3.91 (s, 3H), 3.77 (s, 6H). $^{13}$C NMR (101 MHz, CDCl3) δ 173.98, 173.81, 164.93, 151.34, 134.10, 131.99, 126.33, 123.61, 123.38, 55.69, 52.31.

### 3.2.3. Synthesis of Methoxy-diphenoxy-*s*-triazine (MPhT)

An aqueous solution of sodium hydroxide (NaOH, 3.05 equivalents, 5%) was prepared, to which 2.4 equivalents of phenol were added. The mixture was stirred under a nitrogen atmosphere at room temperature for 2 hours. Subsequently, 1 equivalent of compound ST1, dissolved in THF, was added to the reaction mixture. The reaction was monitored using TLC. Once the reaction was complete, the mixture was washed three times with DCM. The collected DCM phases were then washed with a 5% aqueous NaOH solution and water. The DCM phase was dried over anhydrous Na2SO4 and filtered. A clear solution was obtained and subsequently dried using a rotary evaporator. The resulting white crystals were obtained with a yield of 44%, and their melting point was determined to be 150 °C by DSC analysis.$^{1}$H NMR (400 MHz, CDCl3) δ 7.31 (t, J = 7.9 Hz, 4H), 7.17 (t, J = 7.4 Hz, 2H), 7.09 (d, J = 8.5 Hz, 4H), 3.86 (s, 3H). $^{13}$C NMR (101 MHz, CDCl3) δ 174.13, 173.64, 151.79, 129.64, 126.17, 121.60, 55.72.

### 3.2.4. Synthesis of Triphenoxy-*s*-triazine (TPT)

3.05 equivalents of phenol were added to the aqueous solution of NaOH (3.9 eq. 5wt%) under a $N_2$ atmosphere. After 2 hours, 1 equivalent of cyanuric chloride was dissolved in THF and added to the reaction mixture drop by drop. Reaction was monitored *via* thin layer

chromatography. After the reaction was complete, the reaction mixture was washed with DCM, and the organic phases were collected. The organic phase was then washed with aqueous NaOH solution (5wt%). The clear solution was dried over Na2SO4 and filtered. A clear solution was obtained and subsequently dried using a rotary evaporator. White powder with a 237 °C melting point was obtained. $^{1}$H NMR (400 MHz, CDCl3) δ 7.35 (t, J = 7.8 Hz, 2H), 7.22 (t, J = 7.4 Hz, 1H), 7.14 (d, J = 7.8 Hz, 2H). $^{13}$C NMR (101 MHz, CDCl3) δ 173.80, 151.70, 129.58, 126.18, 121.52.

### 3.2.5. Synthesis of Trimequinol-*s*-triazine (TMT)

3.05 equivalents of 4-methoxyphenol were added to the aqueous solution of NaOH (3.15 eq. 5wt%) under a $N_2$ atmosphere. After 2 hours, 1 equivalent of cyanuric chloride was dissolved in THF and added to the reaction mixture drop by drop. Reaction was monitored *via* thin layer chromatography. After the reaction was complete, the reaction mixture was washed with DCM, and the organic phases were collected. The organic phase was then washed with aqueous NaOH solution (5wt%). The clear solution was dried over Na2SO4 and filtered. A clear solution was obtained and subsequently dried using a rotary evaporator. White powder with a 201 °C melting point was obtained. $^{1}$H NMR (400 MHz, CDCl3) δ 7.05 (d, J = 9.0 Hz, 2H), 6.86 (d, J = 8.9 Hz, 2H), 3.79 (s, 3H). $^{13}$C NMR (101 MHz, CDCl3) δ 174.08, 157.46, 145.26, 122.30, 114.55, 55.67.

### 3.2.6. Synthesis of Methoxy-dimequinol-*s*-triazine (MDMT)

An aqueous solution of sodium hydroxide (NaOH, 3.05 equivalents, 5%) was prepared, to which 2.4 equivalents of 4-methoxyphenol were added. The mixture was stirred under a nitrogen atmosphere at room temperature for 2 hours. Subsequently, 1 equivalent of compound ST1, dissolved in THF, was added to the reaction mixture. The reaction was monitored using TLC. Once the reaction was complete, the mixture was washed three times

with DCM. The collected DCM phases were washed with a 5% aqueous NaOH solution and water. The DCM phase was dried over anhydrous $Na_2SO_4$ and filtered. A clear solution was obtained and subsequently dried using a rotary evaporator. The resulting viscous liquid was dissolved in THF and precipitated in ice-water with a yield of 51%, and its melting point was determined to be 103 °C by DSC analysis. $^1$H NMR (400 MHz, CDCl3) δ 7.08 (d, J = 8.9 Hz, 4H), 6.89 (d, J = 8.9 Hz, 4H), 3.93 (s, 3H), 3.80 (s, 6H). $^{13}$C NMR (101 MHz, CDCl3) δ 174.09, 173.96, 157.49, 145.35, 122.37, 114.62, 68.11, 55.71, 55.67, 25.74.

### 3.3. Melt Polymerization Reactions

MMST monomer, BPA, and LiOMe were charged to a glass cylindrical melt reactor (100 mL). The reactor was purged with $N_2$. The reaction mixture was heated in a silicon oil bath while stirred with an overhead mechanical stirrer. Temperature and pressure were controlled differently during polymerization, P1 and P2, which will be explained below. Torque values were recorded throughout

For P1, the polymerization was kept stirring for 3 hours. The temperature was kept at 180 °C for approximately 75 minutes, then heated up to 240 °C in 95 minutes. A vacuum was applied at 75 minutes, gradually decreasing the pressure from $10^3$ mbar to 1 mbar in 45 minutes, and kept at 1 mbar for 1 hour.

For P2, the polymerization was kept stirring for 7.5 hours. The temperature was increased from ~150 °C to 240 °C in 30-40 °C increments while waiting 30-60 minutes for each temperature increase. A vacuum was applied at the 6th hour, dropping the pressure sharply from $10^3$ mbar to 1 mbar and kept at 1 mbar until the end of the polymerization.

After polymerization was complete, the following solids were dissolved in THF and precipitated in excess MeOH solution.

**P1** $^1$H NMR (400 MHz, CDCl3) δ 8.04, 7.53, 7.31, 7.14, 7.02, 6.72, 3.59, 3.55, 3.35, 1.65.

**P2** $^1$H NMR (400 MHz, CDCl3) δ 7.25, 7.07, 6.93, 6.65, 3.52, 3.48, 3.28, 1.60.

### 3.4. Solution Polymerization Reactions

1 equivalent of MMST and BPA was charged into a 50 mL round-bottom flask. NaOH (0.1 wt% MMST) was added as a catalyst. The mixture was dissolved in 30 mL o-DCB and heated to 110 °C. The reaction mixture was kept stirring overnight. After the reaction was complete, the reaction mixture was precipitated in excess hexane and filtered. $^{1}$H NMR (400 MHz, $CDCl_3$) δ 7.42 – 7.34 (m,), 7.21 – 7.09 (m,), 7.07 – 6.95 (m), 6.81 (t, J = 7.6 Hz), 6.65 (d, J = 7.9 Hz), 3.87 (s), 1.61 (s), 1.57 (s), 1.50 (s).

### 3.5. Thermal Exposure Experiments

Apart from MMST, all samples were heated in an aluminum pan under a $N_2$ atmosphere. Heating was monitored *via* differential scanning calorimetry (DSC). After heating, the aluminum pan was cracked open and collected by dissolving in THF or $CHCl_3$. Samples were heated from room temperature to 300 °C. If the exotherm on DSC was no longer visible, heating was stopped to avoid degradation.

MMST samples were heated in glass cylinders using a silicon-oil bath under a $N_2$ atmosphere. Samples were heated from room temperature to 240 °C.

### 3.6. Kinetic and Thermal Analysis

Differential scanning calorimetry (DSC) thermograms were obtained by heating samples with varying heating rates (β = 1, 3, 5, 7, 10 °C per minute) from room temperature to 300 °C. Samples were stopped heating to avoid degradation if the exotherm on the DSC thermogram was deemed to finish. All DSC samples were about 4-5 mg and heated under a $N_2$ atmosphere.

Peak temperatures ($T_p$) were obtained directly from DSC thermograms. Activation energies ($E_a$) were calculated from the linear fit of $\ln(\beta/T_p^2)$ versus $1/T_p$.

Enthalpy values were calculated from the area of the exotherms and reported as an average.

### 3.7. Measurements

$^{1}H$ NMR, $^{13}C$ NMR, $^{1}H$-$^{13}C$ HSQC, and $^{1}H$-$^{15}N$ HMBC NMR analyses were conducted on a Brucker 400 MHz spectrometer. $CDCl_3$ was used as NMR solvent and TMS was used as an internal reference solvent. Samples for $^{1}H$ NMR analysis had at least 128 scans , while for $^{13}C$ NMR 1028 scans. $^{1}H$-$^{15}N$ HMBC NMR analyses conducted on 200mg/mL concentration samples.

Differential scanning calorimetry (DSC) analyses were conducted on Exstar SII 7020. Calibrated with indium and Tin. Analyses were conducted under nitrogen with different heating rates. The sample masses were approximately 4 mg.

FTIR analyses were conducted on a Thermo Fisher Scientific Nicolet 380 FTIR. FTIR samples were recorded on a range of 3500-600 $cm^{-1}$ with 32 scans. Spectra were then analyzed with Omnic software.

Gel permeation chromatography (GPC) analyses were conducted on Viscotek VE2001 gel permeation chromatography with THF flow at a rate of 0.5mL/min at 25 °C. Samples were dissolved in THF at a 4mg/mL concentration.

# 4. RESULTS AND DISCUSSION

## 4.1. Synthesis of Activated *s*-Triazines

Methoxy-bis(methyl salicyl)-s-triazine (MMST) monomer was synthesized from commercially available cyanuric chloride (CC) through a two-step process. The resulting monomer, MMST, was then used in melt-polycondensation with bisphenol-A (BPA) (Figure 4.1).

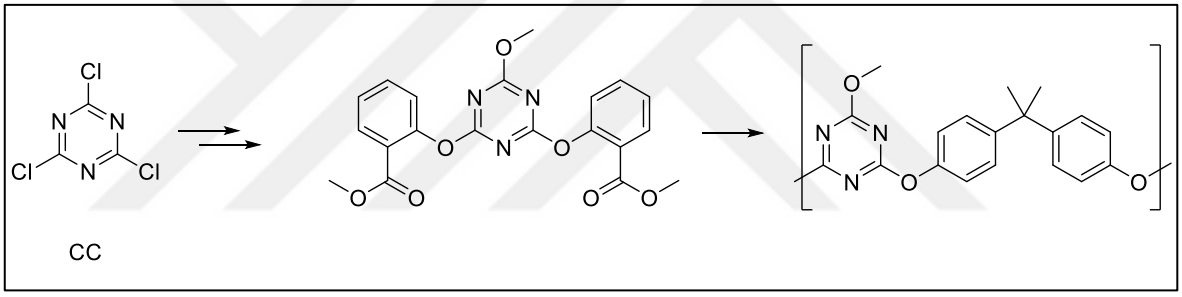



Figure 4.1. Synthetic pathway for the synthesis of polycyanurates.

The first step is the conversion of CC to dichloro-methoxy-s-triazine (ST1). ST1 was synthesized from CC at below 0 °C (ice-salt bath) in MeOH (Figure 4.2). $NaHCO_3$ was used stoichiometrically to neutralize HCl formed during the reaction. Reaction was followed by thin-layer chromatography (TLC). After consumption of all the CC, the reaction mixture was washed with distilled water, and the organic phase was extracted with dichloromethane (DCM). After drying, a white powder of ST1 was isolated in 79-83% yield and stored at ≤ 4 °C in a refrigerator. Throughout the study, ST1 was freshly synthesized and used within 3-4 days since ST1 showed signs of hydrolysis, similar to CC.

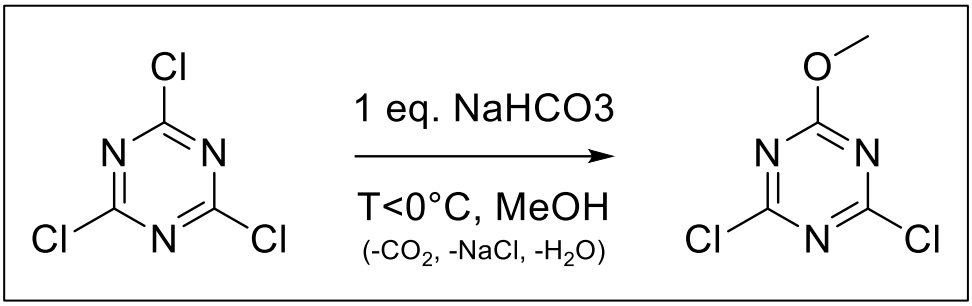



Figure 4.2. Synthesis of ST1 from CC.

The second step of the synthesis of MMST was performed using two different procedures. For the first procedure (Procedure A), methyl salicylate was deprotonated with the help of NaH and reacted with ST1 in N-methyl-pyrrolidone (NMP) at 80 °C. The product was isolated as white powder in 21-54% yields. For the second procedure (Procedure B), the sodium salt of methyl salicylate is first prepared separately from methyl salicylate and NaOH. Sodium salt of methyl salicylate (NaMS) was dissolved in dimethyl formamide (DMF) and reacted with ST1 at 40 °C. A white powder product was obtained with yields ranging from 12% to 48% (Figure 4.3).

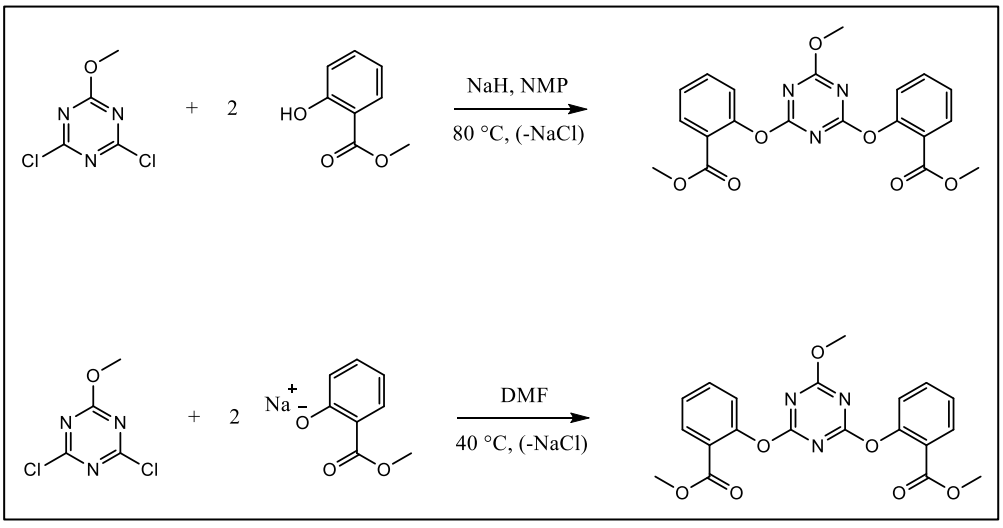



Figure 4.3. Procedure A-B for the synthesis of MMST monomer.

For both procedures, purification was similar, where the reaction solution was washed with acid and base and collected in DCM (complete sequence in Experimental). It is apparent that the yield percentages for both procedures are low. This can be mainly attributed to the extensive work-up procedure required to remove DMF and NMP, which are challenging since they are soluble in both organic and water phases. On the other hand, DMF and NMP are essential solvents to dissolve organic salts. Alternative routes where the tertiary amine catalyzed substitution of CC were also attempted, but the reaction showed very low conversion.

## 4.2. Melt Polymerization of Activated *s*-Triazines

MMST monomers were then employed in the target polycondensation reaction (150-240 °C, 7 g scale) with bisphenol A (BPA) under reduced pressure (Figure 4.4). A base catalyst, LiOMe (1 mol%), was employed to promote the transesterification reaction. Methyl salicylate was removed as a *by*-product to drive the reaction forward.

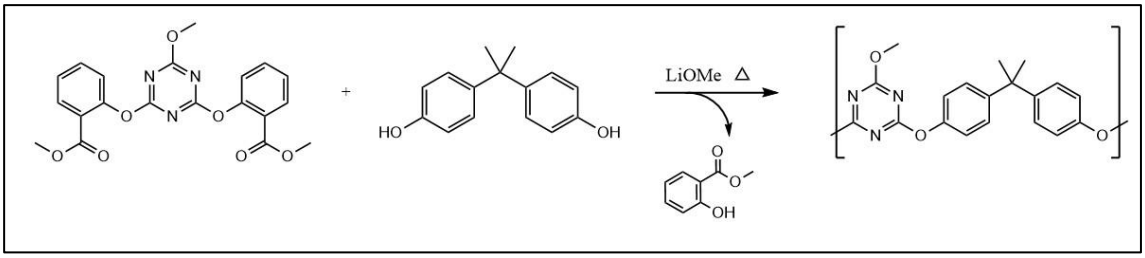



Figure 4.4. Targeted polycondensation reaction of MMST and BPA.

According to the expected mechanism, LiOMe first should deprotonate BPA to its corresponding phenolate, once deprotonated, BPA is expected to trigger a transesterification reaction, liberating the methyl salicylate. Vacuum distillation was used to collect the *by*-product methyl salicylate. The suggested mechanism is shown below (Figure 4.5).

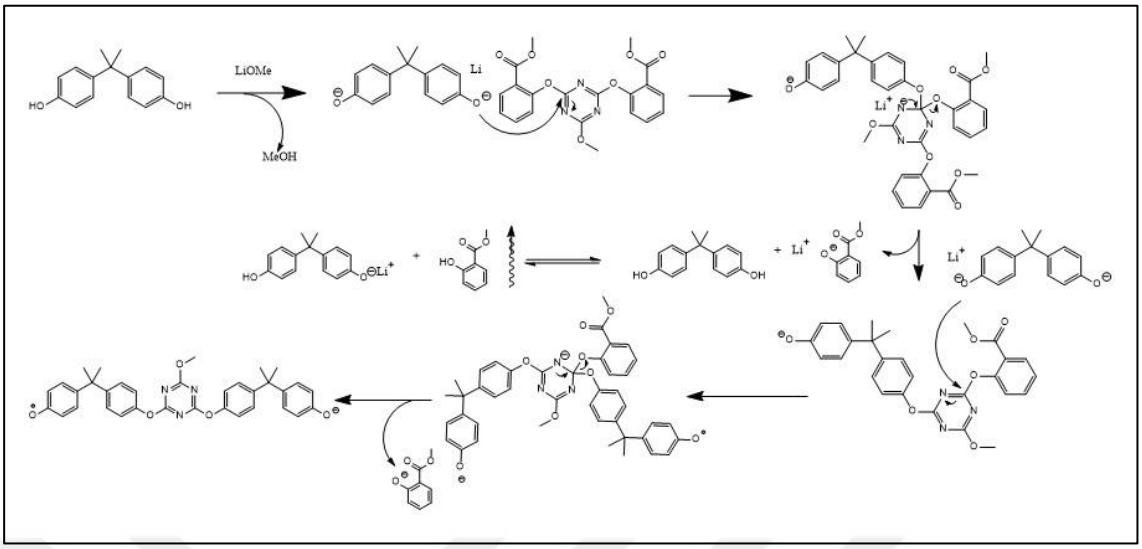



Figure 4.5. LiOMe Catalyzed targeted polymerization of MMST and BPA.

Two melt polycondensation procedure were followed which differed in temperature and pressure profiles; torque values were recorded to monitor the molecular weight increases through viscosity changes. The first polymerization process (P1) was conducted according to a previous study in our group, where the temperature was increased from 180 °C to 230 °C and the pressure was decreased concurrently from $10^3$ mbar to 1 mbar. After 150 minutes, the torque exceeded 30 Nm (Figure 4.6).

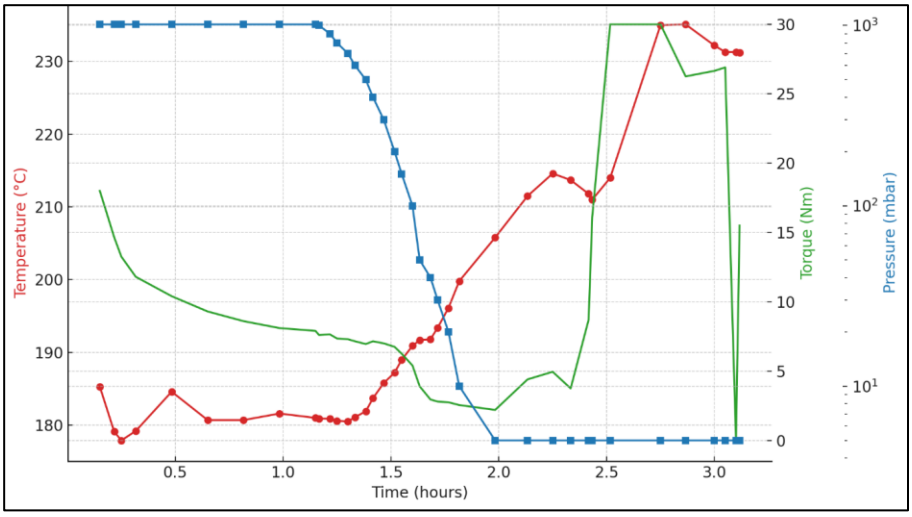



Figure 4.6. Temperature, pressure, and torque values recorded for P1.

For the second process (P2), the temperature was increased from 150 °C to 240 °C over a more extended period, and the pressure was decreased from $10^3$ mbar to 1 mbar at the late polymerization stages. In P2, contrary to the former polymerization-P1, torque values increased only to 3.5 - 4.0 at the 6$^{th}$ hour of polymerization (Figure 4.7).

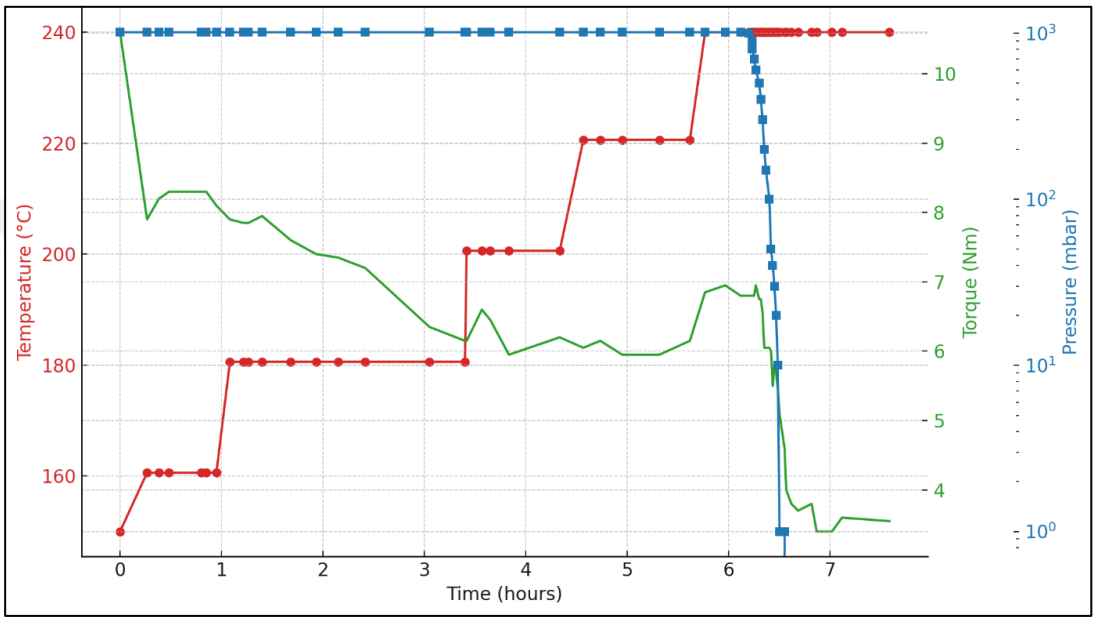



Figure 4.7. Temperature, pressure, and torque values recorded for P2.

Size-exclusion chromatography (SEC) values correlate with the torque values. P1 has an $M_n$ of 3,924 Da, whereas P2 has an Mn of 1,947 Da. Differential scanning calorimetry (DSC) yielded $T_g$ values that decreased, as expected, with the molecular weights of the polymers (Table 1).

Table 1. Synthesis ratios, SEC, and DSC results of polymers P1 and P2.

| **Polymer** | **Moles of MMST** | **LiOMe (Mole% MMST)** | **Mn (kDa)** | **Mw (kDa)** | **PDI** | **$T_g$ (°C)** |
|---|---|---|---|---|---|---|
| P1 | 0.01094 | 1 | 3.9 | 4.9 | 1.2 | 174 |
| P2 | 0.01022 | 1 | 1.9 | 2.4 | 1.2 | 121 |

When P1 was characterized through 1H-NMR, the -CH3 peak from monomer MMST at 3.9 ppm was found to be absent, but a new peak at 3.5 ppm was detected (Figure 4.8, Figure 4.9). Excessive shifting of the methyl peak was particularly intriguing and suggested a structural change.

Upon studying possible side reactions reported in the literature, the possibility of a thermal rearrangement was investigated through a series of experiments. These experiments and their results will be discussed later in the chapter concerning the thermal rearrangement in Section 4.3.4.

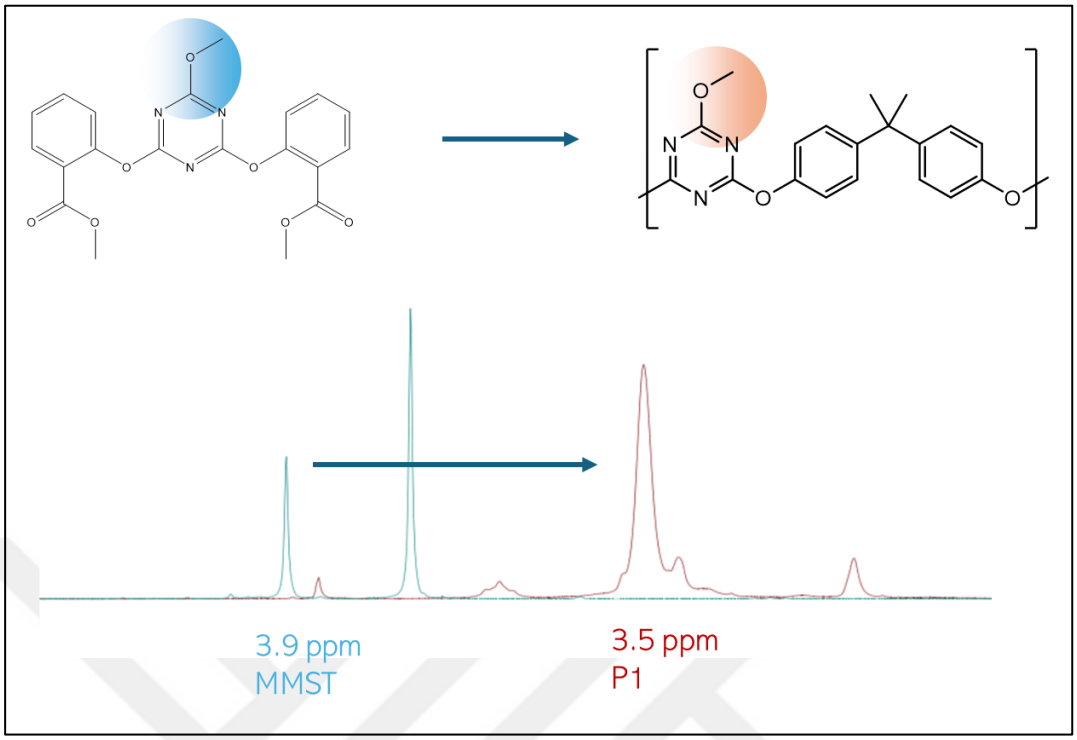



Figure 4.8. The [1]H-NMR spectrum shows the shift of the methyl signal from MMST to the possible repeating unit structure of the P1.

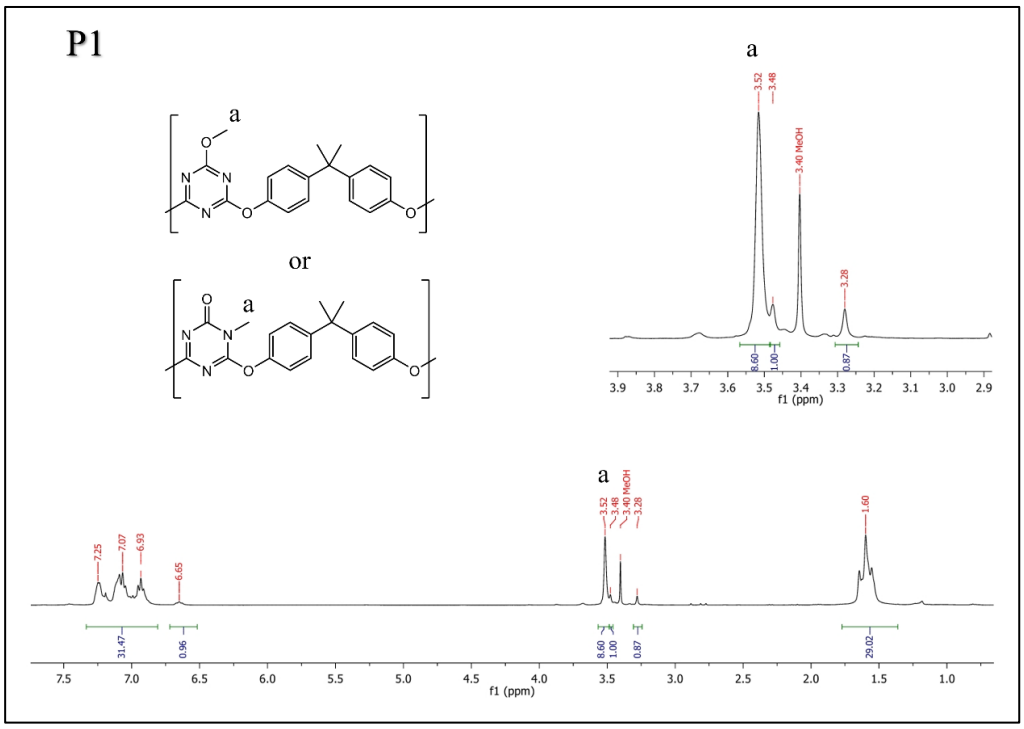



Figure 4.9. [1]H-NMR spectrum of P1.

Samples were taken during the polymerization of P2 and were subjected to NMR analyses to track the polymerization (Figure 4.10 – Figure 4.11).

In the first sample, which was taken at the second hour, the byproduct free methyl salicylate can be observed by the sharp methyl peak from methyl ester at 3.87 ppm overlapping with the methoxy-capped oligomeric species at 3.87 ppm.

In the second sample at the third hour, the $^{1}$H-NMR spectrum showed the disappearance of the shoulder at 3.96 ppm and the appearance of newly emerged peaks at 3.3, 3.5, and 3.6 ppm. The final polymer exhibits the same peaks as well. Though a shift to the 3.5 region is expected from P1, multiple methyl peaks demand a comprehensive explanation. The presence of multiple methyl peaks can be attributed to the polymer's low molecular weight, which gave rise to oligomer and end-group signals (Figure 4.11). Additionally, in pursuit of explaining multiple methyl peaks, the likelihood of a side reaction where aryl groups shift to the neighbouring nitrogen was considered. A detailed investigation is provided in Section 4, specifically under aryl shift (Section 4.3.4).

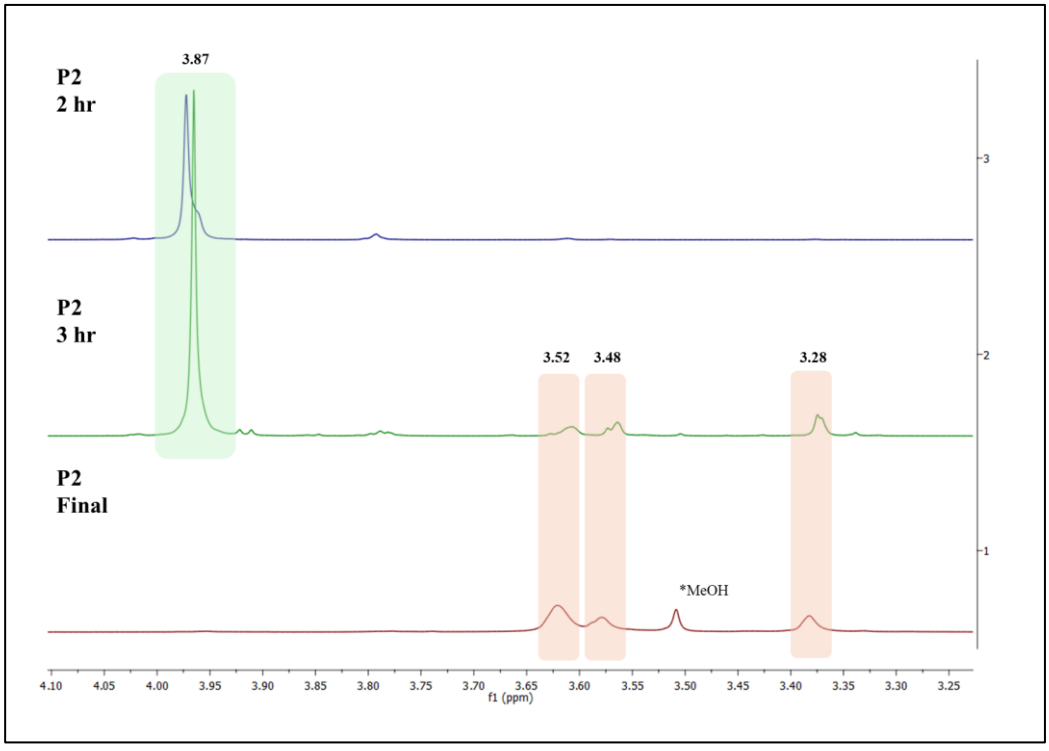



Figure 4.10. $^{1}$H-NMR spectra of polymerization P2 at the second and third hours.

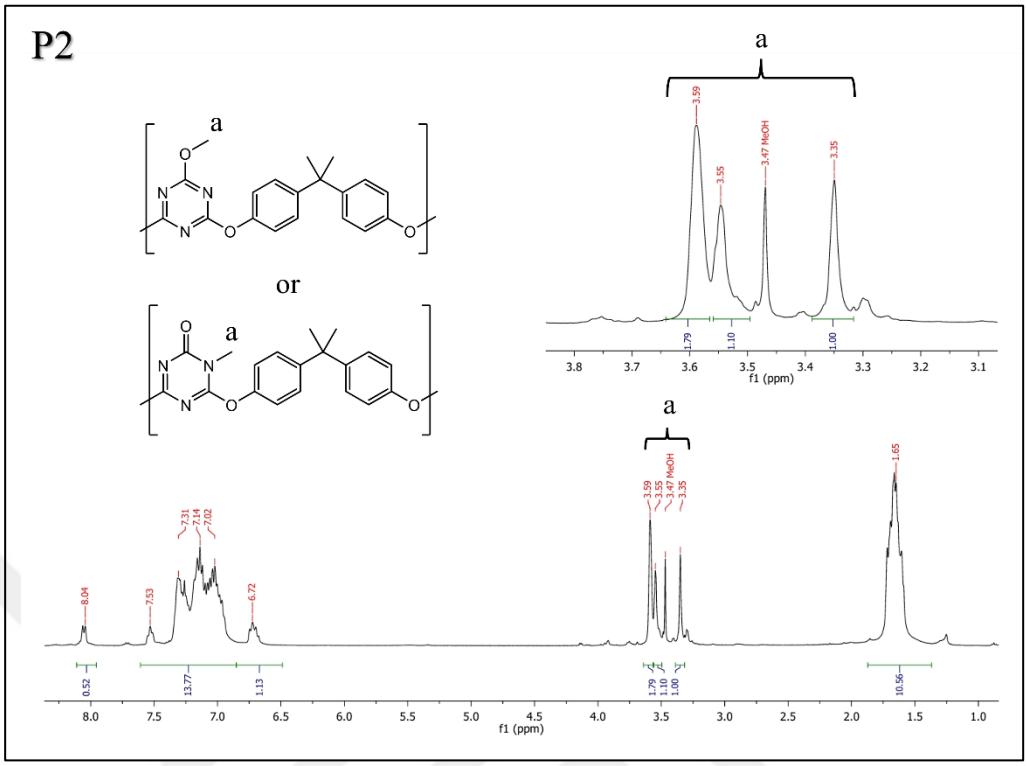



Figure 4.11. $^{1}$H-NMR spectrum of P2.

### 4.3. Thermal Rearrangement

Cyanurates were shown to undergo a thermal rearrangement reaction where the alkyl groups migrate to the nitrogens, forming an amide-like functionality [42]. It is most likely that cyanurate monomer, MMST, and/or newly formed polymer chains undergo thermal rearrangement during melt polymerization due to the excessive heat (Figure 4.12).

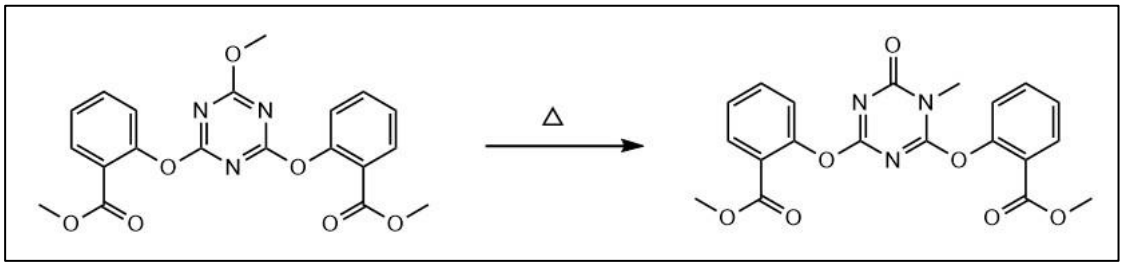


Figure 4.12. The possible thermal rearrangement of MMST.

### 4.3.1. Alkyl Rearrangement

A heating experiment was conducted on MMST monomer to prove the structural change that may be caused by the expected thermal rearrangement. In an inert atmosphere and reduced pressure, a sample of MMST was heated to 240 °C. After 4 minutes, the clear colorless melt became vivid red, and its color intensified rapidly. Samples taken at 10, 30, and 45 minutes were run on TLC. TLC shows that a new spot emerged after 10 minutes, and many spots emerged in 30 to 45 minutes (Figure 4.13).

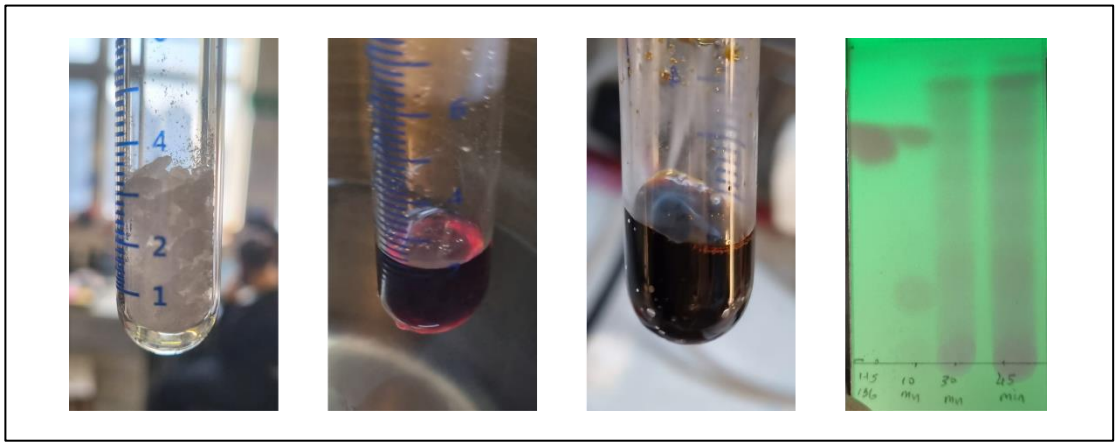


Figure 4.13. Photos of the heating experiment of MMST and TLC Plate (Mobile Phase Hexane: EtOAc)

Heated samples were analyzed by FTIR to track the changes (Figure 4.14). Formation of a new vibration at 1676 $cm^{-1}$ was attributed to an amide-like ($(N)_2C=O$) carbonyl in the rearranged structure. Additional vibrations were also present at 1753 $cm^{-1}$ and 1712 $cm^{-1}$ as a shoulder in the carbonyl region that requires further analysis for complete assignment.

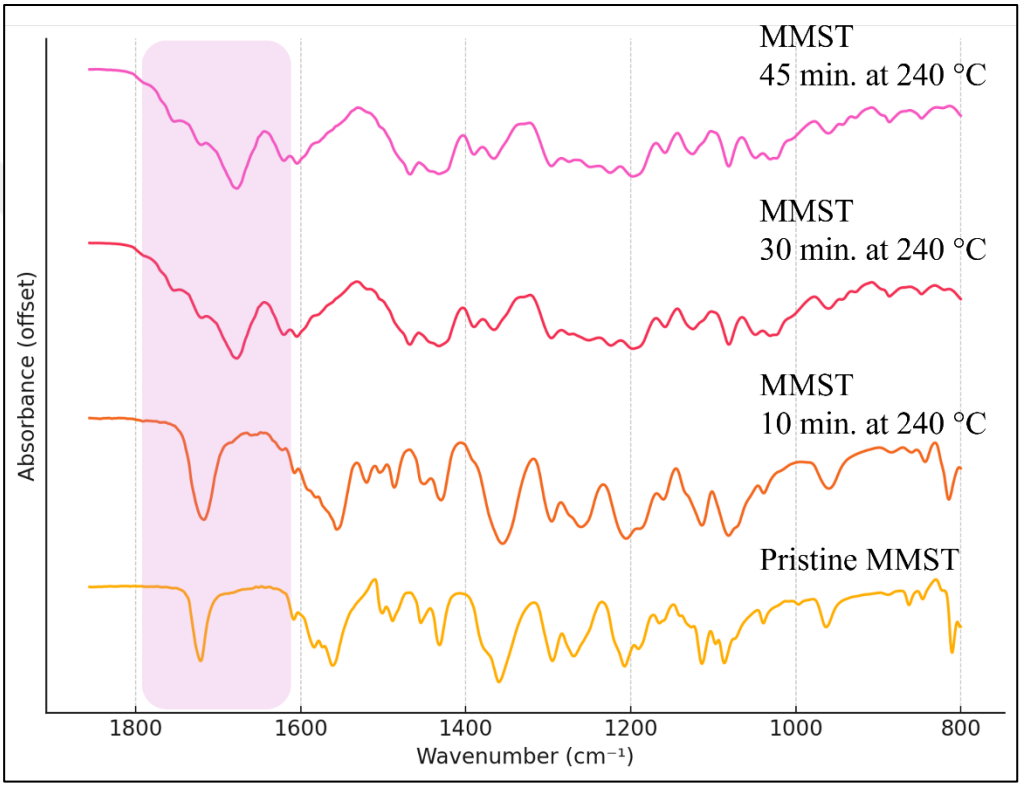



Figure 4.14. FTIR spectra of MMST and heated MMST samples.

Studying both $^{13}C$-NMR and $^{1}H$-NMR of the heated samples confirmed the structural change as well. $^{1}H$-NMR of MMST exposed to 240 °C for 10 minutes showed a new singlet at 3.6 ppm (Figure 4.15). Likewise, $^{13}C$-NMR showed a new peak emerging at 29.8 ppm, which was attributed to the newly formed N-methyl protons and carbons, respectively. Affirming these points, $^{13}C$-$^{1}H$ Heteronuclear single quantum coherence spectroscopy (HSQC) analysis indicates that the 3.6 ppm peak correlates with the 29.8 ppm peak.

Moreover, $^{13}$C-NMR also yielded new ring carbons. 169.7 ppm and 164.2 ppm were assigned to carbons involved in N=C-N, whereas the isocyanurate character carbon ($(N)_2C=O$) showed up at 156.7 ppm. Assignments were done according to the relevant literature by Tosato [42].

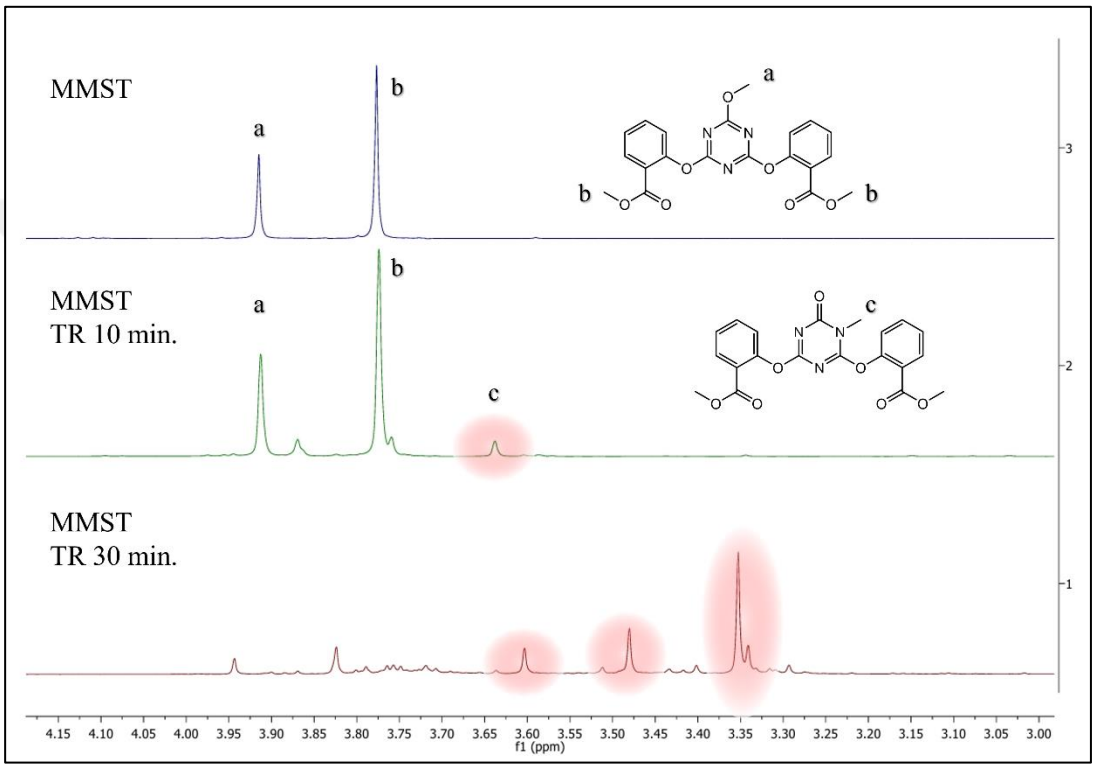



Figure 4.15. The 1H-NMR spectra of MMST and 10 min/30 min thermal exposure. $^{15}$N-$^{1}$H HMBC correlations highlighted.

In addition, $^{15}$N-$^{1}$H Heteronuclear Multiple Bond Correlation NMR ($^{15}$N-$^{1}$H HMBC), a less commonly employed new technique, was also used. $^{15}$N-$^{1}$H HMBC is an NMR method that provides the correlation of hydrogen and nitrogens that correlate through up to 3 bonds. It is important to note that, in cyanurates, methyl protons are at a four-bond distance to the triazine nitrogen. However, thermal rearrangement alters the structure in a way that methyl protons are then two bonds away from the closest nitrogen, making them visible in the $^{15}$N-$^{1}$H HMBC NMR spectrum (Figure 4.16). $^{15}$N-$^{1}$H HMBC was employed on a heated MMST

sample, and newly emerged peaks were found to be visible, confirming again the rearranged structure (Figure 4.15).

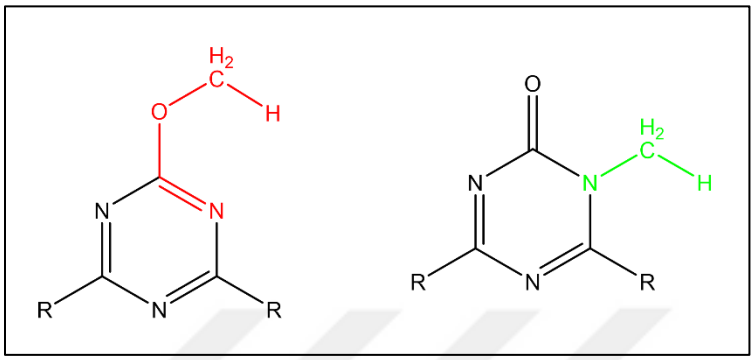



Figure 4.16. Comparison of $^{15}$N-$^{1}$H HMBC invisible (left) and visible (right) structures.

The $^{15}$N-$^{1}$H HMBC NMR spectra confirm the correlation of methyl peaks in both P1 and P2, indicating that a thermal rearrangement reaction occurred during the melt polymerization. Interestingly, thermal rearrangement reactions are typically reported only in neutral or acidic media. However, in the present case, a base catalyst, LiOMe, was used. Therefore, to the best of our knowledge, this is the first instance of a thermal rearrangement reported in basic media.

A similar analysis was conducted on methoxy-diphenoxy-*s*-triazine (MPhT), which is easier to synthesize and bears structural similarity (Figure 4.17). In the thermal exposure experiment of the MPhT, the sample was heated to 280 °C in an inert atmosphere (N2 purge) in an aluminum pan to avoid hydrolysis. In the $^{1}$H-NMR, the methoxy signal at 3.97 ppm had diminished entirely as a fresh N-methyl peak arose at 3.62 ppm. Likewise, in $^{13}$C-NMR, the methoxy signal at 55.72 ppm was replaced by a newly emerged peak at 29.75 ppm (Figure 4.17).

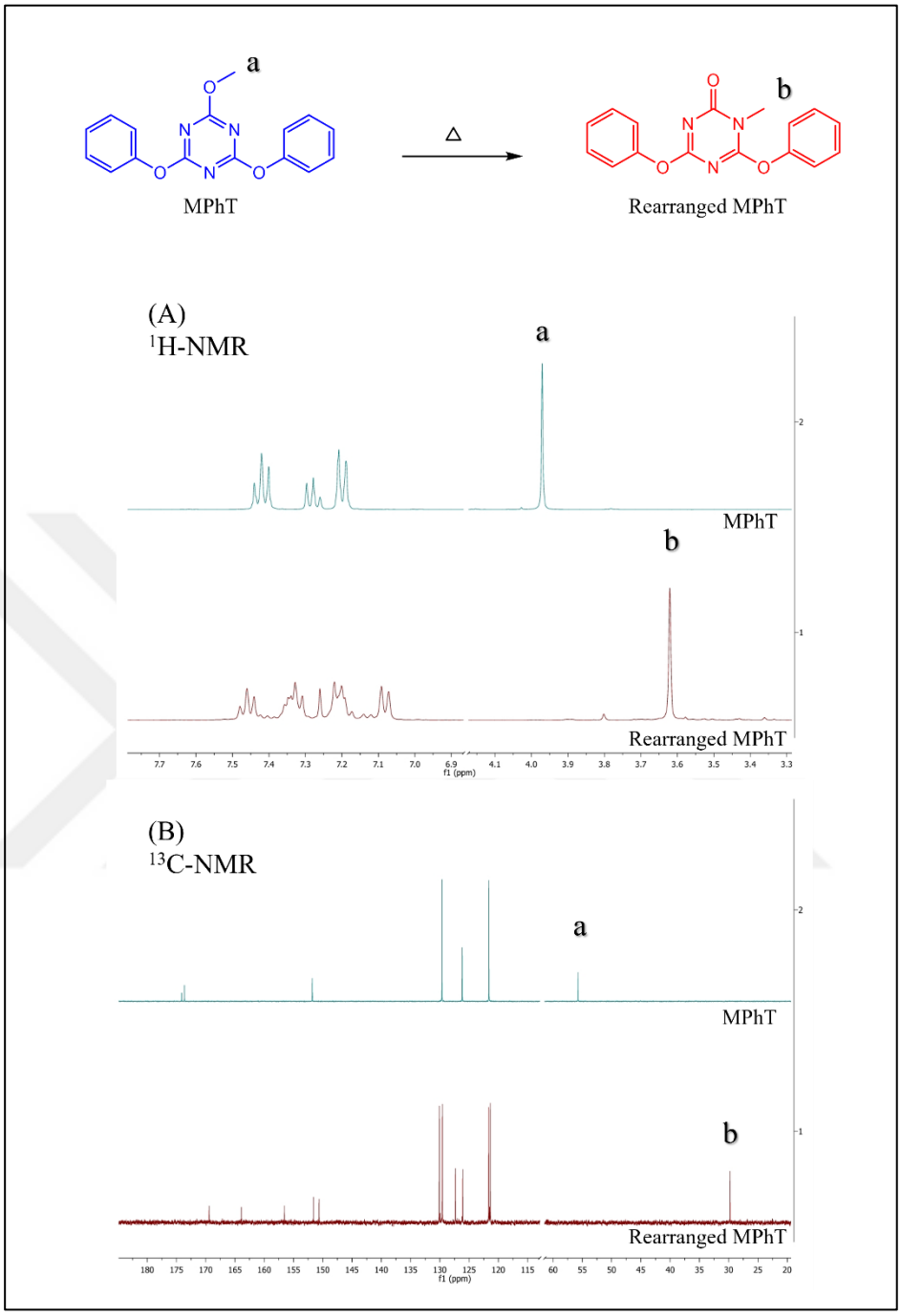



Figure 4.17. $^{1}$H-NMR (A) and $^{13}$C-NMR (B) spectra of MPhT before and after rearrangement.

Thermal exposure experiments on MMST and MPhT and their instrumental analysis showed that the thermal rearrangement of cyanurates is triggered at elevated temperatures.

Rearranged structures of cyanurates can explain the shift of methyl peaks on polycyanurates synthesized in melt-polycondensation.

### 4.3.2. Kinetic and Thermodynamic Study

It is documented that cyanurate thermal rearrangement is an exothermic reaction that exhibits a clear exotherm in the DSC thermogram [32]. Considering the literature, DSC experiments were conducted with different heating rates on MPhT and MMST (Figure 4.18). All the samples showed an exotherm where peak temperatures ranged from 237.9 °C to 286.1 °C (Figure 4.19). To calculate the enthalpy of the reaction, the area of the exotherms was calculated. Enthalpy of the rearrangement was found to be from -15.1 ± 2.7 kJ/mol for MPhT and -41.3 ± 2.7 kJ/mol for MMST.

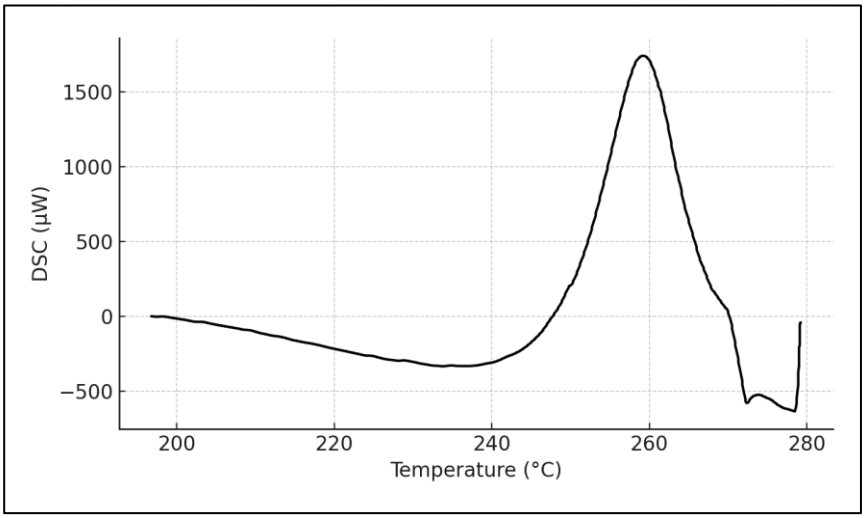



Figure 4.18. DSC thermogram of MPhT at 3 °C $min^{-1}$ heating rate.

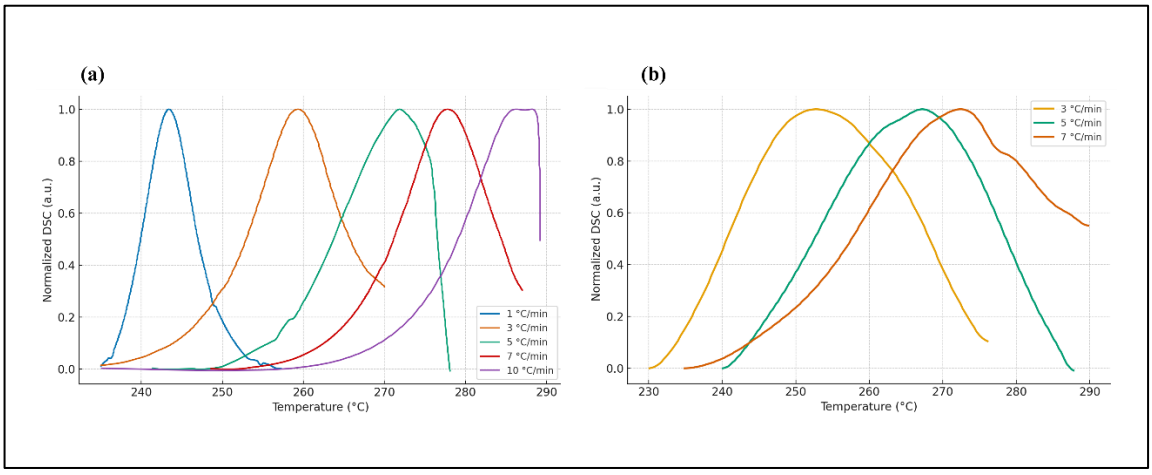



Figure 4.19. Close-up of normalized, DSC exotherms of MPhT (a) and MMST (b) in different heating rates.

Moreover, exotherms can be used to extract activation energies ($E_a$), as well. Kissinger stated an equation where several differential thermal scans with different heating rates can yield activation energy [43]. The Kissinger equation is

$$\ln( \beta / Tp^2 ) = - ( Ea / R ) \cdot ( 1 / Tp ) + C \quad (1.1)$$

where β is the heating rate, R is the gas constant, and Tp is the peak temperature for the given heating rate. Peak temperatures of the samples for different heating rates were recorded, and the Kissinger Equation was solved. Results were then plotted, and $E_a$ was calculated from the slope. The MMST sample was heated, and peak temperatures (Tp) were used to plot the Kissinger plot. The slope of the plot resulted in Ea being 87.95 kJ/mol (Figure 4.20).

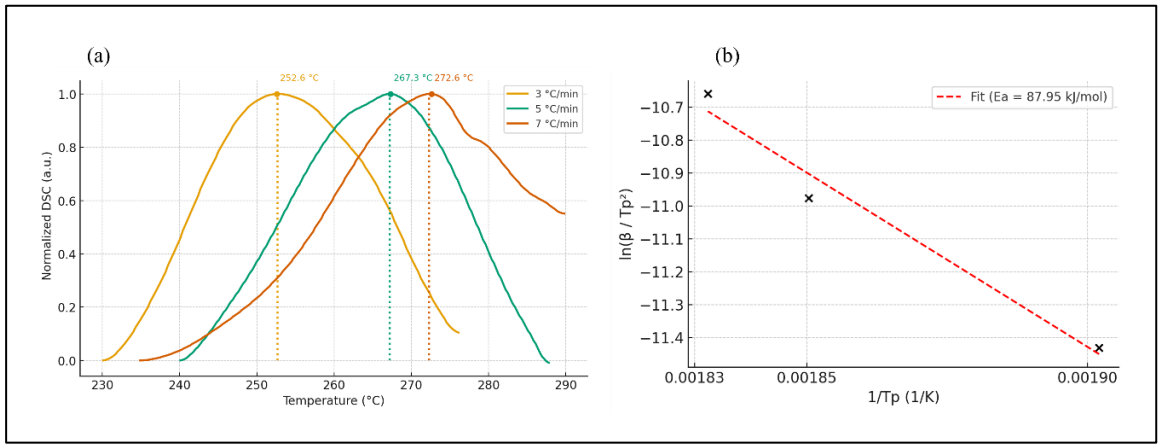



Figure 4.20. DSC Graph of MMST (a) with different heating rates 3, 5, 7 °C °C/min and Kissinger Kinetic Analysis Plot (b).

The same procedure was applied, and the activation energy was calculated for MPhT. The slope of the linear fit of the Kissinger plot yielded an activation energy of 119 kJ/mol (Table 2). When compared to MMST, the energy activation of MPhT is higher. This could be attributed to the presence of electron-withdrawing methyl esters located in the ortho positions of MMST. Hamerton and co-workers state the enthalpy of MPhT to be -13.6 kJ/mol [44]. Tosato and co-workers report the activation energy for the rearrangement of trimethoxy-s-triazine as 118.4 kJ/mol [29]. Therefore, the calculated kinetic and thermodynamic parameters are in line with the literature (Table 2)

.

Table 2. $T_p$'s of exotherms, activation energies, regression of linear fit, and enthalpies of MPhT and MMST.

| Molecule | $T_p$ at 1 °C min$^{-1}$ (°C) | $T_p$ at 3 °C min$^{-1}$ (°C) | $T_p$ at 5 °C min$^{-1}$ (°C) | $T_p$ at 7 °C min$^{-1}$ (°C) | $T_p$ at 10 °C min$^{-1}$ (°C) | $R^2$ | Ea (kJ/mol) | $\Delta H$ (kJ/mol) |
|---|---|---|---|---|---|---|---|---|
| **MPhT** | 243.6 | 259.2 | 271.9 | 277.8 | 286.1 | 0.99 | **119** | -15.1 ± 2.7 |
| **MMST** | — | 252.6 | 267.3 | 272.6 | — | 0.97 | **88** | -41.3 ± 2.7 |

### 4.3.3. Solution Polymerization

The DSC analysis has shown that the exotherm starts around 230 °C for MPhT and MMST (Figure 4.19). Hamerton and co-workers report that the onset temperature for the rearrangement in methoxy-substituted linear aromatic polycyanurates can be as low as 163 °C [44]. Therefore, a new polymerization procedure was used to avoid thermal rearrangement, in which the temperature did not exceed 163 °C, and solution polymerization was used.

Solution polymerizations (SP) were conducted with equimolar MMST and BPA in o-DCB at 90 °C. Reactions were catalyzed with NaOH. To the best of our knowledge, this is the first instance of solution polymerization that involves the transesterification of *s*-triazines (Figure 4.21).

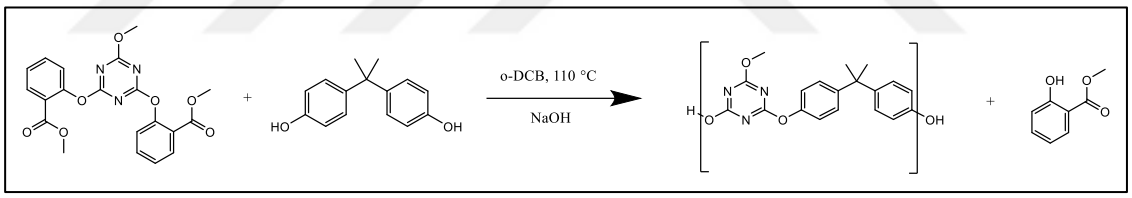



Figure 4.21. Solution polymerization scheme of MMST with BPA in o-DCB.

$^{1}$H-NMR and $^{13}$C-NMR spectra of SP showed no sign of rearrangement (Figure 4.22).The methoxy signal of SP appeared at 3.87 ppm and 55.73 ppm, which are closer to the signals of MMST, meaning that the repeating unit consists of a methoxy group instead of the potentially rearranged N-methyl groups.

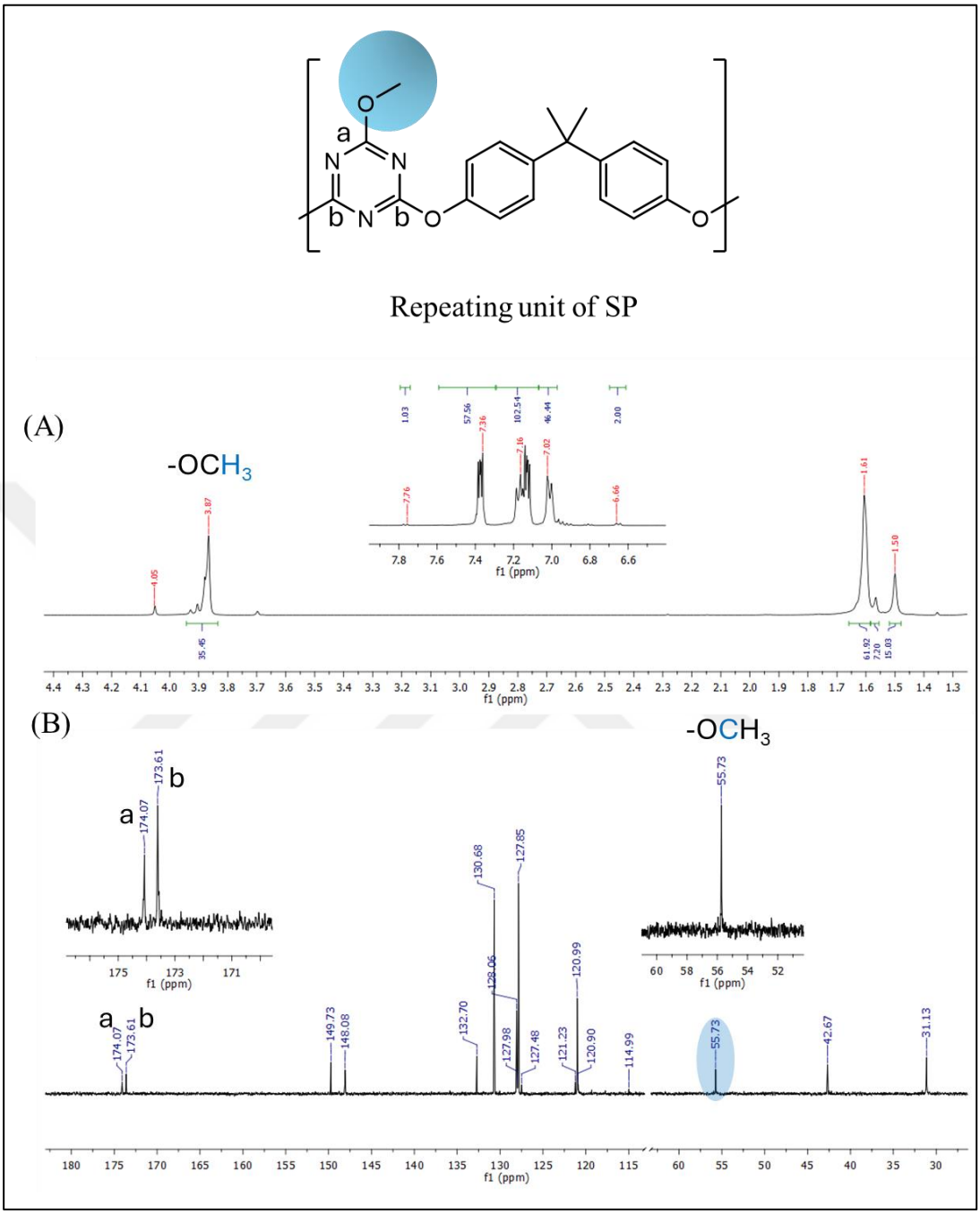



Figure 4.22. $^{1}$H-NMR (A) and $^{13}$C-NMR (B) spectra of SP.

Polymer SP was subjected to a thermal exposure experiment to investigate thermal rearrangement in polymer chains, as well as to obtain rearranged polycyanurate to compare with the readily rearranged P1 sample. SP was heated to 210 °C, and then the temperature was increased to 250 °C at a rate of 1 °C/min to trigger thermal rearrangement. After thermal

exposure, all the methoxy moieties disappeared and were converted to N-methyl moieties, which show signals at 3.59 ppm in $^{1}$H-NMR and 29.78 ppm in $^{13}$C-NMR (Figure 4.23). The $^{1}$H-NMR of the rearranged sample resembled P1 as if it had also undergone melt polymerization. Additionally, it has been observed that SP was insoluble in tetrahydrofuran (THF) but became soluble after thermal rearrangement. For this reason, GPC analysis was run only after thermal rearrangement. GPC results yielded Mn of 9.4 kDa and Mw of 16 kDa, resulting in a 1.7 polydispersity. Similarly, molecular weight is calculated as 9.4 kDa from $^{1}$H-NMR.

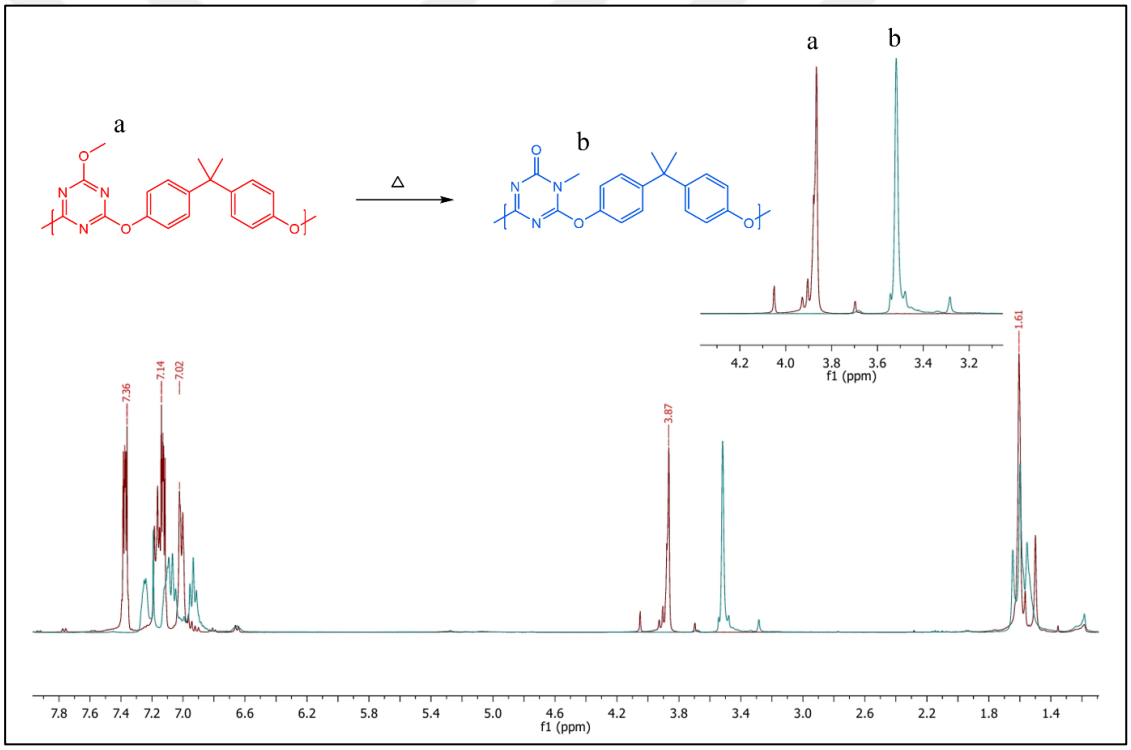



Figure 4.23. $^{1}$H-NMR spectra of pristine SP (red) and thermally rearranged SP (blue).

Lastly, a kinetic and thermodynamic analysis of SP was conducted through DSC experiments, similar to the analysis performed in Section 4.3.2. The kinetic analysis of thermal rearrangement in SP is of significant importance, as it offers valuable insights into the mechanisms of rearrangement within long-chain structures, as well as during

polymerization processes. SP samples were heated to 290 °C at various heating rates. The resulting exothermic reactions produced an average enthalpy of -31.4 ± 3.5 kJ/mol. The activation energy of SP was determined to be 112 kJ/mol, calculated using the Kissinger equation with the peak temperatures ($T_p$).

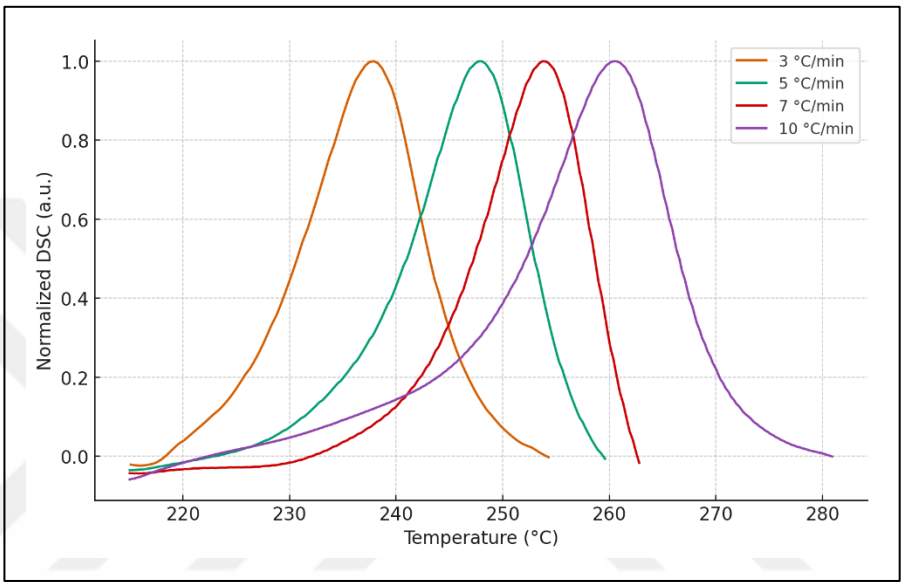



Figure 4.24. Close-up of normalized, DSC exotherms of SP in different heating rates.

### 4.3.4. Aryl Shift

In earlier (Section 4.2), it was mentioned that P2 resulted in multiple methyl peaks in $^1$H-NMR, which were then potentially attributed to the various forms of oligomeric end groups. A potential side reaction, the aryl shift, was still investigated to ensure the accurate structural characterization.

The main reference for the aryl shift is the work of Tschiya and co-workers [35] (Figure 4.25). Up-to-date articles state that the rearrangement of aryl cyanurates to the corresponding isocyanurates seems unlikely. Since Tschuiya's work opposes the literature, further investigation was necessary.

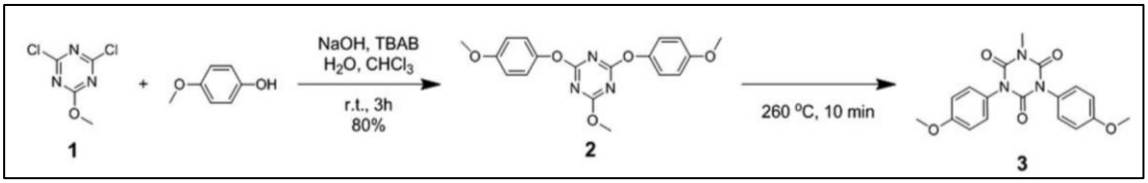



Figure 4.25. Synthesis and thermal rearrangement of the model compound from the work of Tsuchiya and co-workers. Used as it is from Ref [35].

Though it is unlikely, the possibility of an aryl shift was found worth analyzing because it could be an alternative (alternative to the oligomer end group explanation) explanation for the presence of multiple peaks in P2 (Figure 4.26). It is postulated that repeating groups without aryl shift (a), semi-aryl shift (b), and full-aryl shift (c) would yield three distinct methyl signals. This assumption can explain three signals in $^{1}$H-NMR at around 3.5 ppm and $^{13}$C-NMR at around 29.5 ppm.

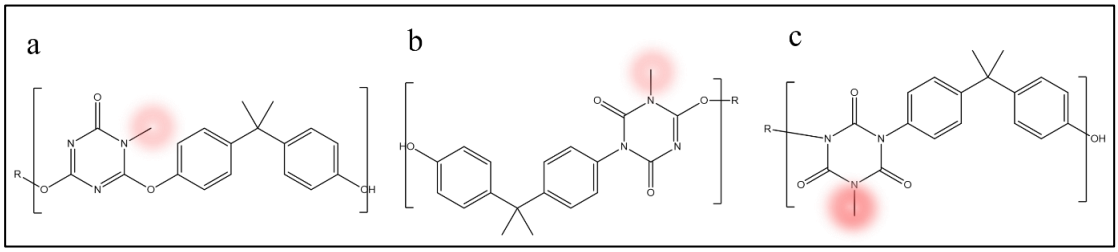



Figure 4.26. Possible structures of repeating units where no aryl shift (a), semi-aryl shift (b), and complete aryl shift (c) occur.

Firstly, a model compound of triphenoxy-*s*-triazine (TPT) was synthesized. TPT was heated to 270 °C for 90 minutes to trigger the aryl shift. No difference in FTIR, and no new carbonyl peaks emerged throughout the thermal exposure (Figure 4.27).

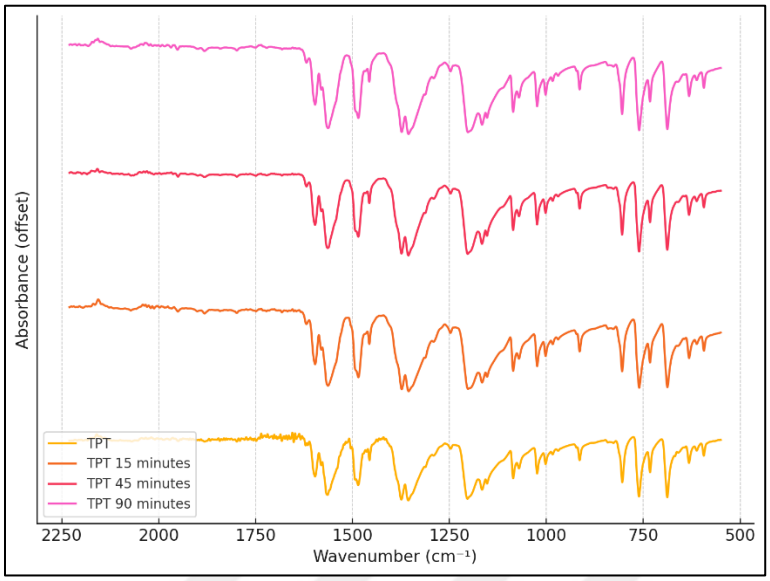



Figure 4.27. FTIR spectra of TPT, heated TPT samples at 15, 45, and 90 minutes (from top to bottom).

Similarly, another model compound was synthesized where mequinol (4-methoxyphenol) was used as a substituent to mimic the model compound of Tschuiya and co-workers. Trimequinol-*s*-triazine (TMT) was synthesized and subjected to thermal exposure experiments, as well. To have an analogous reaction, tetrabutylammonium bromide (TBAB) was added and heated to 240 °C for 30 minutes. Upon seeing no change in the FTIR, the temperature increased to 270 °C and was kept there for an additional 30 minutes. No visible change was detected in the FTIR (Figure 4.28).

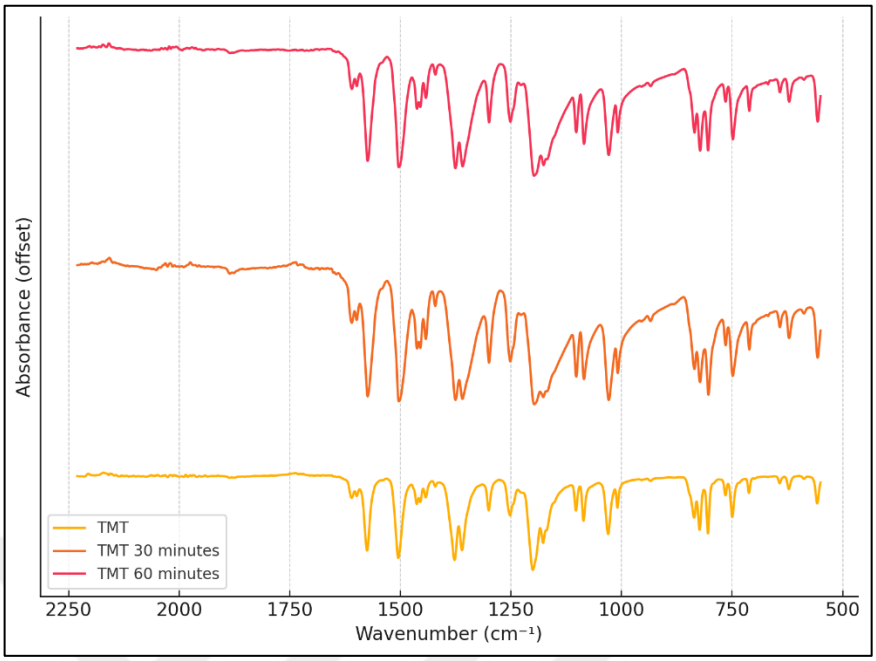



Figure 4.28. FTIR spectra of TMT and heated TMT samples at 30 and 60 minutes (from top to bottom).

Finally, DSC analysis of TPT and TMT was conducted. DSC thermograms only showed endotherms of the melting point and no exotherms, which the latter should be present if the modal compounds were to go through an aryl shift.

Since two model compounds did not undergo aryl shift, it was necessary to revisit the characterization of Tschuiya's model compound. Model compound methoxy-dimequniol-*s*-triazine (MDMT) was synthesized and heated to 240 °C for 40 minutes. The product was then characterized by $^{13}$C-NMR. $^{13}$C-NMR was explicitly chosen because triazine and isocyanurate rings exhibit specific chemical shifts. For instance, triazine rings display signals around 170 ppm, while isocyanurate rings show peaks around 150 ppm [42]. MDMT, however, displays a hybrid-ring containing triazine and isocyanurate character. Ring carbons were assigned (Figure 4.29). In brief, it is most likely that the authors of the original work on aryl shift mischaracterized the ring carbons, misinterpreted the rearrangement of the methyl group as a complete isomerization of cyanurate to isocyanurate.

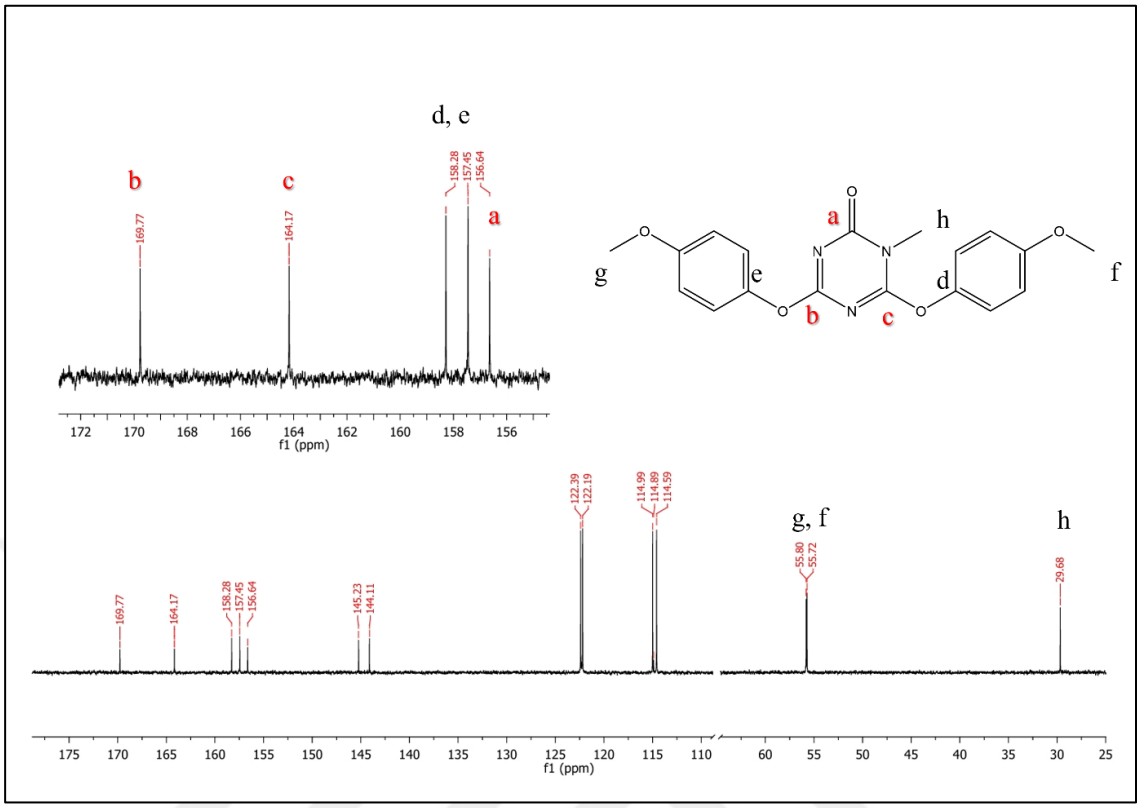



Figure 4.29. $^{13}$C-NMR spectrum of the rearranged MDMT.

To sum up, evidence for an aryl shift is nonexistent. Hybrid rearranged structures may lead to falsely attributed structures, but detailed analysis shows that aryl triazine structures are thermally stable.

# 5. CONCLUSION

An activated *s*-triazine monomer with methyl salicylate leaving groups was designed and synthesized in two successive steps. The monomer and Bisphenol A were polymerized with LiOMe by a melt-polycondensation process, where the methyl salicylate byproduct was removed. Polymers were characterized *via* NMR, leading to an additional investigation of the thermal rearrangement of *s*-triazines.

Heating experiments were conducted on activated *s*-triazine monomer and similar cyanurate molecules. Samples were analyzed through FTIR and several NMR techniques namely $^{1}H$, $^{13}C$, $^{1}H$ -$^{13}C$ HSQC and $^{1}H$ –$^{15}N$ HMBC. The results showed that thermal rearrangement of *s*-triazines is triggered at high temperatures.

A kinetic analysis of thermal rearrangement was carried out with the Kissinger method. Samples were heated with different heating rates in differential scanning calorimetry. The resulting activation energies and enthalpies were comparable to those found in the literature.

Solution polymerization strategy was employed to lower the temperature of the polymerization. Activated *s*-triazines and bisphenol A were polymerized in ortho-dichlorobenzene with the help of NaOH catalysis. This approach successfully reduced the polymerization temperature by at least 120 °C when compared to the melt-polycondensation trials. Consequently, the resulting polymer showed no sign of rearrangement. It has been found that solution polymerization delivered Mn of 9.4 kDa, more than twice what has been achieved with other trials.

Lastly, a potential thermal rearrangement of aryl-*s*-triazines was investigated. Model *s*-triazines with aryl substitutions failed to rearrange under any tested conditions.

# 6. FUTURE WORK

Activated s-triazines exhibit significant potential in the synthesis of linear polycyanurates, as the leaving group, methyl salicylate, serves to enhance the rate of polymerization. To fully leverage the potential of activated s-triazines, it is crucial to optimize the synthesis of these monomers. Our study revealed a pronounced decrease in the yield of activated s-triazines, primarily resulting from the cumbersome work-up procedures associated with the solvent removal. Investigating alternative solvent systems may prove advantageous for improving reaction efficiency.

Using mild temperature profiles during melt polycondensation is recommended to minimize the risk of thermal rearrangement and to enhance the molecular weights of the polycyanurates. Furthermore, additional research into the solution polymerization of activated s-triazines is recommended.

Lastly, a thorough exploration of the thermal rearrangement mechanism is advisable. Performing computational analyses on the transition state will be beneficial for further investigations. It is noteworthy that thermal rearrangement has traditionally been reported in acidic and neutral conditions; however, we have identified thermal rearrangement occurring in basic media during melt polycondensation. Future studies should address the media-dependent nature of the thermal rearrangement reaction to deepen the understanding of the reaction mechanisms involved.

# REFERENCES


1. Kushwaha, N., and C. S. Sharma, “The Chemistry of Triazine Isomers: Structures, Reactions, Synthesis and Applications”, *Mini-Reviews in Medicinal Chemistry*, Vol. 20, No. 20, pp. 2104–2122, 2021.

2. Katritzky, A. R., C. W. Rees, and E. F. V. Scriven (Eds.), *Comprehensive Heterocyclic Chemistry II*, Pergamon, Oxford, 1996.

3. Matsui, K., K. Hagiwara, and A. Hayashi, “Reaction of Cyanuric Chloride with Alcohols. I”, *Journal of Synthetic Organic Chemistry*, Vol. 18, No. 2, pp. 97–104, 1960.

4. Dudley, J. R., J. T. Thurston, F. C. Schaefer, D. Holm-Hansen, C. J. Hull, and P. Adams, “Cyanuric Chloride Derivatives. III. Alkoxy-s-Triazines”, *Journal of the American Chemical Society*, Vol. 73, No. 7, pp. 2986–2990, 1951.

5. Blotny, G., “Recent Applications of 2,4,6-Trichloro-1,3,5-Triazine and Its Derivatives in Organic Synthesis”, *Tetrahedron*, Vol. 62, No. 41, pp. 9507–9522, 2006.

6. Eicher, T., and S. Hauptmann, *The Chemistry of Heterocycles: Structure, Reactions, Syntheses and Applications*, Second, completely revised and enlarged edition, Wiley-VCH, Weinheim, 2003.

7. Katritzky, A. R., C. A. Ramsden, J. A. Joule, and V. V. Zhdankin, *Handbook of Heterocyclic Chemistry*, Third Edition, Elsevier, Oxford, 2010.

8. Hamerton, I. (Ed.), *Chemistry and Technology of Cyanate Ester Resins*, Springer Netherlands, Dordrecht, 1994.

9. Smolin, E. M., and L. Rapoport, *Chemistry of Heterocyclic Compounds*, Vol. 13, Interscience, New York, 1959.

10. Pérez-Manríquez, L., A. Cabrera, L. E. Sansores, and R. Salcedo, “Aromaticity in Cyanuric Acid”, *Journal of Molecular Modeling*, Vol. 17, No. 6, pp. 1311–1315, 2011.

11. de Lange, P. G., and T. A. Misev, *Powder Coatings: Chemistry and Technology*, Second edition (expanded and completely revised), Vincentz Network, Hannover; William Andrew, Norwich, 2004.

12. Driest, P. J., *Poly(urethane-isocyanurate) Networks: Synthesis, Properties and Applications*, Ph.D. Thesis, Universiteit Twente, 2020.

13. Linder, T., M. Schnürch, and M. D. Mihovilovic, “One-Pot Synthesis of Triazines as Potential Agents Affecting Cell Differentiation”, *Monatshefte für Chemie – Chemical Monthly*, Vol. 149, No. 7, pp. 1257–1284, 2018.

14. Dudley, J. R., J. T. Thurston, F. C. Schaefer, C. J. Hull, D. Holm-Hansen, and P. Adams, “Cyanuric Chloride Derivatives. VII. Transesterification Reactions of Alkoxy-s-Triazines. Polyammelide Ethers”, *Journal of the American Chemical Society*, Vol. 73, No. 7, pp. 2999–3004, 1951.

15. Kropa, E. I., “Reaction Products of a Cyanuric Tri-Ester and a Polyhydric Alcohol and Methods of Preparing the Same”, U.S. Patent 2,557,667, June 19, 1951. Available: https://patents.google.com/patent/US2557667A/en, Accessed on August 19, 2025.

16. Yameen, B., H. Duran, A. Best, U. Jonas, M. Steinhart, and W. Knoll, “Polycyanurate Thermoset Networks with High Thermal, Mechanical, and Hydrolytic Stability Based on Liquid Multifunctional Cyanate Ester Monomers with Bisphenol A and AF Units”, *Macromolecular Chemistry and Physics*, Vol. 209, No. 16, pp. 1673–1685, 2008.

17. Coscia, A. T., R. L. Kugel, and J. Pellon, “Polymerization of 2,4-Dimethyl-6-Vinyl-s-Triazine”, *Journal of Polymer Science*, Vol. 55, No. 161, pp. 303–309, 1961.

18. Braun, D., and T. Ziser, “Triazine-Based Polymers, 1. Synthesis of Poly[(2,4-Dichloro-6-Ethoxy-s-Triazine)-alt-(Bisphenol A)]”, *Die Angewandte Makromolekulare Chemie*, Vol. 219, No. 1, pp. 27–42, 1994.

19. Nakamura, Y., K. Mori, K. Tamura, and Y. Saito, “Relation of the Chemical Structure of Polycyanurates to Thermal and Mechanical Properties”, *Journal of Polymer Science Part A-1: Polymer Chemistry*, Vol. 7, No. 11, pp. 3089–3100, 1969.

20. Grigat, E., R. Putter, and R. Sundermann, “Process for Preparation of S-Triazine Prepolymers”, U.S. Patent 4,049,630, Sept. 6, 1977. Available: https://patents.google.com/patent/US4049630A/en, Accessed on August 19, 2025.

21. Sundermann, R., “*s*-Triazine Prepolymers and a Process for Their Production”, U.S. Patent 4,042,567, Aug. 9, 1977. Available: https://patents.google.com/patent/US4042567A/en, Accessed on August 19, 2025.

22. Aldalbahi, A., B. S. AlOtaibi, B. M. Thamer, and A. El-Faham, “Synthesis of New *s*-Triazine Bishydrazino and Bishydrazido-Based Polymers and Their Application in Flame-Retardant Polypropylene Composites”, *Polymers*, Vol. 14, No. 4, Article 784, 2022.

23. Schaefer, F. C., “Reaction Products of a Polyhydric Alcohol and a Triazine Derivative and Methods of Preparing the Same”, U.S. Patent 2,481,156, Aug. 30, 1949. Available: https://patents.google.com/patent/US2481156A/en, Accessed on August 19, 2025.

24. Nakamura, Y., A. Sato, and Y. Sato, “Preparation of Polymers from 2-Amino-4,6-Diphenoxy-s-Triazine and Bisphenol A, and Its Cross-Linking Reaction”, *The Journal of the Society of Chemical Industry*, Vol. 68, No. 7, pp. 1284–1287, 1965.

25. Hofmann, A. W., and O. Olshausen, “Ueber die Isomeren der Cyanursäure-Aether”, *Berichte der Deutschen Chemischen Gesellschaft*, Vol. 3, No. 1, pp. 269–276, 1870.

26. Klason, P., “Ueber Cyanursäure, Di- und Trithiocyanursäure”, *Journal für Praktische Chemie*, Vol. 33, No. 1, pp. 116–132, 1886.

27. Schaefer, F. C., J. R. Dudley, and J. T. Thurston, “Cyanuric Chloride Derivatives. VI. Rearrangement Reactions of 2,4-Dialkoxy-6-Amino-*s*-Triazines”, *Journal of the American Chemical Society*, Vol. 73, No. 7, pp. 2996–2999, 1951.

28. Bacon, W. E., J.-L. Kuo, and G. H. Brown, “Nematic Solvent Effects in the Isomerization of 2,4,6-Trimethoxy-s-Triazine”, *Molecular Crystals and Liquid Crystals*, Vol. 56, No. 1, pp. 13–17, 1979.

29. Paoloni, L., M. L. Tosato, and M. Cignitti, “Tautomeric Forms of Oxy- and Oxo-Derivatives of 1,3,5-Triazine. Part VI. Isomerization Mechanism and Thermal Stability of the Methyl Esters of Cyanuric Acid”, *Journal of Heterocyclic Chemistry*, Vol. 5, No. 4, pp. 533–544, 1968.

30. Kaftory, M., *Organic Solid-State Reactions*, Springer, Dordrecht, 2002.

31. Kaftory, M., and E. Handelsman-Benory, “Thermal Rearrangement of Cyanurates in the Solid State”, *Molecular Crystals and Liquid Crystals Science and Technology, Section A: Molecular Crystals and Liquid Crystals*, Vol. 240, No. 1, pp. 241–249, 1994.

32. Taycher, H., M. Botoshansky, V. Shteiman, and M. Kaftory, “Alkyl Rearrangement of Derivatives of 2-Anilino-4,6-Dialkoxy-1,3,5-Triazines in the Solid- and Liquid-State”, *Supramolecular Chemistry*, Vol. 13, No. 1, pp. 181–192, 2001.

33. Harrington, P. J., and I. H. Sanchez, “Application of the Cyanurate-Isocyanurate Rearrangement to Amine Synthesis: Preparation of 2-(2-Thienyl)Ethylamine”, *Synthetic Communications*, Vol. 23, No. 9, pp. 1307–1314, 1993.

34. Higashihara, T., M.-C. Fu, T. Uno, and M. Ueda, “Synthesis and Characterization of Polycyanurates as Dismantlable Adhesives”, *Journal of Polymer Science Part A: Polymer Chemistry*, Vol. 54, No. 8, pp. 1153–1158, 2016.

35. Saito, Y., H. Matsumoto, T. Higashihara, and M. Ueda, “Synthesis of Transparent and Thermally Stable Polycyanurates and Their Thermal Rearrangement”, *Journal of Polymer Science Part A: Polymer Chemistry*, Vol. 51, No. 18, pp. 3950–3955, 2013.

36. Tsuchiya, K., Y. Ishida, T. Higashihara, A. Kameyama, and M. Ueda, “Refractive Index Modulation by Tunable Thermal Rearrangement of Polycyanurates”, *Chemistry Letters*, Vol. 44, No. 8, pp. 1110–1112, 2015.

37. Piron, F., C. Oprea, C. Cismaş, A. Terec, J. Roncali, and I. Grosu, “Synthesis of Podands with Cyanurate or Isocyanurate Cores and Terminal Triple Bonds”, *Synthesis*, 2010, No. 10, pp. 1639–1644.

38. Chapman, A. W., “Imino-Aryl Ethers. Part V. The Effect of Substitution on the Velocity of Molecular Rearrangement”, *J. Chem. Soc.*, 1927, pp. 1743–1751.

39. Ueda, M., H. Tomoya, S. Yoshitaka, O. Takahashi, and U. Takaaki, “Polymer Production Method and Polymer”, JP Patent JP2014185309A, Oct. 6, 2014. Available: https://patents.google.com/patent/JP2014185309A/en, Accessed on August 19, 2025.

40. Kamps, J. H., T. Hoeks, E. Kung, J. P. Lens, P. J. McCloskey, B. A. J. Noordover, and J. P. A. Heuts, “Activated Carbonates: Enabling the Synthesis of Differentiated Polycarbonate Resins via Melt Transcarbonation”, *Polymer Chemistry*, Vol. 7, No. 33, pp. 5294–5303, 2016.

41. Aerts, A., C. Kroonen, J. H. Kamps, R. P. Sijbesma, and J. P. A. Heuts, “High Molar Mass Polycarbonate via Dynamic Solution Transcarbonation Using Bis(methyl salicyl) Carbonate, an Activated Carbonate”, *Macromolecular Chemistry and Physics*, Vol. 222, No. 18, Article 2100186, 2021.

42. Tosato, M. L., “Systematic Analysis of Substituent Effects on the 13C Chemical Shifts of the Ring Carbons in Trimethyl-Cyanurates and -Thiocyanurates”, *Journal of the Chemical Society*, Perkin Transactions 2, No. 10, pp. 1593–1599, 1984.

43. Kissinger, H. E., “Variation of Peak Temperature with Heating Rate in Differential Thermal Analysis”, *Journal of Research of the National Bureau of Standards*, Vol. 57, No. 4, pp. 217–221, 1956.

44. Hamerton, I., B. J. Howlin, and D. A. Tilbrook, “Examining Structure–Property Relationships in Coatings Based on Substituted Linear Aromatic Polycyanurates” *Reactive and Functional Polymers*, Vol. 73, No. 8, pp. 1046–1057, 2013.

# APPENDIX A: SUPPLEMENTARY DATA

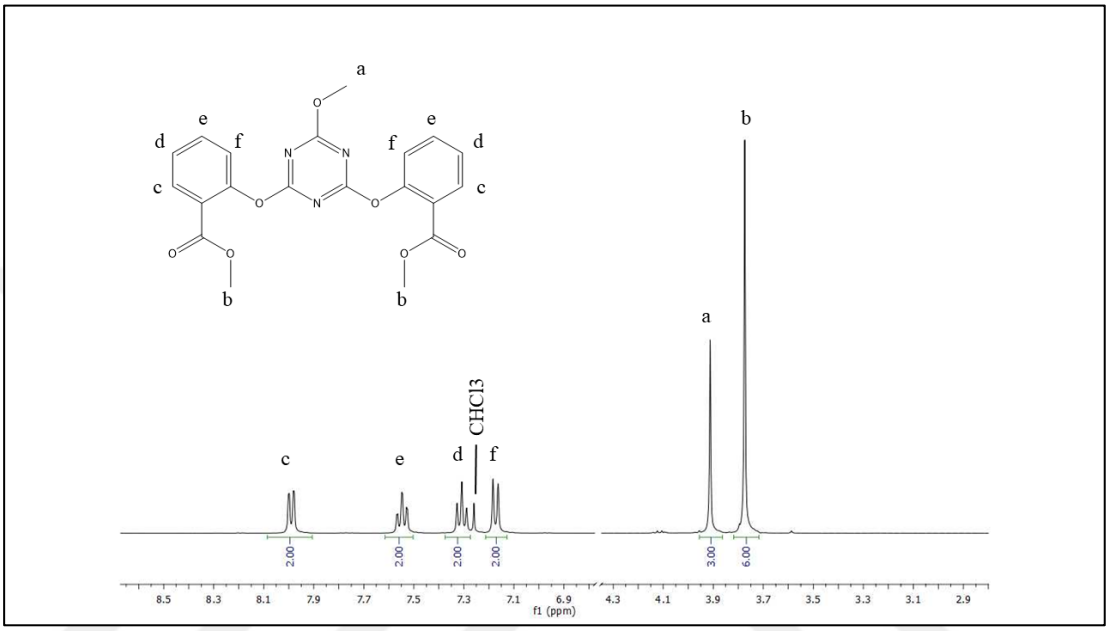



Figure A.1. $^{1}$H-NMR spectrum of MMST.

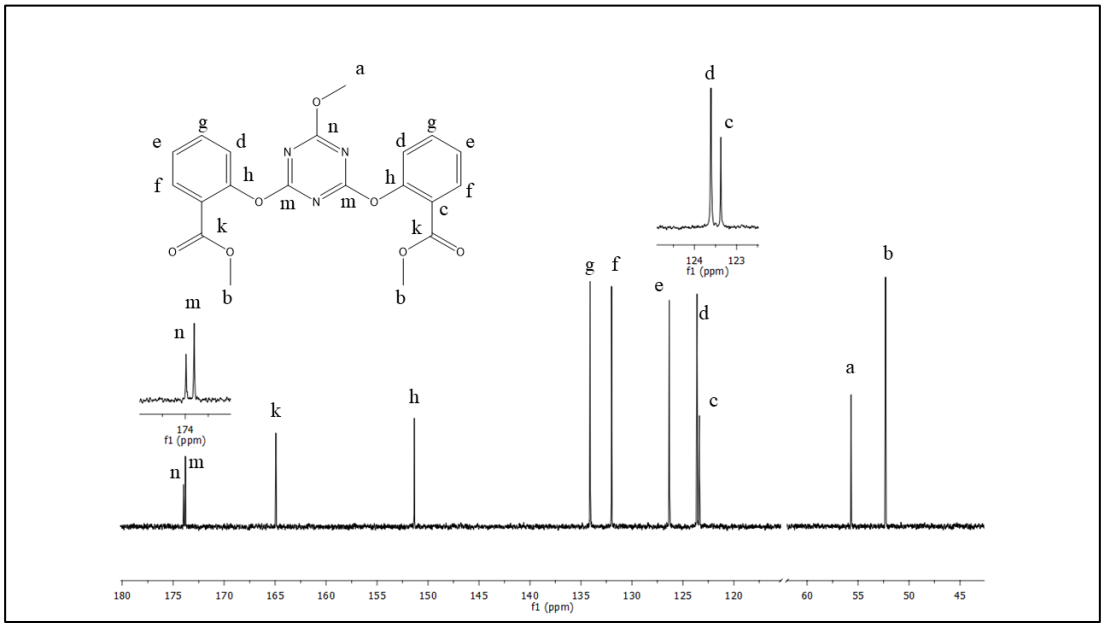



Figure A.2. $^{13}$C-NMR spectrum of MMST.

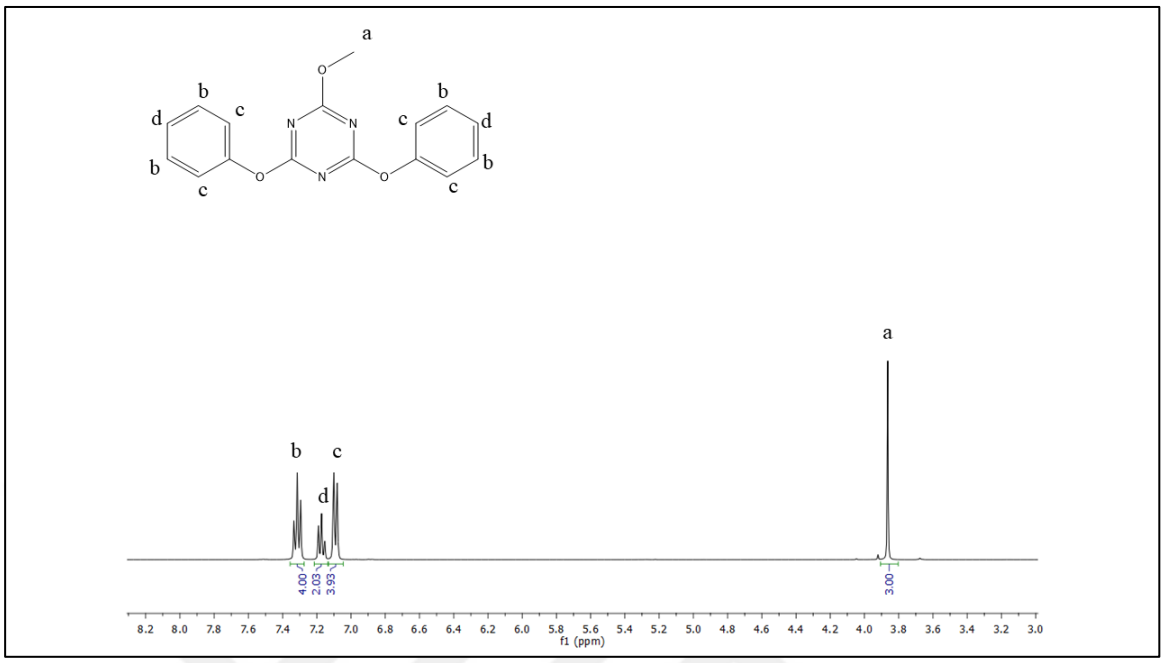



Figure A.3. $^{1}$H-NMR spectrum of MPhT.

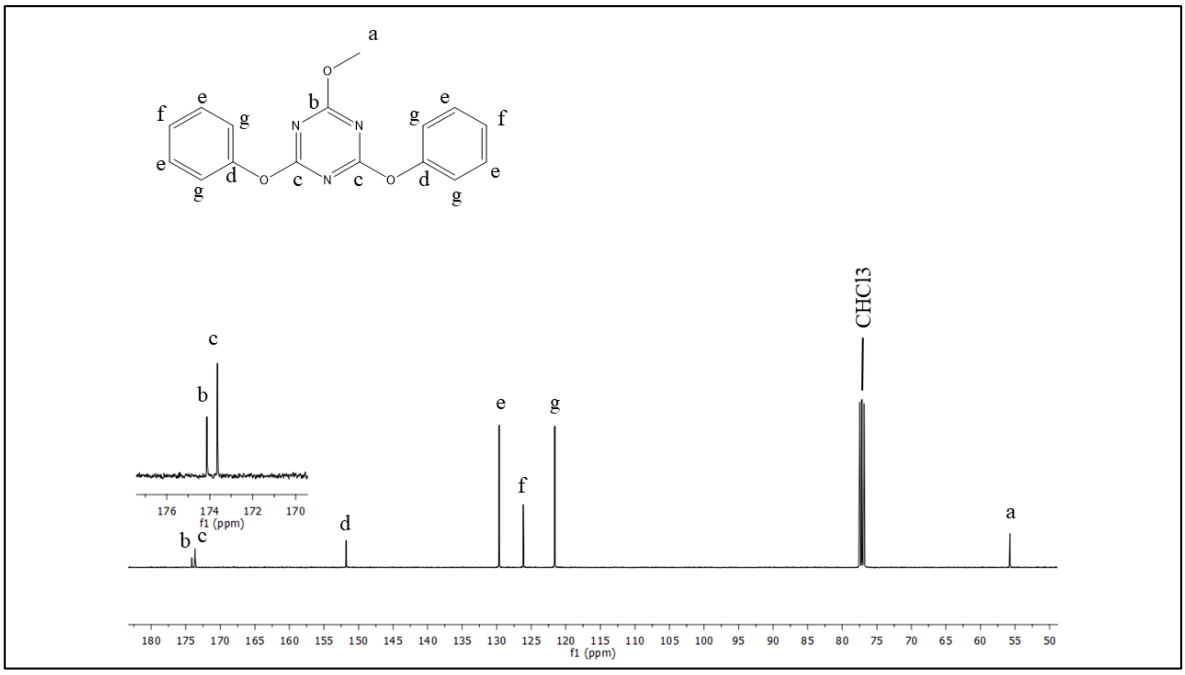



Figure A.4. $^{13}$C-NMR spectrum of MPhT.

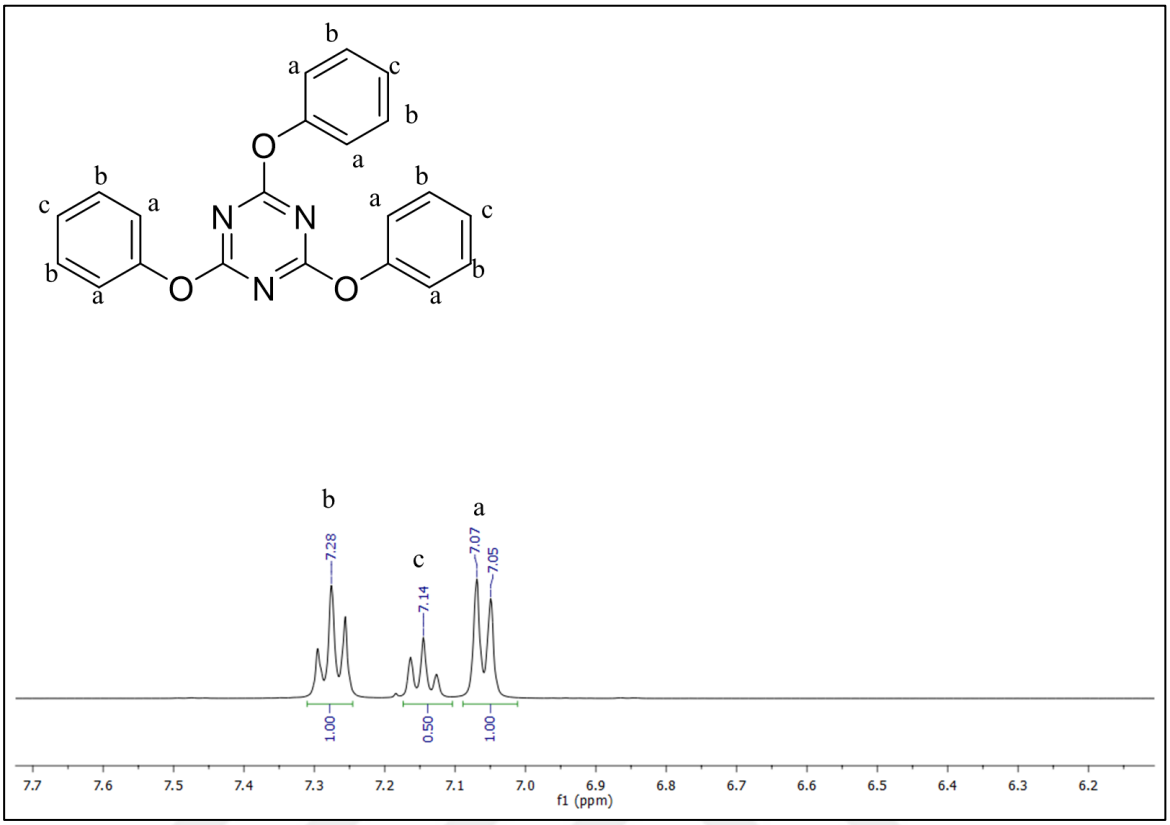



Figure A.5. $^{1}$H-NMR spectrum of TPT.

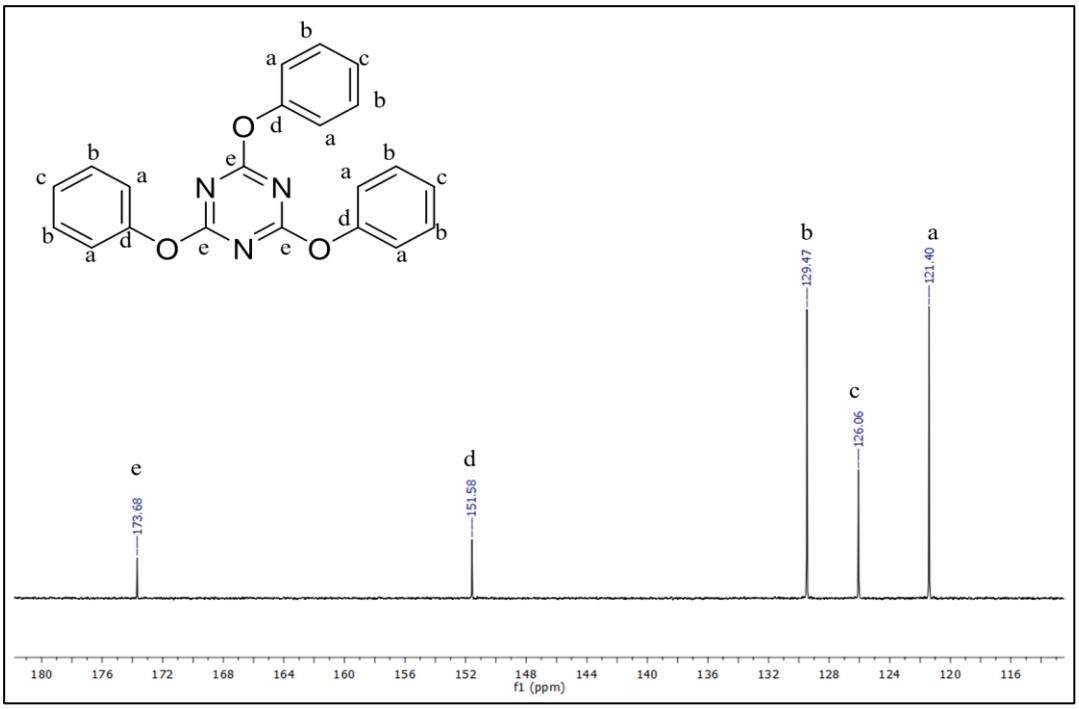



Figure A.6. $^{13}$C-NMR spectrum of TPT.

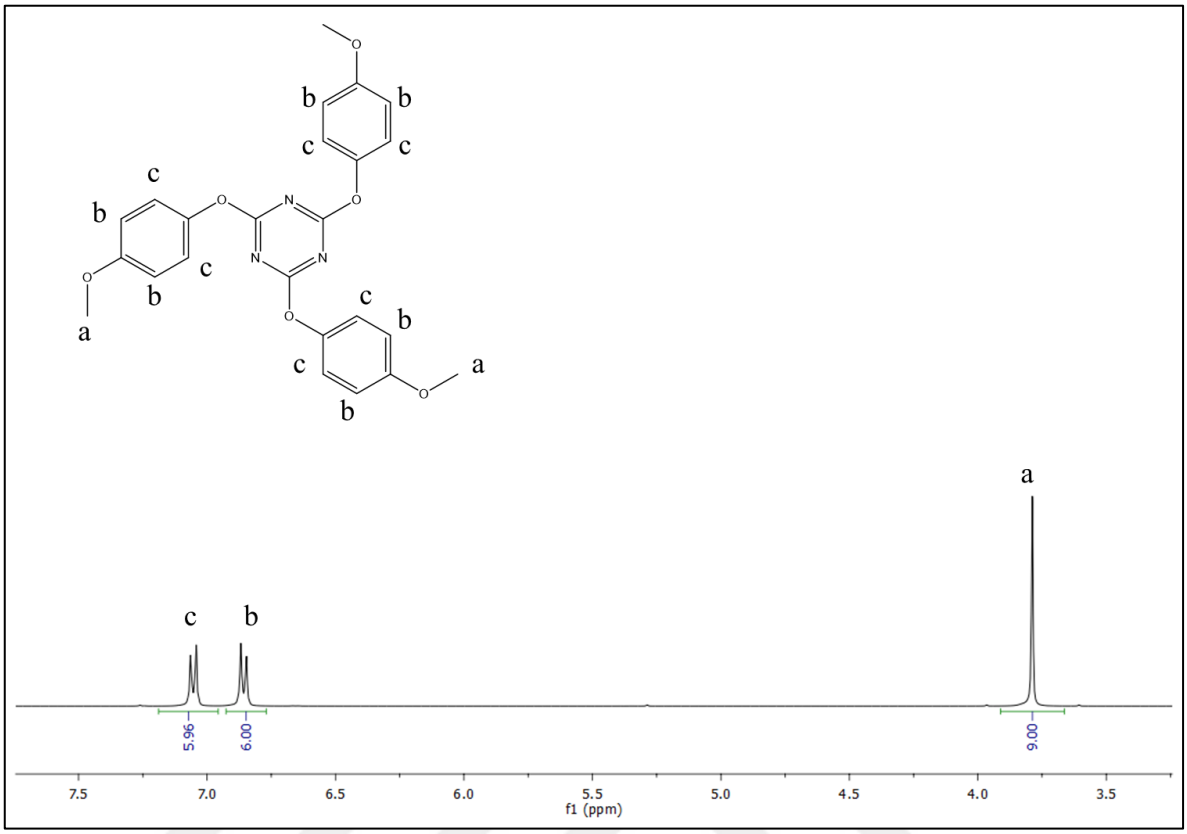



Figure A.7. $^{1}$H-NMR spectrum of TMT.

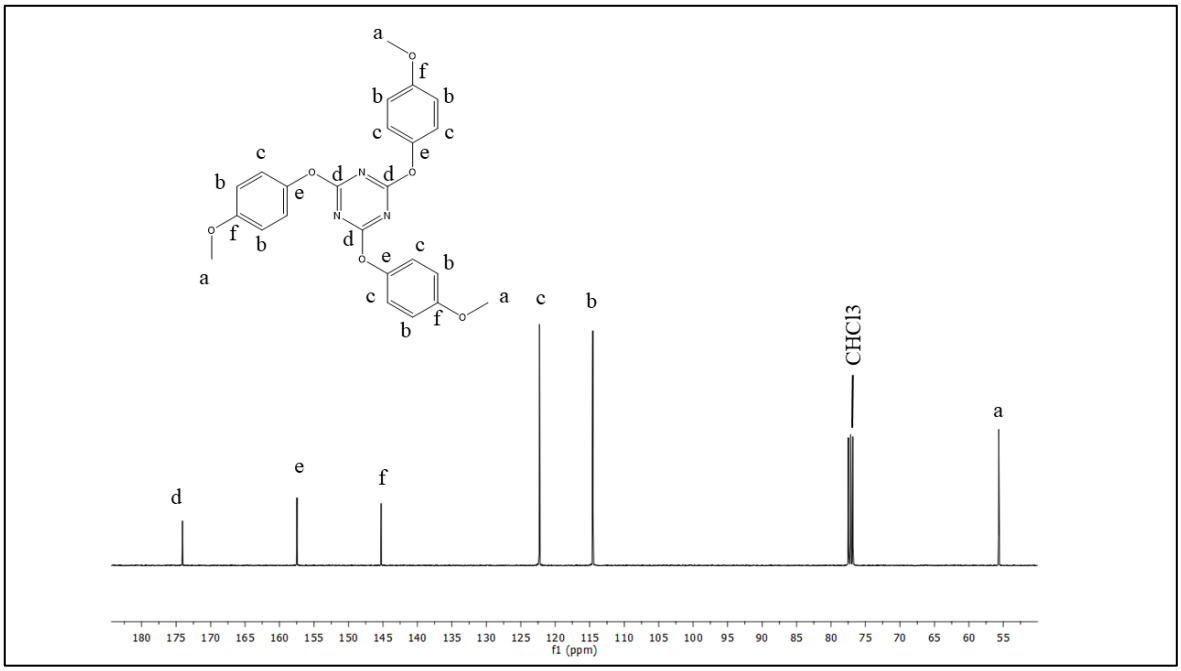



Figure A.8. $^{13}$C-NMR spectrum of TMT.

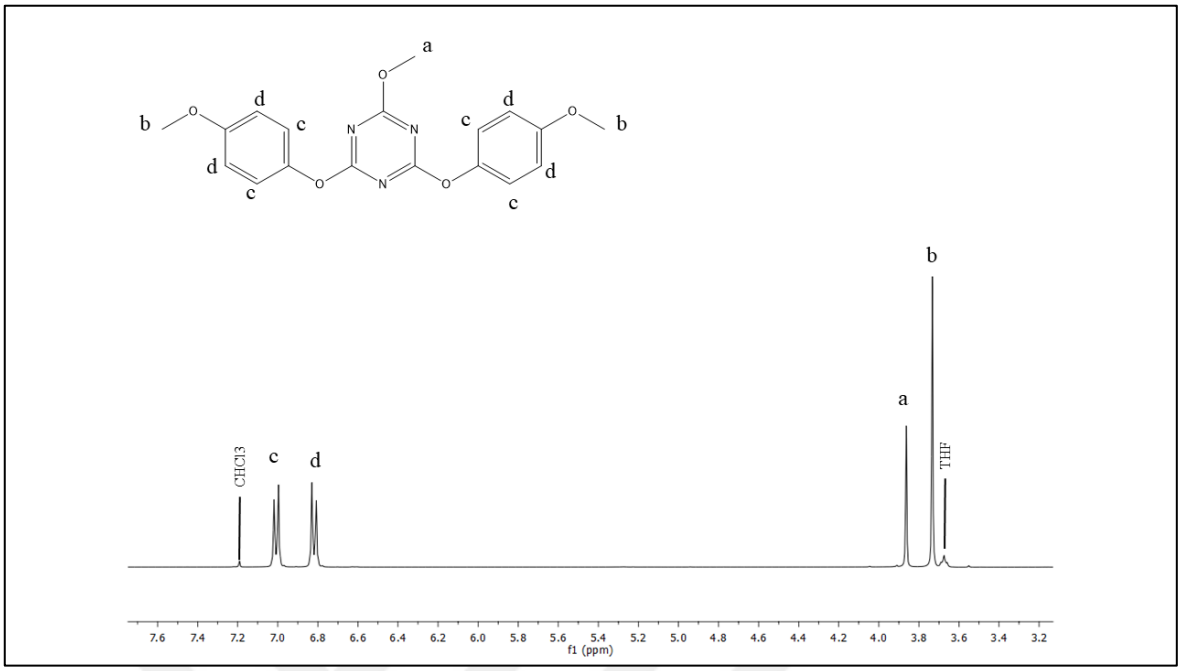



Figure A.9. $^{1}$H-NMR spectrum of MDMT.

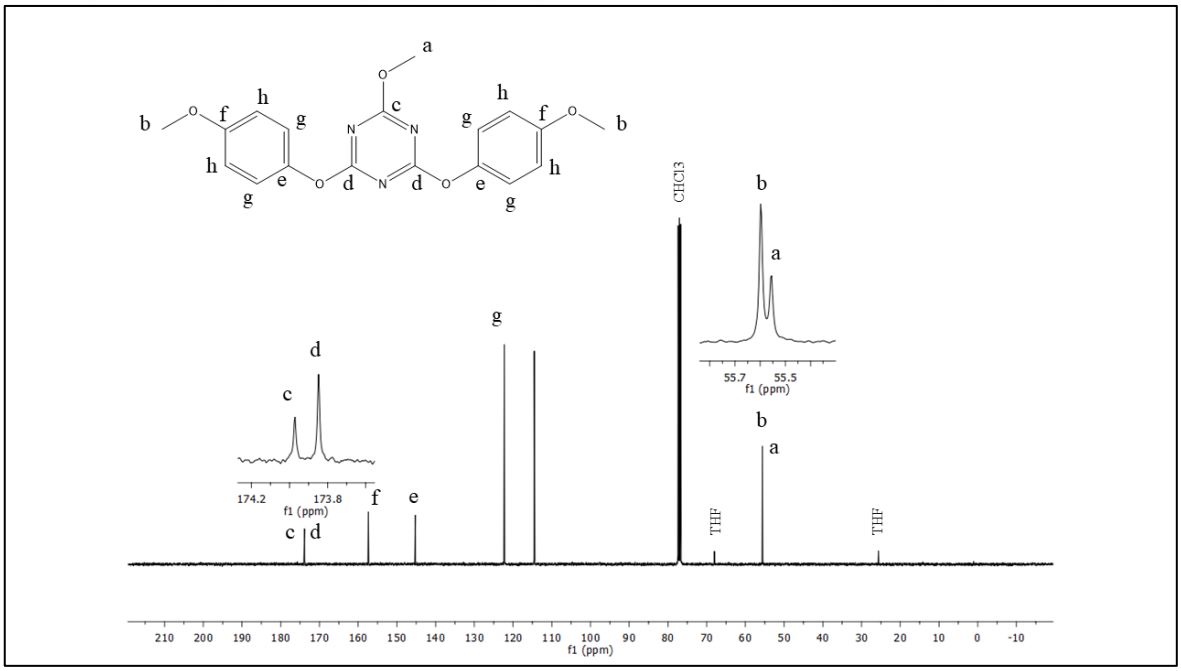



Figure A.10. $^{13}$C-NMR spectrum of MDMT.

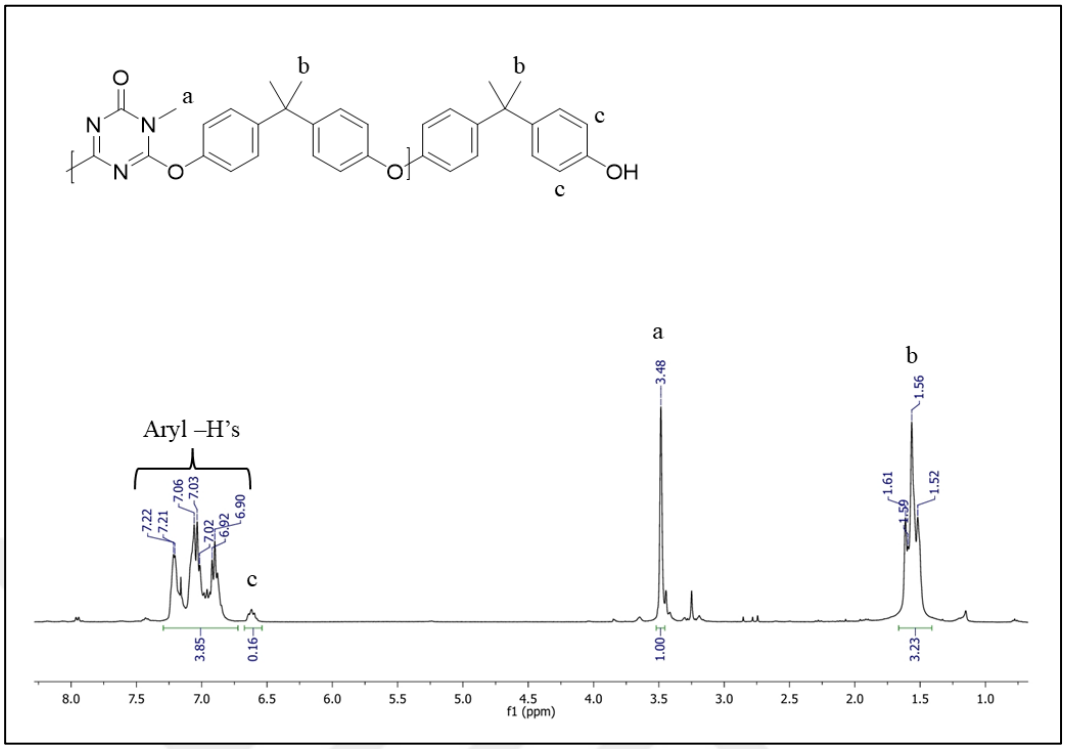



Figure A.11. $^{1}$H-NMR spectrum of P1.

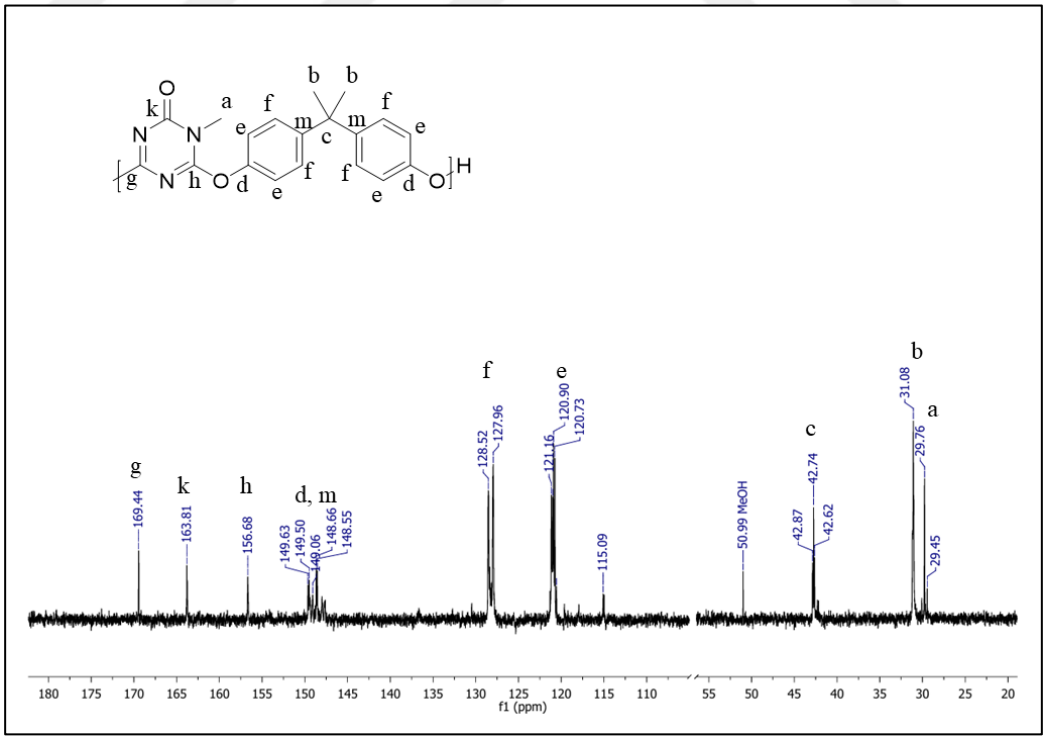



Figure A.12. $^{13}$C-NMR spectrum of P1.

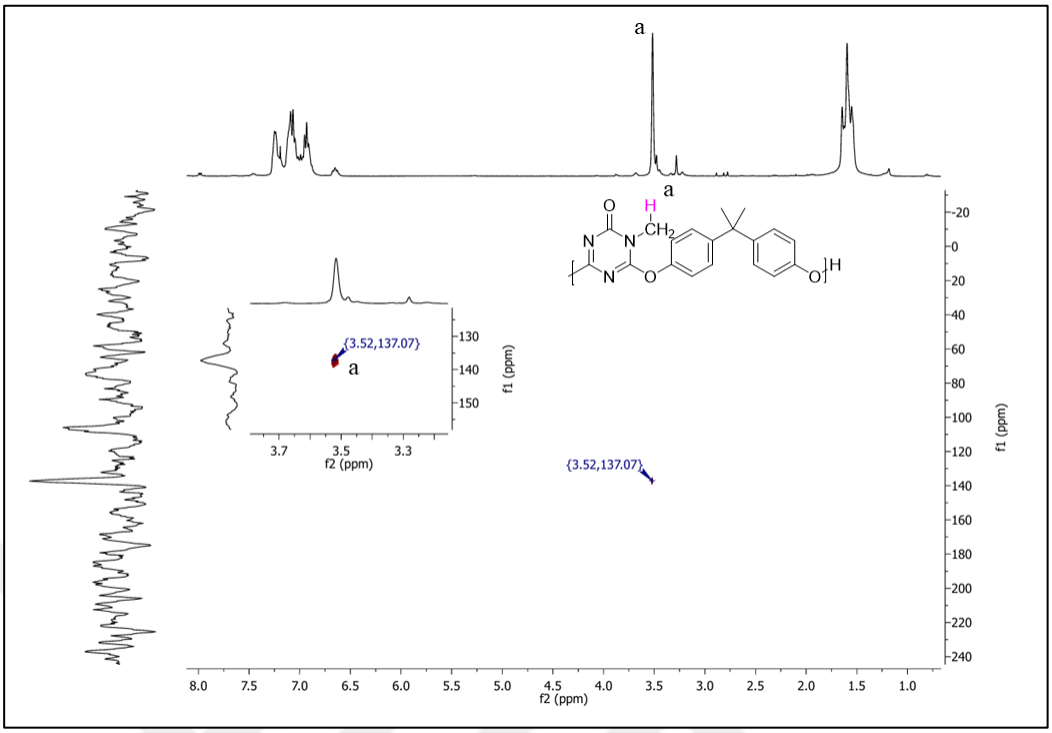



Figure A.13. $^{15}$N-$^{1}$H HMBC NMR spectrum of P1.

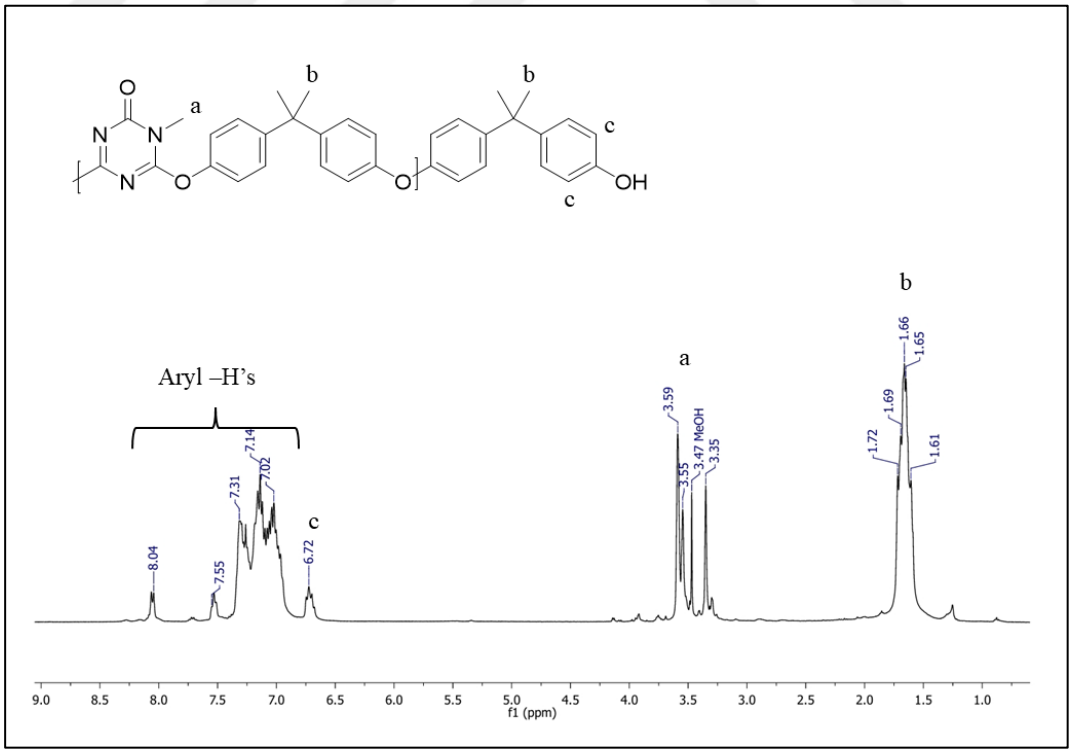



Figure A.14. $^{1}$H-NMR spectrum of P2.

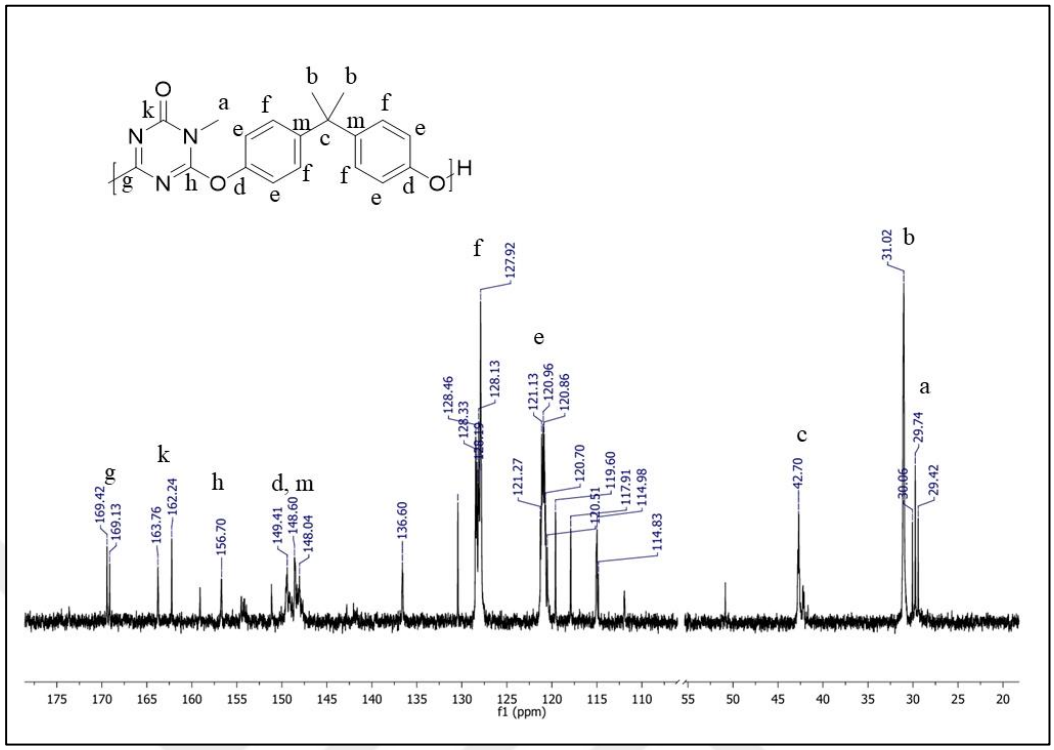



Figure A.15. $^{13}$C-NMR spectrum of P2.

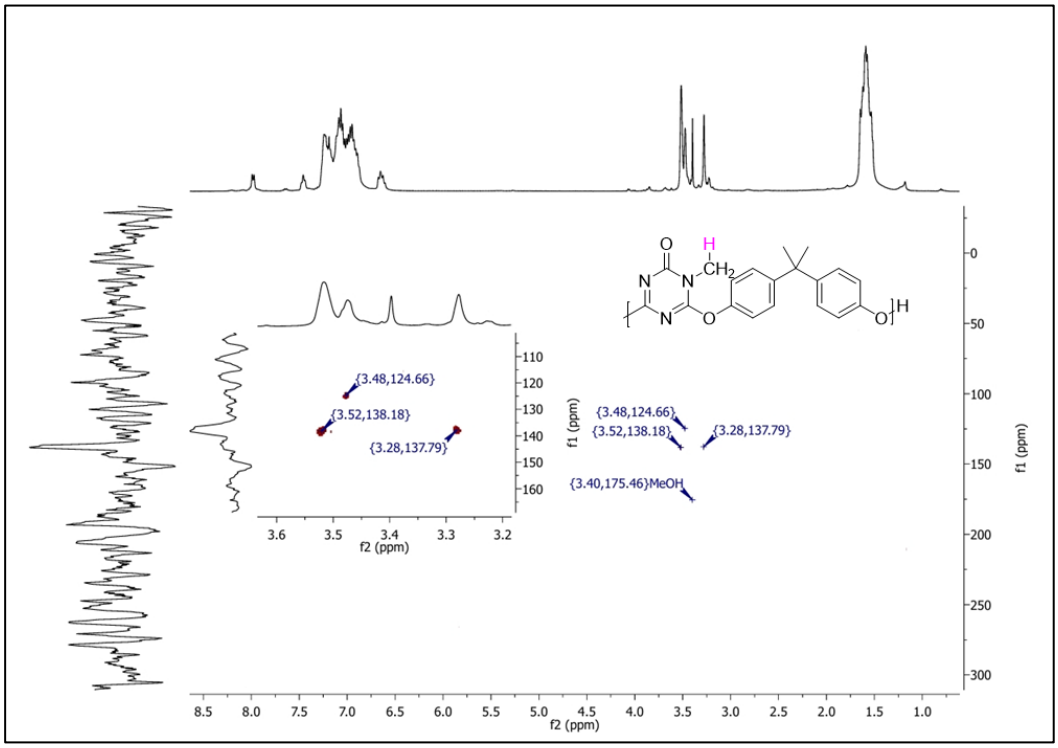



Figure A.16. $^{15}$N-$^{1}$H HMBC NMR spectrum of P2.

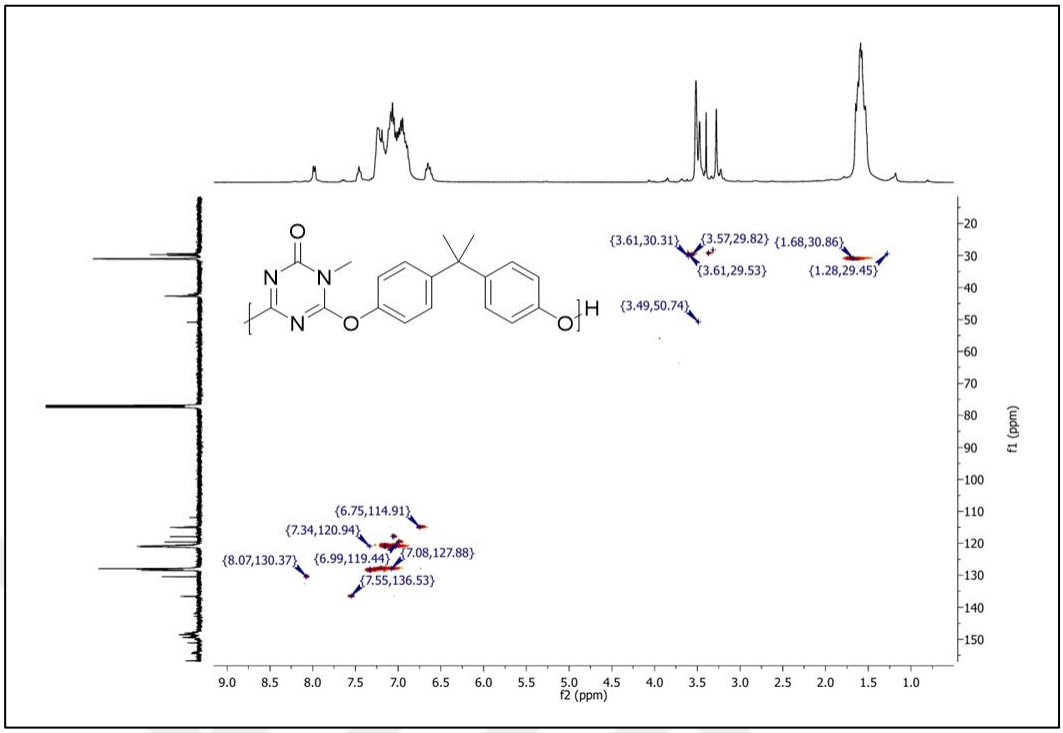



Figure A.17. $^{1}H$-$^{13}C$ HSQC NMR spectrum of P2.

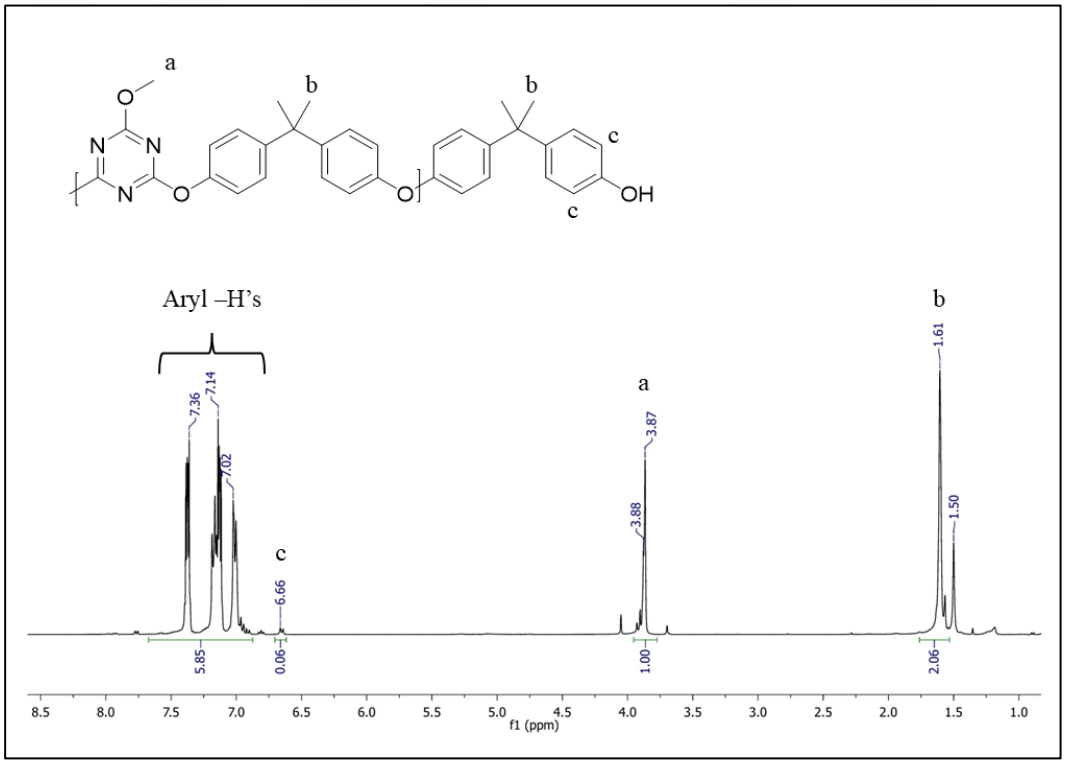



Figure A.18. $^{1}H$-NMR spectrum of SP.

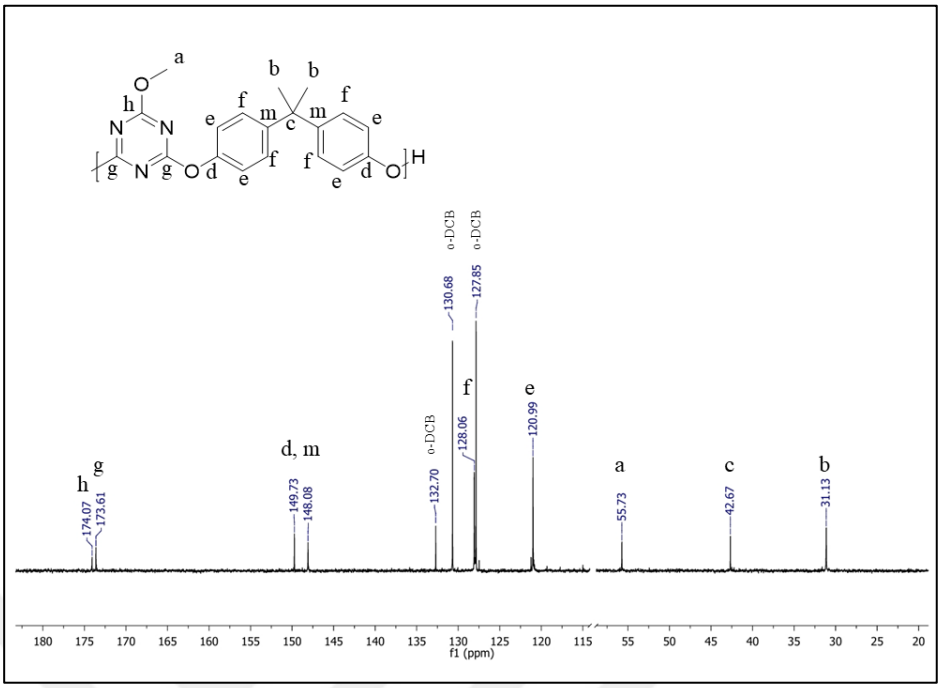



Figure A.19. $^{13}$C-NMR spectrum of SP.

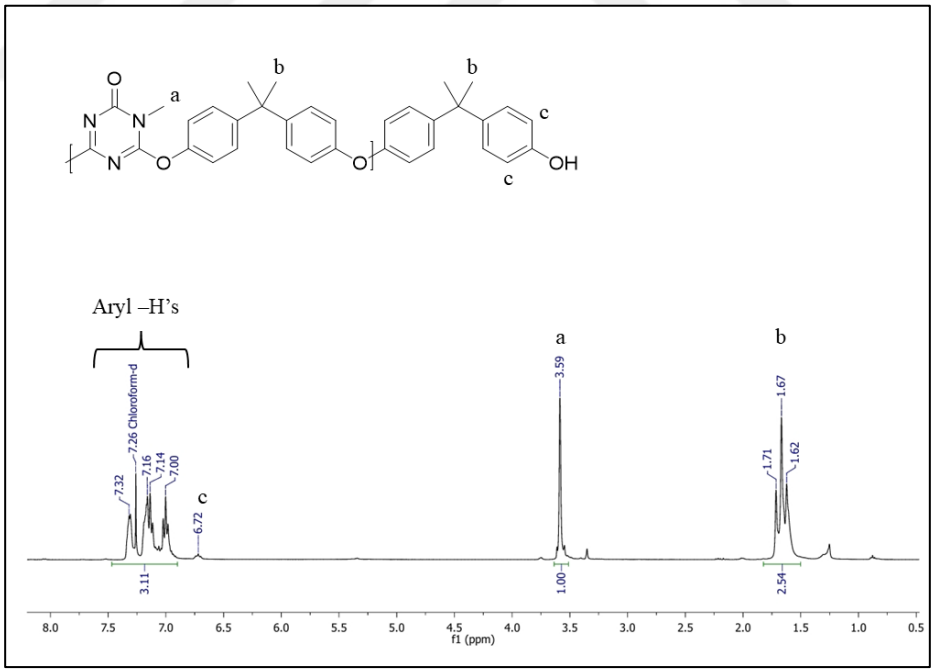



Figure A.20. $^{1}$H-NMR spectrum of thermally rearranged SP.

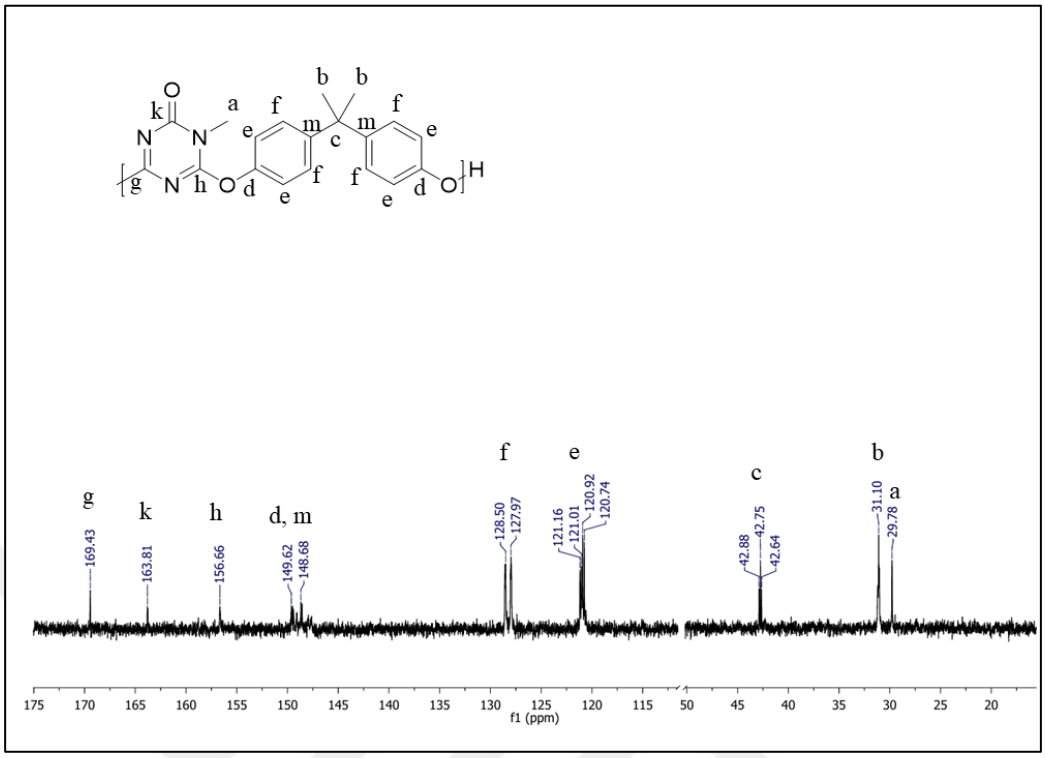



Figure A.21. $^{13}$C-NMR spectrum of thermally rearranged SP.

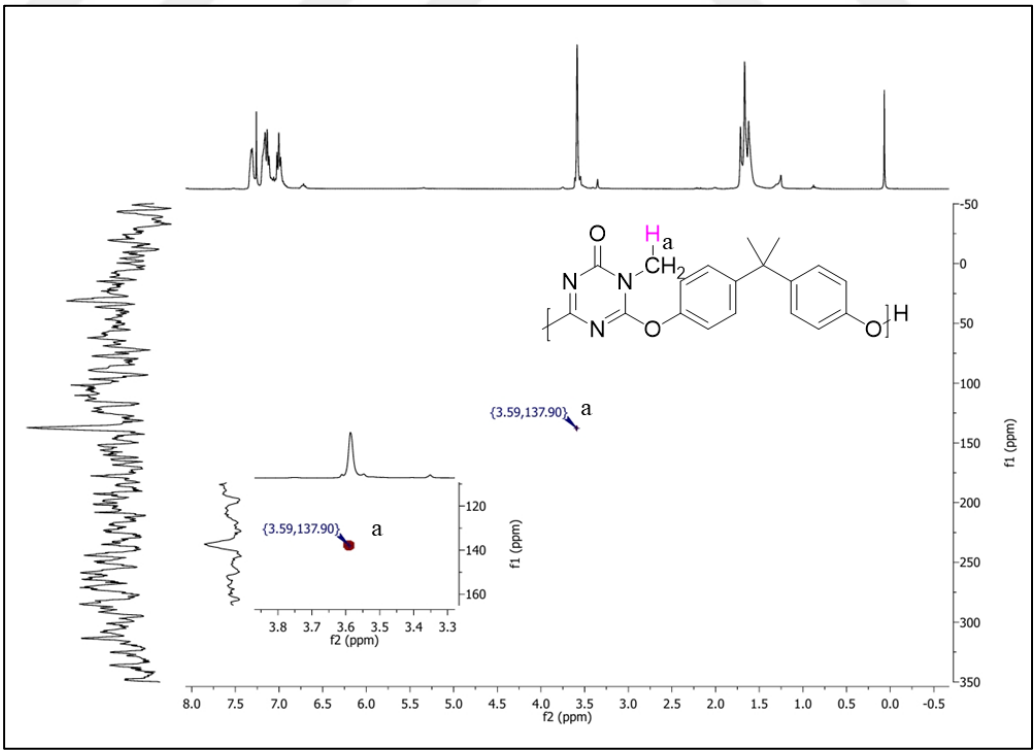



Figure A.22. $^{15}$N-$^{1}$H HMBC NMR spectrum of thermally rearranged SP.

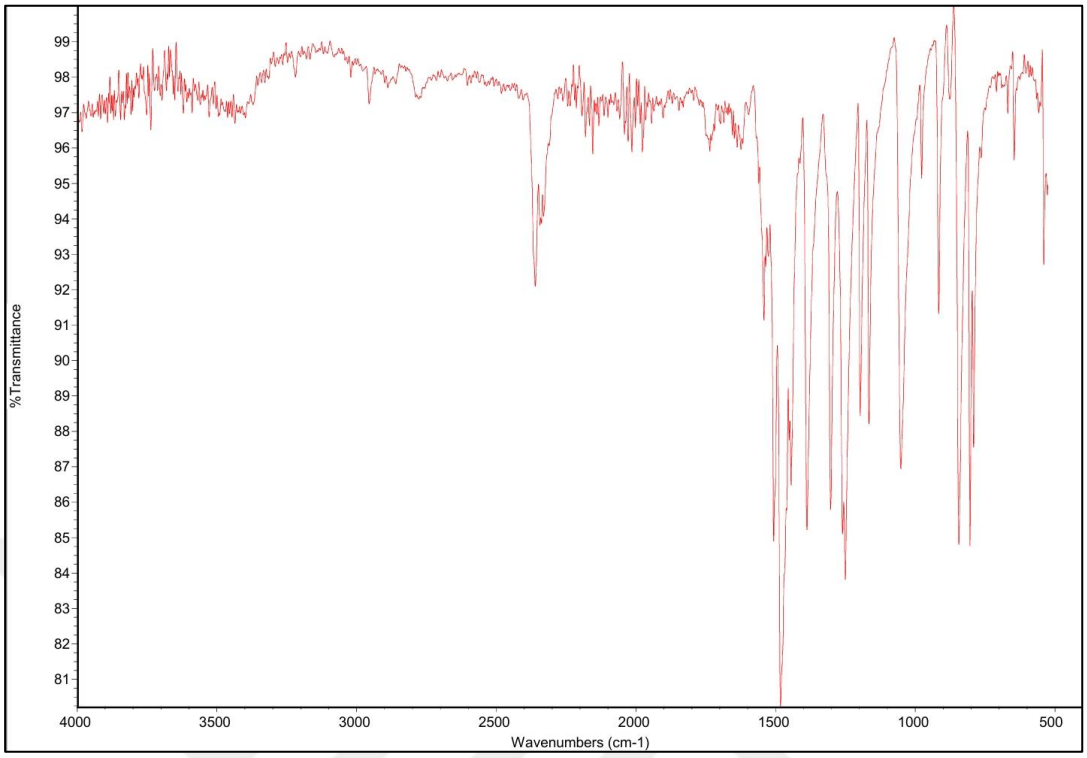



Figure A.23. FTIR spectrum of ST.

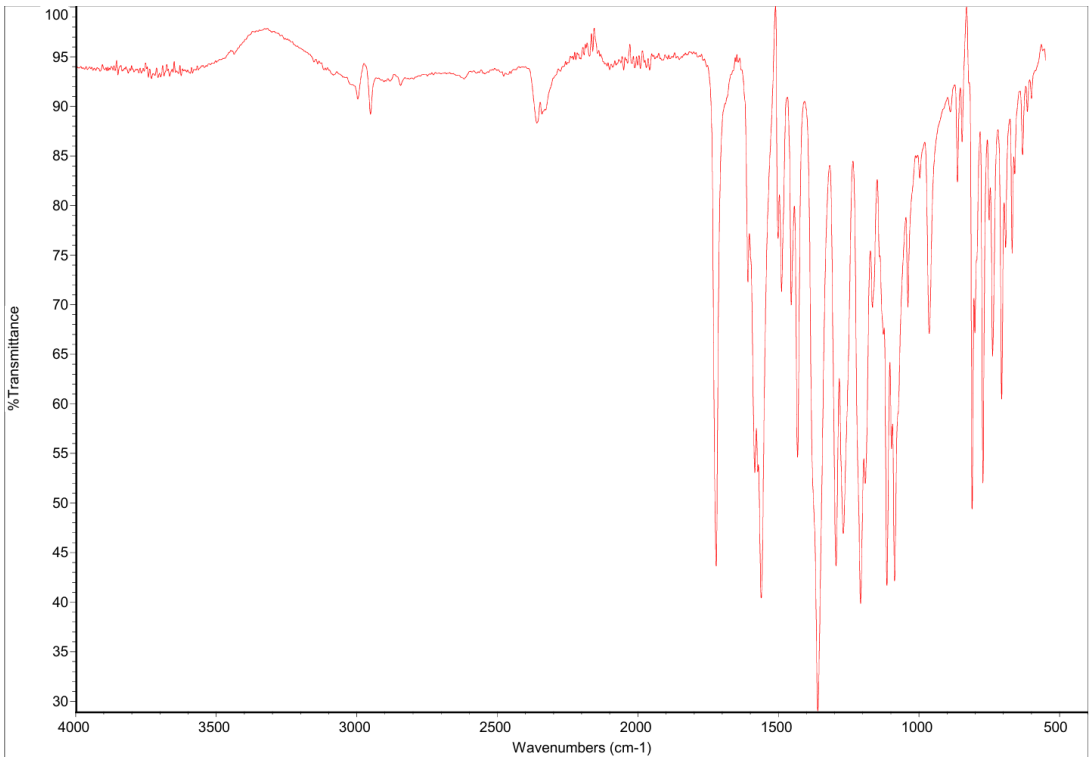



Figure A.24. FTIR spectrum of MMST.

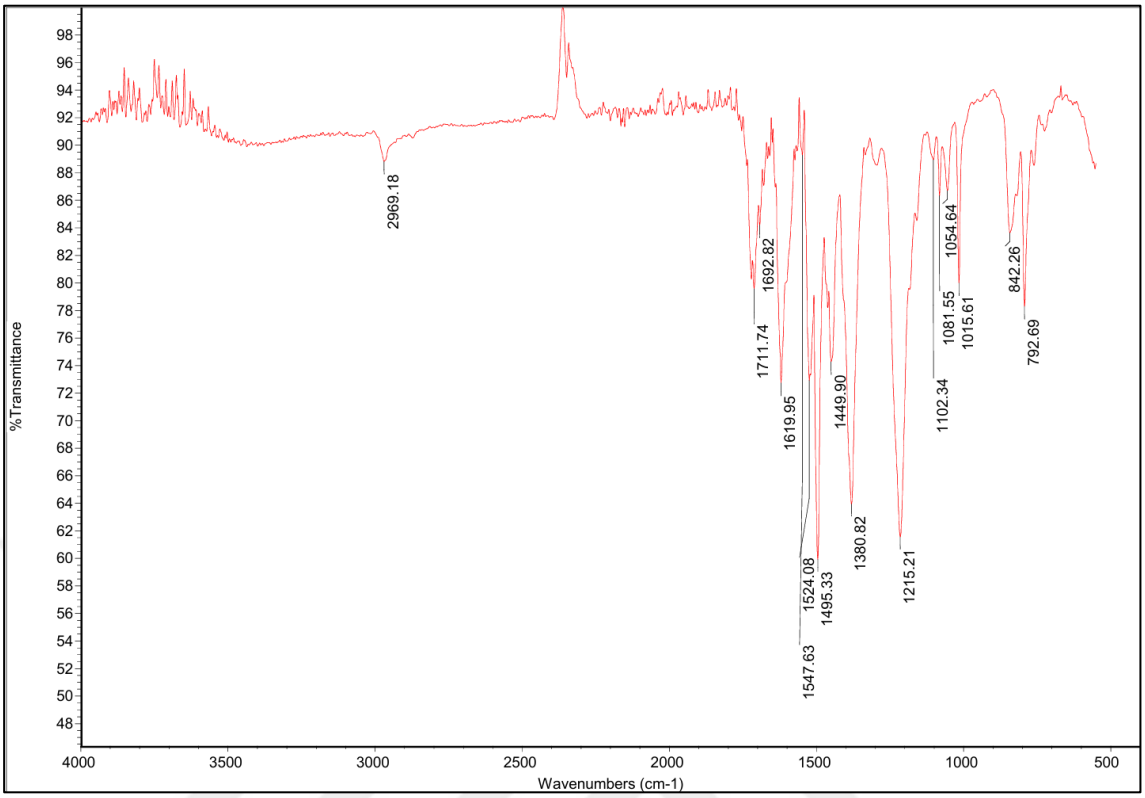



Figure A.25. FTIR spectrum of P1.

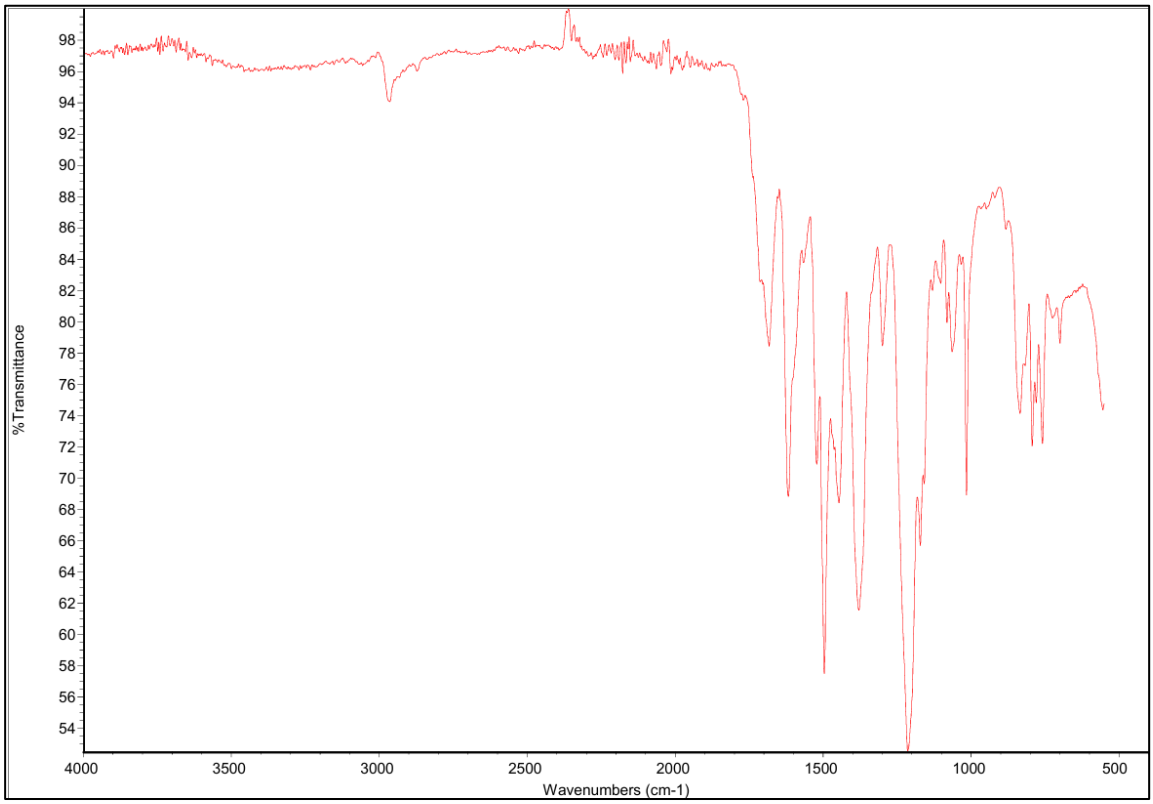



Figure A.26. FTIR spectrum of P2.

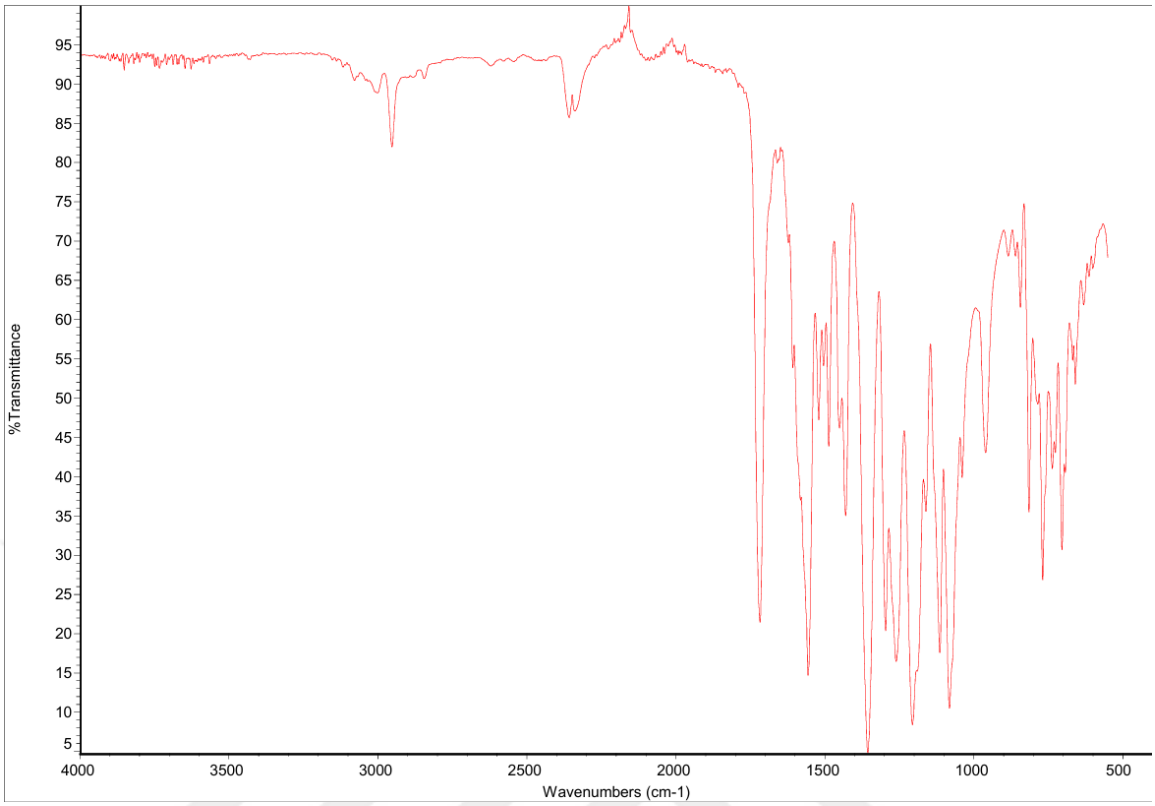



Figure A.27. FTIR spectrum of MMST heated for 10 minutes at 240 °C.

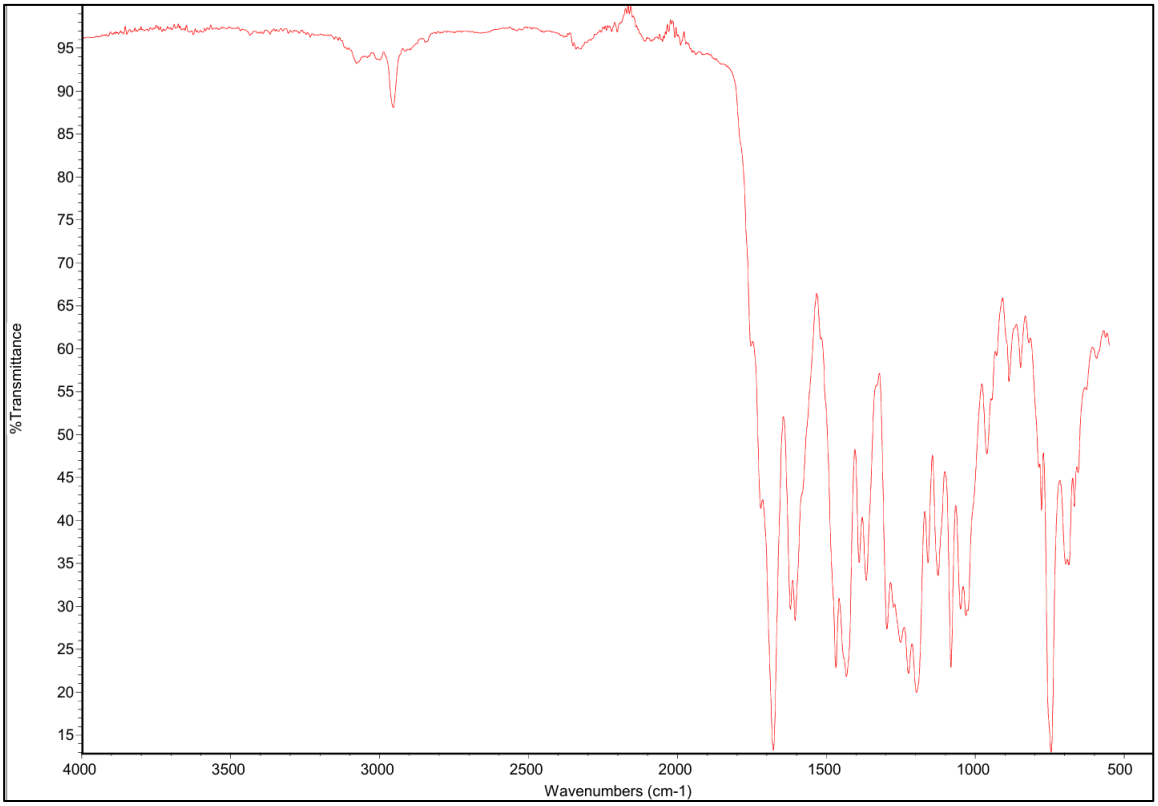



Figure A.28. FTIR spectrum of MMST heated for 30 minutes at 240 °C.

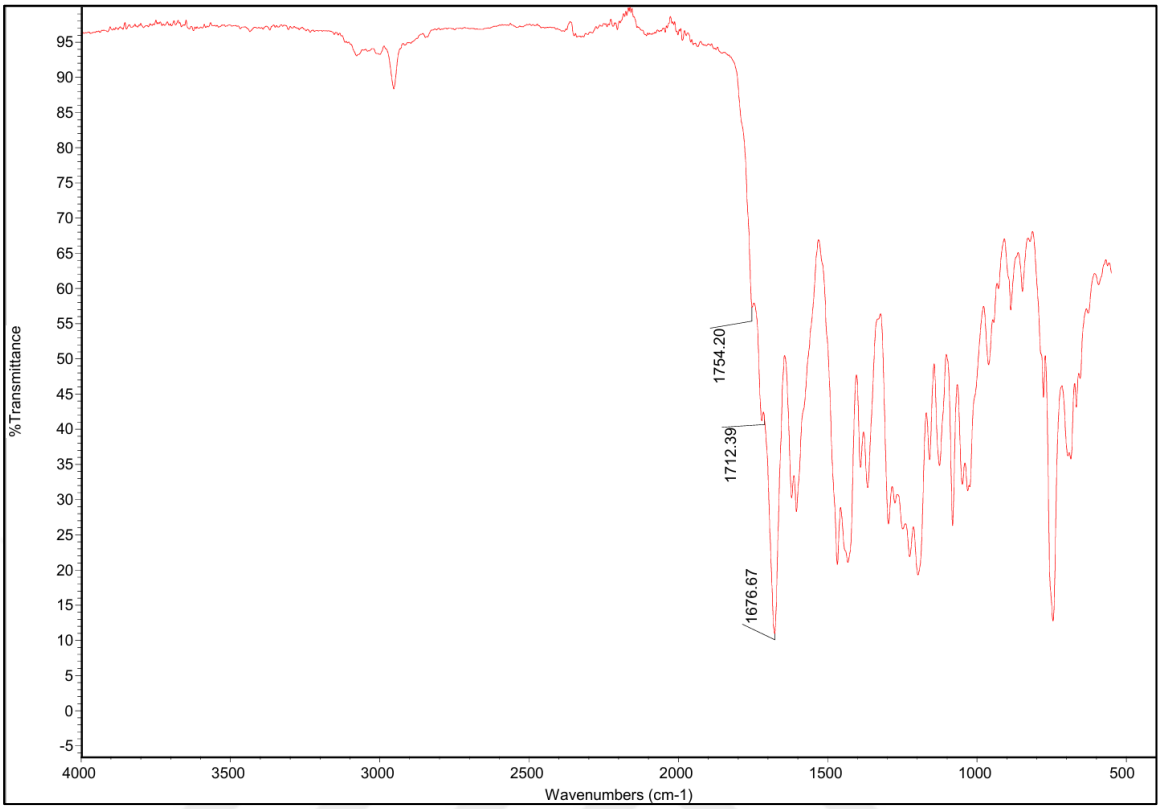



Figure A.29. FTIR spectrum of MMST heated for 45 minutes at 240 °C.

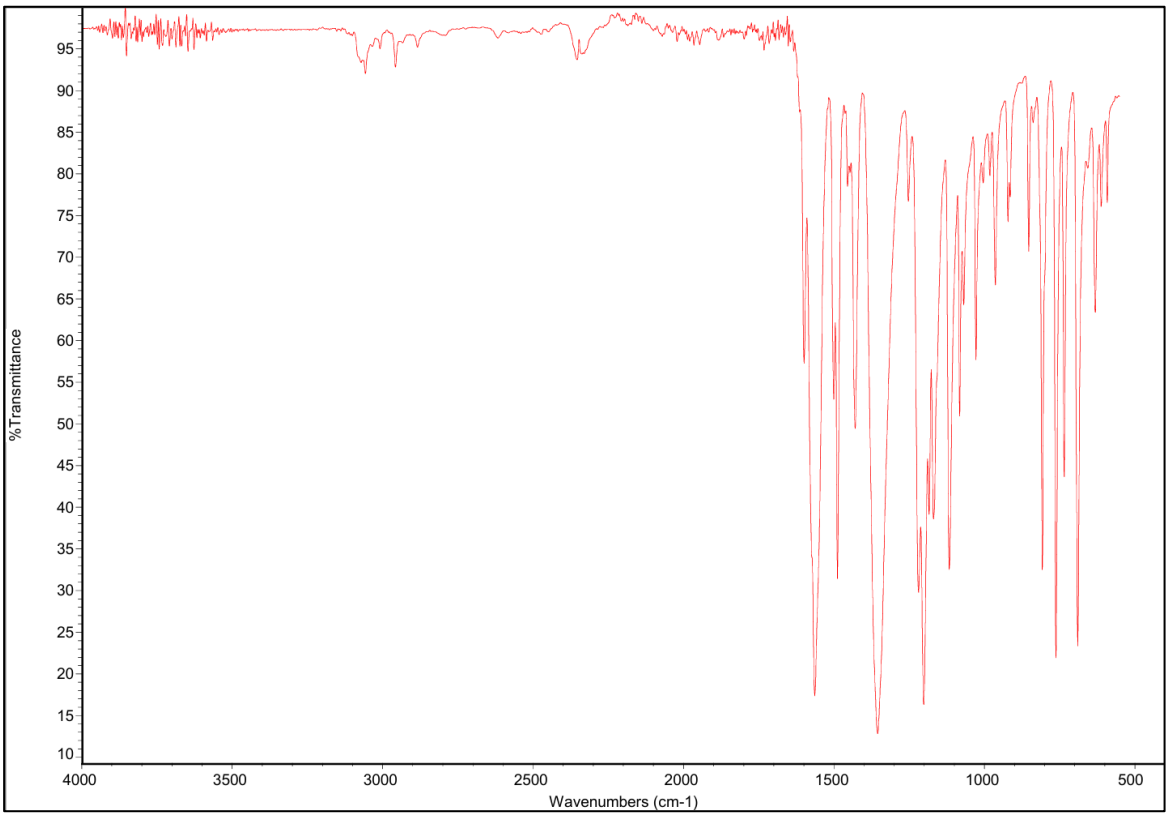



Figure A.30. FTIR spectrum of MPhT.

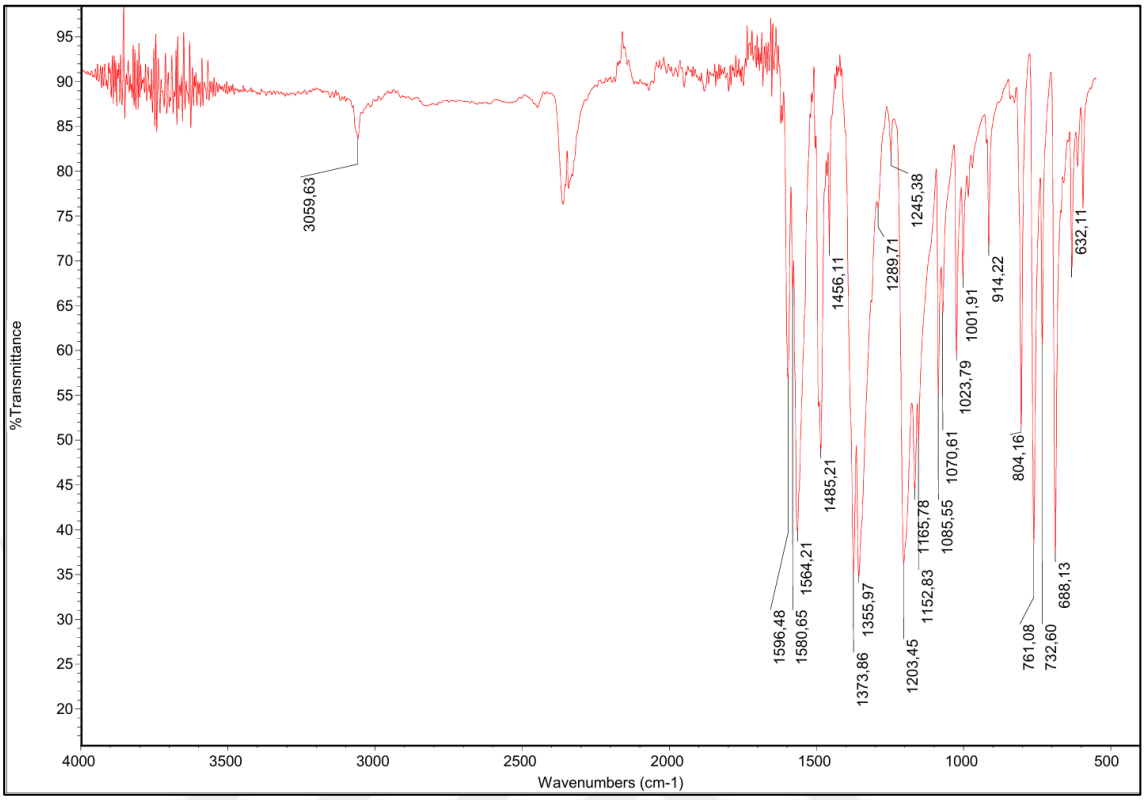



Figure A.31. FTIR spectrum of TPT.

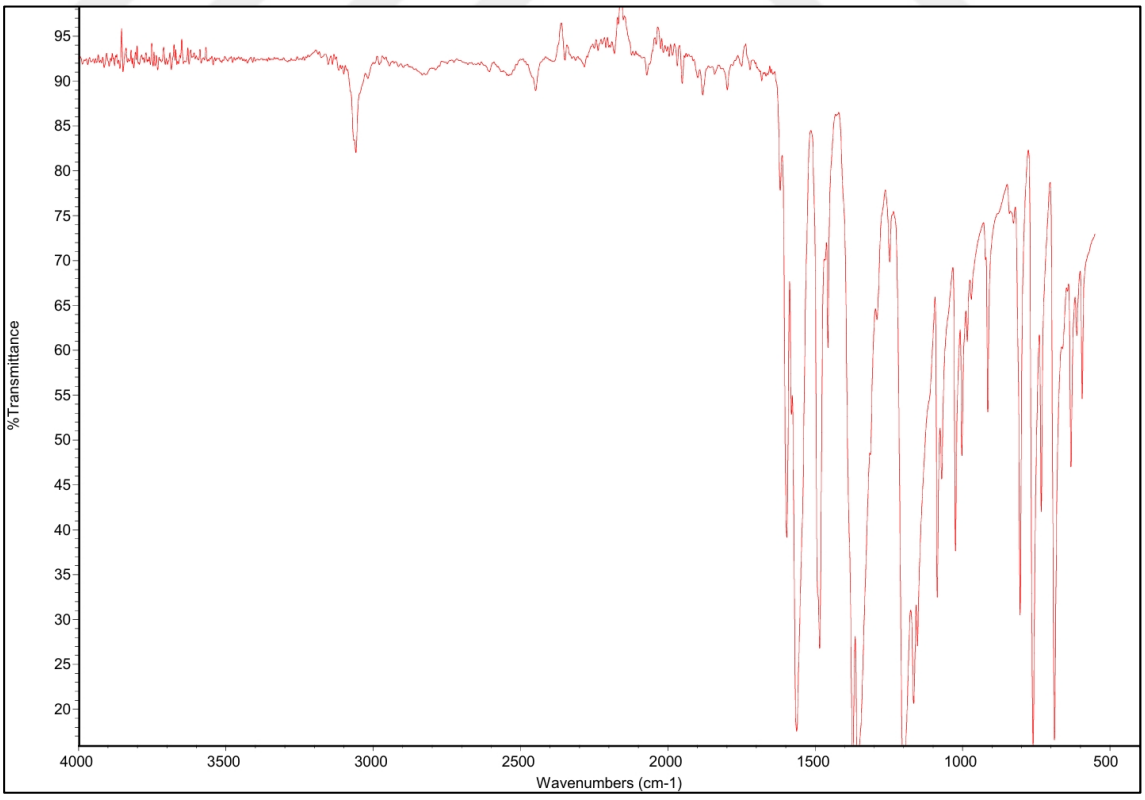



Figure A.32. FTIR spectrum of TPT heated for 90 minutes.

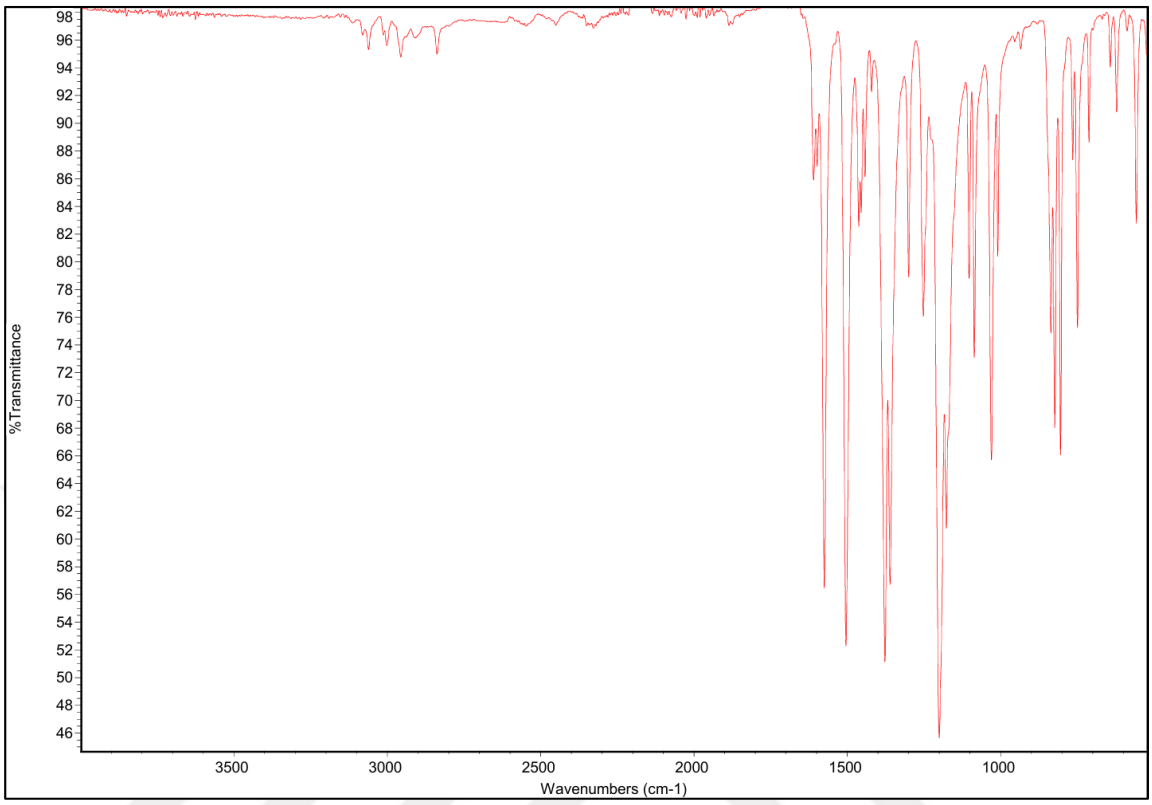



Figure A.33. FTIR spectrum of TMT.

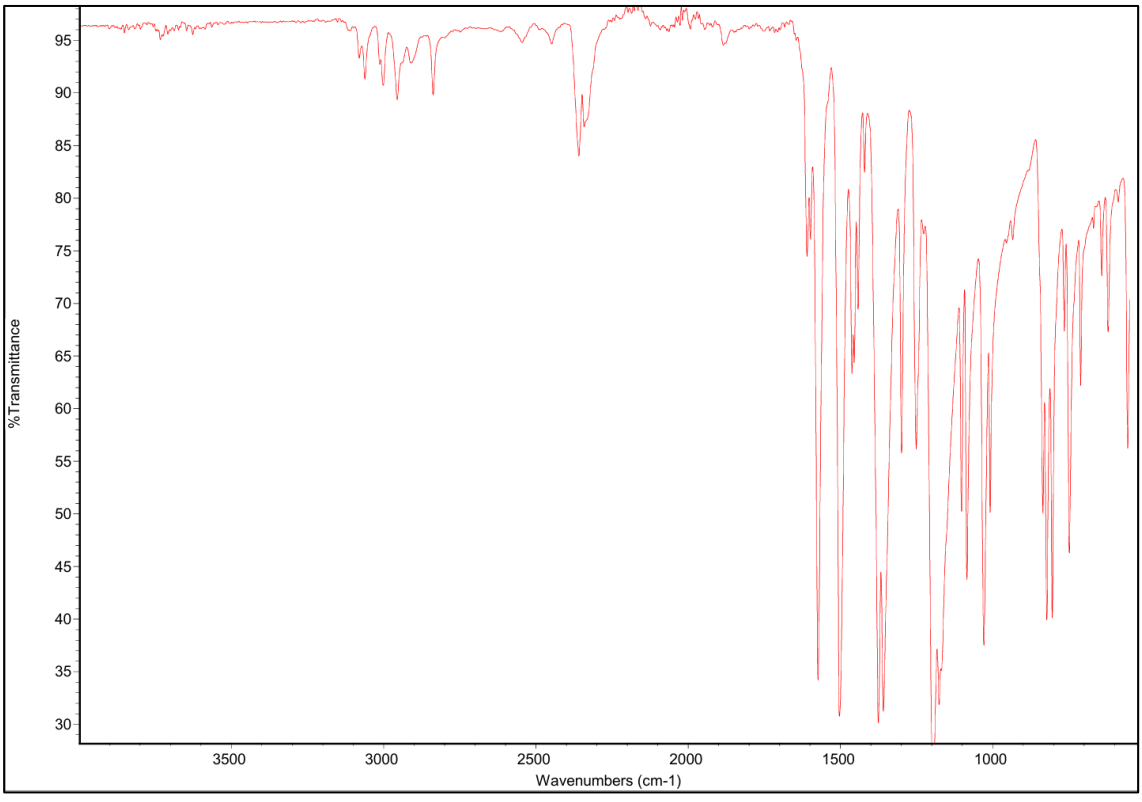



Figure A.34. FTIR spectrum of TMT heated for 60 minutes.

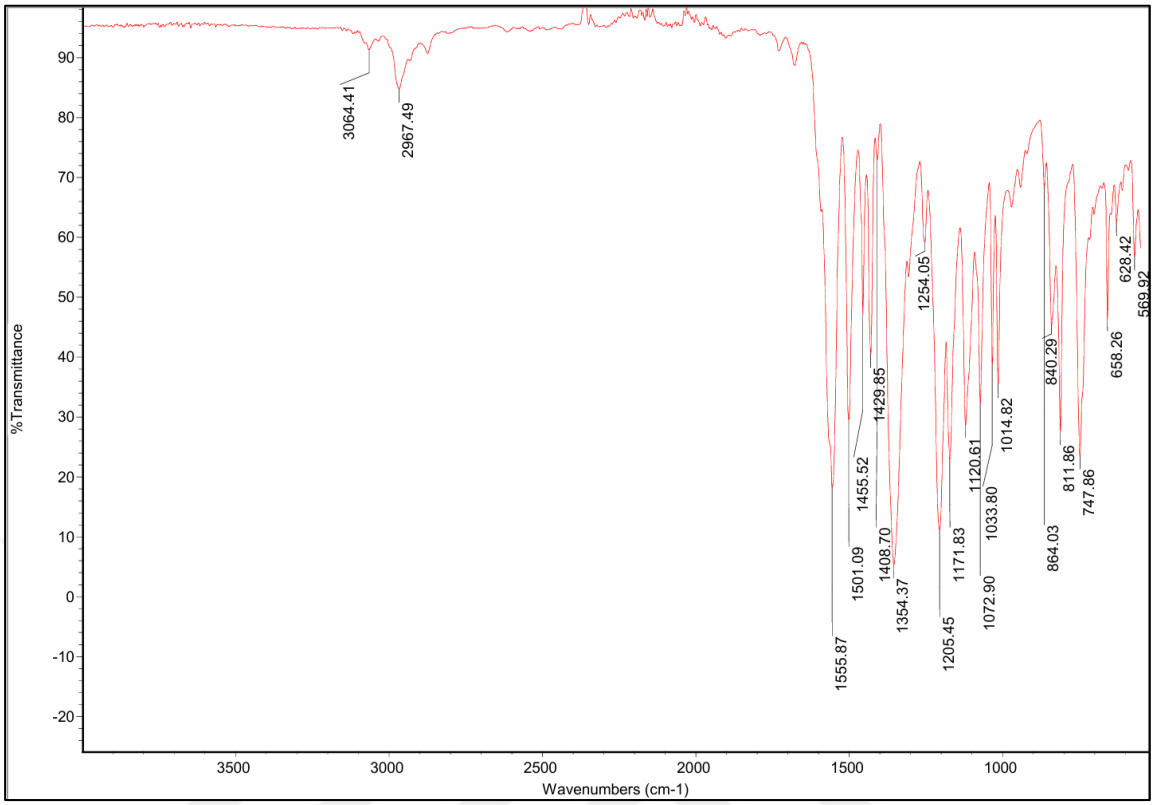



Figure A.35. FTIR spectrum of SP.

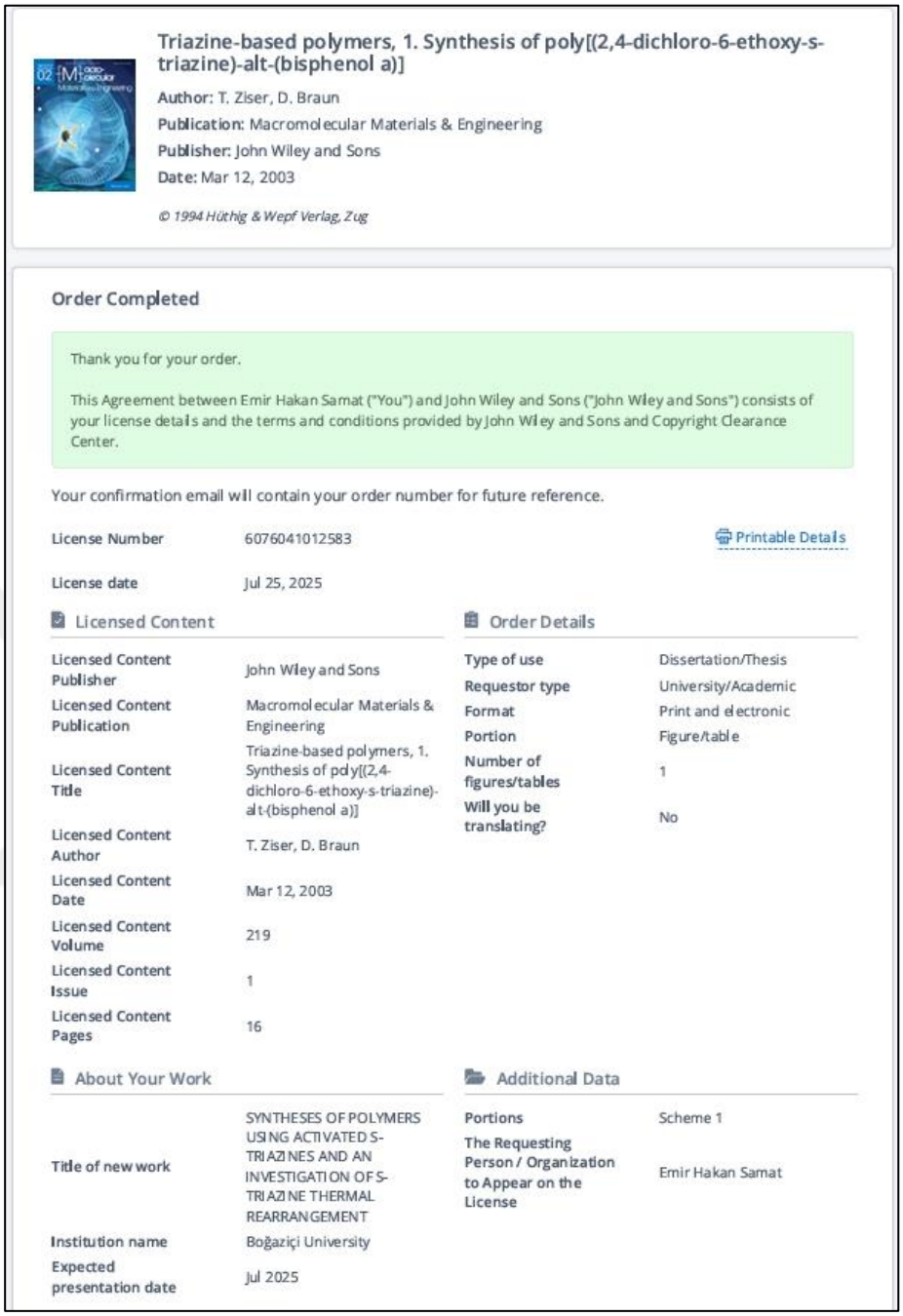
# APPENDIX B: COPYRIGHT LICENCES

Copyright permissions for the images used from the literature presented in this section.

Figures 1.13 and 1.15 are reprinted by permission of Informa UK Limited, trading as Taylor & Francis. Related articles below.

Alkyl Rearrangement of Derivatives of 2-Anilino-4,6-dialkoxy-1,3,5-triazines in the Solid- and Liquid-state. Vitaly Shteiman, Mark Botoshansky, Hellena Taycher, et al, . Supramolecular Chemistry, © 2006, reprinted by permission of Informa UK Limited, trading as Taylor & Francis Group, https://www.tandfonline.com.

Application of the Cyanurate-Isocyanurate Rearrangement to Amine Synthesis: Preparation of 2-(2-Thienyl)ethylamine. Ignacio H. Sanchez, Peter J. Harrington. Synthetic Communications, © 2006, reprinted by permission of Informa UK Limited, trading as Taylor & Francis Group, https://www.tandfonline.com.



**Triazine-based polymers, 1. Synthesis of poly[(2,4-dichloro-6-ethoxy-s-triazine)-alt-(bisphenol a)]**

**Author:** T. Ziser, D. Braun
**Publication:** Macromolecular Materials & Engineering
**Publisher:** John Wiley and Sons
**Date:** Mar 12, 2003

*© 1994 Hüthig & Wepf Verlag, Zug*

**Order Completed**

Thank you for your order.

This Agreement between Emir Hakan Samat ("You") and John Wiley and Sons ("John Wiley and Sons") consists of your license details and the terms and conditions provided by John Wiley and Sons and Copyright Clearance Center.

Your confirmation email will contain your order number for future reference.

| | |
|---|---|
| License Number | 6076041012583 |
| License date | Jul 25, 2025 |

Printable Details

**Licensed Content**

| | |
|---|---|
| Licensed Content Publisher | John Wiley and Sons |
| Licensed Content Publication | Macromolecular Materials & Engineering |
| Licensed Content Title | Triazine-based polymers, 1. Synthesis of poly[(2,4-dichloro-6-ethoxy-s-triazine)-alt-(bisphenol a)] |
| Licensed Content Author | T. Ziser, D. Braun |
| Licensed Content Date | Mar 12, 2003 |
| Licensed Content Volume | 219 |
| Licensed Content Issue | 1 |
| Licensed Content Pages | 16 |

**Order Details**

| | |
|---|---|
| Type of use | Dissertation/Thesis |
| Requestor type | University/Academic |
| Format | Print and electronic |
| Portion | Figure/table |
| Number of figures/tables | 1 |
| Will you be translating? | No |

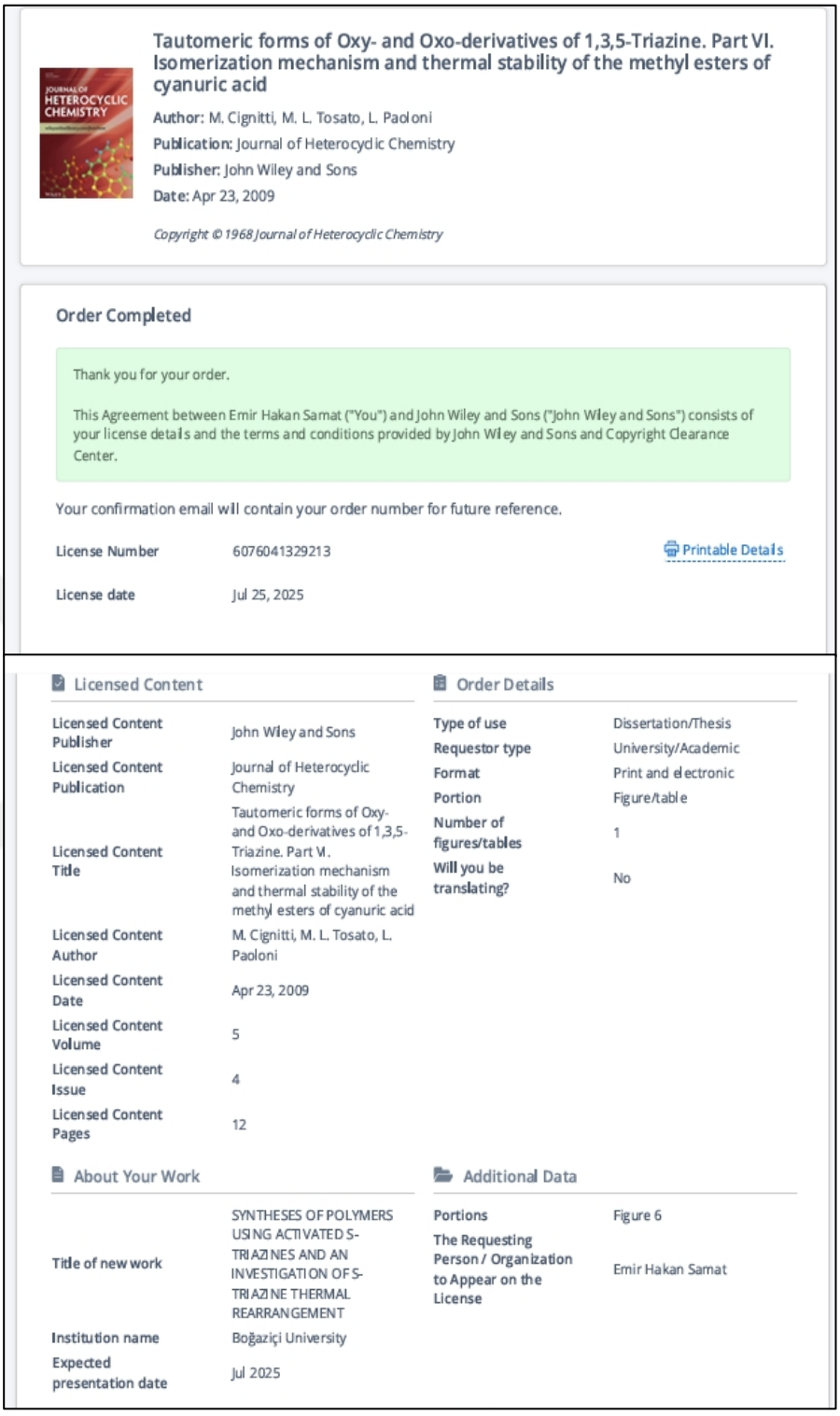
**About Your Work**

| | |
|---|---|
| Title of new work | SYNTHESES OF POLYMERS USING ACTIVATED S-TRIAZINES AND AN INVESTIGATION OF S-TRIAZINE THERMAL REARRANGEMENT |
| Institution name | Boğaziçi University |
| Expected presentation date | Jul 2025 |

**Additional Data**

| | |
|---|---|
| Portions | Scheme 1 |
| The Requesting Person / Organization to Appear on the License | Emir Hakan Samat |

Figure B.1. Copyright of Figure 1.6.



Tautomeric forms of Oxy- and Oxo-derivatives of 1,3,5-Triazine. Part VI. Isomerization mechanism and thermal stability of the methyl esters of cyanuric acid

Author: M. Cignitti, M. L. Tosato, L. Paoloni
Publication: Journal of Heterocyclic Chemistry
Publisher: John Wiley and Sons
Date: Apr 23, 2009

Copyright © 1968 Journal of Heterocyclic Chemistry

Order Completed

Thank you for your order.

This Agreement between Emir Hakan Samat ("You") and John Wiley and Sons ("John Wiley and Sons") consists of your license details and the terms and conditions provided by John Wiley and Sons and Copyright Clearance Center.

Your confirmation email will contain your order number for future reference.

| | |
|---|---|
| License Number | 6076041329213 |
| License date | Jul 25, 2025 |

Printable Details

Licensed Content

| | |
|---|---|
| Licensed Content Publisher | John Wiley and Sons |
| Licensed Content Publication | Journal of Heterocyclic Chemistry |
| Licensed Content Title | Tautomeric forms of Oxy- and Oxo-derivatives of 1,3,5-Triazine. Part VI. Isomerization mechanism and thermal stability of the methyl esters of cyanuric acid |
| Licensed Content Author | M. Cignitti, M. L. Tosato, L. Paoloni |
| Licensed Content Date | Apr 23, 2009 |
| Licensed Content Volume | 5 |
| Licensed Content Issue | 4 |
| Licensed Content Pages | 12 |

Order Details

| | |
|---|---|
| Type of use | Dissertation/Thesis |
| Requestor type | University/Academic |
| Format | Print and electronic |
| Portion | Figure/table |
| Number of figures/tables | 1 |
| Will you be translating? | No |

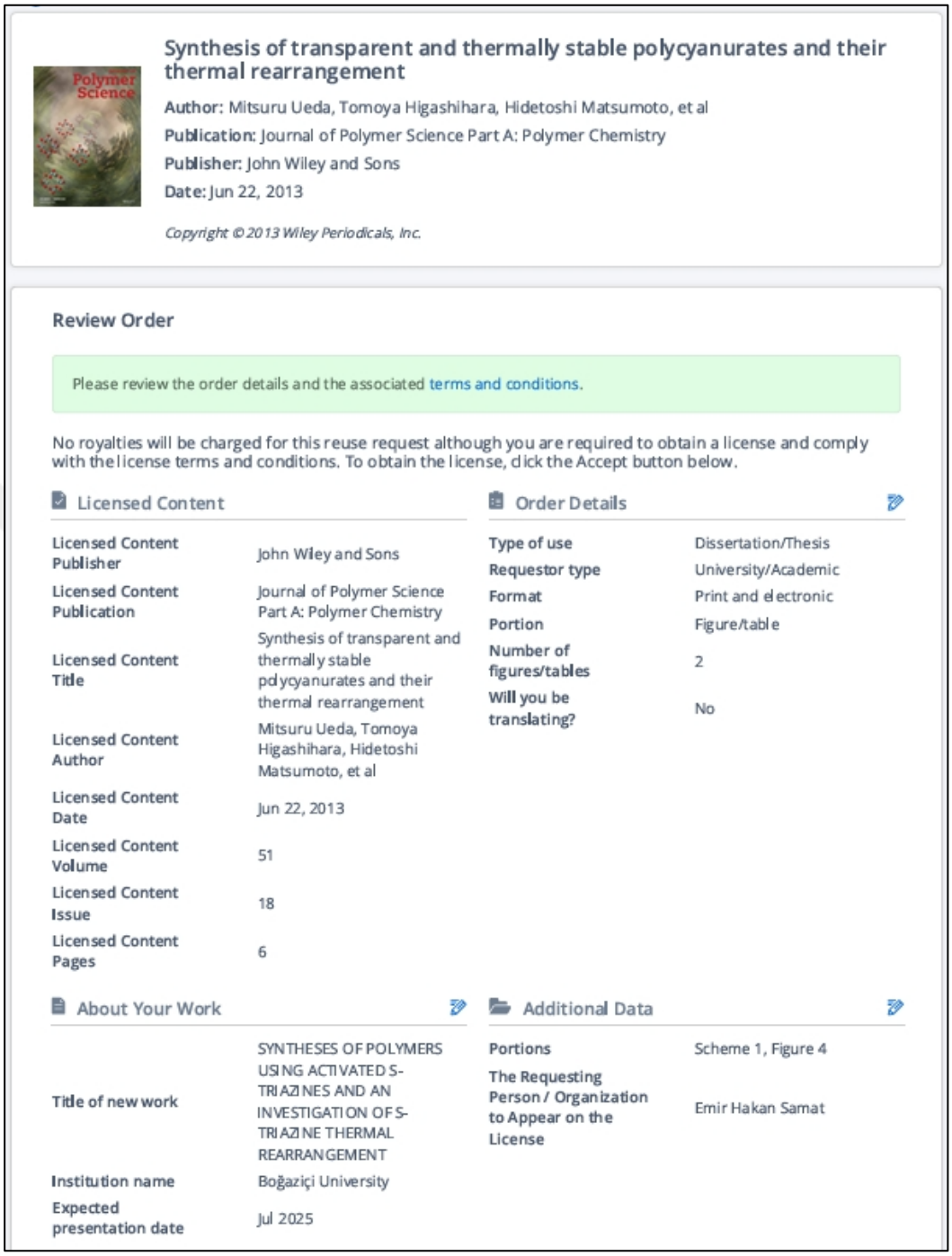
About Your Work

| | |
|---|---|
| Title of new work | SYNTHESES OF POLYMERS USING ACTIVATED S-TRIAZINES AND AN INVESTIGATION OF S-TRIAZINE THERMAL REARRANGEMENT |
| Institution name | Boğaziçi University |
| Expected presentation date | Jul 2025 |

Additional Data

| | |
|---|---|
| Portions | Figure 6 |
| The Requesting Person / Organization to Appear on the License | Emir Hakan Samat |

Figure B.2. Copyright of Figure 1.12.



Synthesis of transparent and thermally stable polycyanurates and their thermal rearrangement

Author: Mitsuru Ueda, Tomoya Higashihara, Hidetoshi Matsumoto, et al
Publication: Journal of Polymer Science Part A: Polymer Chemistry
Publisher: John Wiley and Sons
Date: Jun 22, 2013

Copyright © 2013 Wiley Periodicals, Inc.

Review Order

Please review the order details and the associated terms and conditions.

No royalties will be charged for this reuse request although you are required to obtain a license and comply with the license terms and conditions. To obtain the license, click the Accept button below.

Licensed Content

| | |
|---|---|
| Licensed Content Publisher | John Wiley and Sons |
| Licensed Content Publication | Journal of Polymer Science Part A: Polymer Chemistry |
| Licensed Content Title | Synthesis of transparent and thermally stable polycyanurates and their thermal rearrangement |
| Licensed Content Author | Mitsuru Ueda, Tomoya Higashihara, Hidetoshi Matsumoto, et al |
| Licensed Content Date | Jun 22, 2013 |
| Licensed Content Volume | 51 |
| Licensed Content Issue | 18 |
| Licensed Content Pages | 6 |

Order Details

| | |
|---|---|
| Type of use | Dissertation/Thesis |
| Requestor type | University/Academic |
| Format | Print and electronic |
| Portion | Figure/table |
| Number of figures/tables | 2 |
| Will you be translating? | No |

About Your Work

| | |
|---|---|
| Title of new work | SYNTHESES OF POLYMERS USING ACTIVATED S-TRIAZINES AND AN INVESTIGATION OF S-TRIAZINE THERMAL REARRANGEMENT |
| Institution name | Boğaziçi University |
| Expected presentation date | Jul 2025 |

Additional Data

| | |
|---|---|
| Portions | Scheme 1, Figure 4 |
| The Requesting Person / Organization to Appear on the License | Emir Hakan Samat |

Figure B.3 Copyright of Figure 1.6 and Figure 4.25.